2015-01-01

Nanoceria Exposure To Kidney Beans (phaseolus Vulgaris): Implications On Plant Physiology, Nutrition And Their Transfer To Next Trophic Level

Sanghamitra Majumdar
University of Texas at El Paso, smajumdar@miners.utep.edu

NANOCERIA EXPOSURE TO KIDNEY BEANS (*PHASEOLUS VULGARIS*): IMPLICATIONS ON PLANT PHYSIOLOGY, NUTRITION AND THEIR TRANSFER TO NEXT TROPHIC LEVEL

SANGHAMITRA MAJUMDAR

Department of Chemistry

APPROVED:

Jorge L. Gardea-Torresdey, Ph.D., Chair

Jose R. Peralta-Videa , Ph.D.

Mahesh Narayan , Ph.D.

Jason C. White, Ph.D.

Charles Ambler, Ph.D.
Dean of the Graduate School

Dedication

I would like to dedicate my thesis to *my most precious and beloved parents* for their love, support, relentless motivation and unquestioned confidence on me

I would also like to dedicate my work to my beloved and much treasured *"Dida" and all of my late grandparents* for their blessings and endless love.

NANOCERIA EXPOSURE TO KIDNEY BEANS (*PHASEOLUS VULGARIS*): IMPLICATIONS ON PLANT PHYSIOLOGY, NUTRITION AND THEIR TRANSFER TO NEXT TROPHIC LEVEL

by

SANGHAMITRA MAJUMDAR, M.Sc.

DISSERTATION

Presented to the Faculty of the Graduate School of

The University of Texas at El Paso

in Partial Fulfillment

of the Requirements

for the Degree of

DOCTOR OF PHILOSOPHY

Department of Chemistry

THE UNIVERSITY OF TEXAS AT EL PASO

December 2014

Acknowledgements

I would like to express my deepest gratitude to my mentor, Dr. Jorge Gardea-Torresdey for giving me the opportunity to obtain the highest academic degree in my career under his esteemed tutelage. You have encouraged me to think innovatively as an independent researcher, develop self-confidence and be passionate about my work. You have taught me to write research articles, best represent our research on any platform, and have introduced me to plethora of opportunities. You are a true inspiration for me because of your positivity, enthusiasm and great achievements, along with unparalleled humbleness and caring nature. All my achievement during my doctoral studies and hereafter is dedicated to you.

With immense pleasure, I would like to thank Dr. Jose R. Peralta-Videa for his persistent support throughout my doctoral journey. Under your guidance, I have learned basics of research and to approach problems. It has been exciting every time I came to you to discuss new ideas or share results, as it gave me hope and encouragement. Thanks for all your valuable contribution in my doctoral research and also for teaching me the key words in *Spanish*. Thanks for being so patient while training me in writing manuscripts. Your teachings will always be a treasure throughout my academic career and personal life.

I would also like to thank Dr. Mahesh Narayan for serving my dissertation committee and enriching my doctoral journey with his guidance and insightful comments. I would like to express my sincere thanks to Dr. Jason White for accepting to serve my dissertation committee and providing necessary advice during this period. I am very grateful to you for having confidence in my potential and accepting me as a post-doctoral researcher at your institution. It will be a great honor to work with you in my next endeavor.

I am thankful to Dr. Igor Almeida, Dr. Kyle Johnson, and their lab members for their help during our collaboration. My deepest acknowledgement goes to Dr. Emma Arigi for her assistance in my experiments and deep concern as a very good friend. I would like to thank Vincent Gant and Dr. C. Seong for providing necessary help in the laboratory. I would like to thank Dr. Hyungwon

Choi, National University of Singapore, for being extremely helpful with performing elaborate biostatistics. I would like to thank Dr. Shivendra Sahi, Western Kentucky University, Dr. Genhua Niu and Dr. Youping Sun from Texas AgriLife Research Center at El Paso, Texas A&M University, and Dr. Juan Pedro Flores Margez from Autonomous University of Ciudad Juarez, México for their collaboration. I would like to extend my appreciation to Dr. Chuan Xiao, Dr. Jose Nunez, Dr. Shizue Mito, Dr. Thomas Gill, and Dr. Vanessa Lougheed for allowing me to use their laboratory instruments. I would like to thank Dr. James Kelly, Michigan State University for his generous supply of kidney beans, and Dr. Thomas Dorsey, Department of Agriculture, State of New Jersey for providing us with Mexican bean beetles.

I would like to acknowledge the Chemistry Department for providing necessary resources and supporting me financially through teaching assistantship during this period. Thanks to the Biology Department, Border Biomedical Research Center (BBRC) staffs and resources, for allowing me to use their facility. Special thanks to NSF, EPA, and UC-CEIN for funding me during this period and providing me with ample opportunities to interact with the stalwarts in the field of sustainable nanotechnology. I would like to thank UTEP Graduate School for providing me with George A. Krutilek Memorial Scholarship and Dodson Research grant, towards successful completion of my doctoral studies.

I would like to extend my thanks to other professors in Chemistry Department, especially Dr. Bonnie Gunn and Dr. Katja Michael for showing their confidence in me from time to time. I am very grateful to Frank Reyes, Grace Awad and Lucema Armenta for their administrative assistance at all times. My special thanks goes to all my past and present colleagues and friends in Dr. Gardea's group including Dr. Cyren Rico, Dr. Jesica Trujillo-Reyes, Dr. Jose A. Hernandez, Dr. Lijuan Zhao, Dr. Susmita Bandyopadhyay, Dr. Jie Hong, Dr. Hiram Castillo, Ana Cecilia Barrios for their friendship and assistance during my research and publications. I would also like to thank all other lab members and my friends in Chemistry and Biology department, including Ricardo Mc Creary, Gustavo Avila, Gloria Polanco, Yenni Garcia and Naihsuan C Guy for their support, which have made this ride a very pleasant one. I would like to thank Goutam Banerjee for

his friendship, and providing valuable inputs and motivation during my doctoral research. I would like to pay my sincere gratitude to my past mentor, Dr. Shibani Chatterjee, Visva-Bharati University, for her encouragement and motivation.

I would like to extend my utmost respect and admiration towards my parents for their support and encouragement throughout this journey. I would like to thank my mother for her endless love and sacrifices that she made towards shaping me into what I am today and for being my best friend. I would like to thank my father for his unquestioned confidence and faith in me. You have shown me how to dream big and believe in myself. Special thanks to Mashi, Mesho, and Sujoy for giving me a home away from home, being my only family in United States.

Finally, I would like to thank all those who have contributed directly or indirectly towards my success in this journey. It is a great pleasure to graduate with a PhD in the centennial year of UTEP. Go miners!!

Abstract

Previous studies investigating the effects of cerium oxide nanoparticles (nanoceria, *n*CeO_2) on plants have primarily focused on the physiological and biochemical changes at early growth stages. Comprehensive information on the effects of *n*CeO_2 through the entire life cycle of plants and the nutritional quality of the edible tissues is limited. No studies have been reported on the interactions between *n*CeO_2 and common beans (*Phaseolus vulgaris*). Common beans are leguminous crops, which are societally important due to their nutritional benefits. The beans are rich in proteins and essential nutrients like folate, iron, zinc, molybdenum and magnesium, and are consumed worldwide. This research was performed to comprehend the impact of *n*CeO_2 on plant health, defense mechanisms, yield and nutritional quality of *P. vulgaris* var. red hawk kidney beans, and further transfer of *n*CeO_2 to a primary consumer in a terrestrial food chain. The broad scope of this research was divided into four major phases. Phase I was focused towards the mechanism of uptake and toxicity in a hydroponic system. Phase II evaluated soil organic matter as a factor towards the impact of *n*CeO_2 on plant physiology, metabolism, productivity, and bean nutritional quality. Phase III involved exploring the molecular mechanisms responsible for modulation of bean nutritional quality by *n*CeO_2. In Phase IV, the possible trophic transfer of *n*CeO_2 from the plant to a primary consumer was examined. To accomplish the goals of Phase I, plants were exposed to *n*CeO_2 suspensions (0, 62.5, 125, 250 and 500 mg/L) in hydroponics and analyzed for Ce uptake and translocation after 1, 7, and 15 days of exposure, using ICP-OES. Cerium localization and speciation in roots were studied by using scanning electron microscopy, synchrotron μ-XRF mapping/μ-XANES. Primary indicators of stress like oxidative stress, antioxidant enzyme activities, soluble protein and chlorophyll content were evaluated using biochemical assays. Synchrotron μ-XRF/μ-XANES provided evidence that Ce enters through the root epidermis maintaining its oxidation state, Ce(IV), as in *n*CeO_2, and reaches the vascular system through the region of emergence of lateral roots, due to the gaps in Casparian strip. Prolonged exposure to 500 mg/L *n*CeO_2 negatively affected the radical scavenging enzymes in the

roots, whereas, guaiacol peroxidase played a major role in the leaves to combat stress. In Phase II, the plants were grown in soils varying in their organic matter content (low organic matter soil: 4%, LOMS and organic matter enriched soil: 10%, OMES), amended with 0 to 500 mg/kg *n*CeO_2 through their complete life cycle. Plant tissues were analyzed for Ce accumulation, leaf area, photosynthetic pigments and metabolic activities like net photosynthesis, transpiration, and stomatal conductance. The matured beans harvested upon treatments were assessed for the mineral nutrients and macromolecular composition using ICP-MS, FTIR and colorimetric assays. Organic matter content in soil influenced the response of *n*CeO_2 on metabolic activities and bean quality. Although Ce accumulation in tissues was dose-dependent, Ce translocation to the leaves was significantly higher in plants grown in OMES by 71%, than in LOMS at 500 mg/kg *n*CeO_2. Photosynthesis and transpiration increased significantly compared to control upon *n*CeO_2 exposure at 62.5, 125 and 250 mg/kg *n*CeO_2 in OMES. Plant productivity in the presence of less organic matter was enhanced when amended with 250 and 500 mg *n*CeO_2/kg, but a bell-shaped curve with increasing *n*CeO_2 concentration was noted in the plants grown in OMES. Nanoceria did not affect the macronutrient content in the beans, however Mo was reduced by 38-61% with respect to control, upon *n*CeO_2 exposure in LOMS. On the other hand, in the seeds from OMES, Na content was reduced by 18-31% with respect to control. FTIR studies showed alteration in the carbohydrates, lipids, and amides in the beans harvested from plants exposed OMES amended with *n*CeO_2. However in the beans from LOMS, only the amides were affected at 62.5 mg/kg *n*CeO_2. In Phase III, proteomic analyses performed using LC MS/MS tandem spectrometry on the beans harvested upon *n*CeO_2 exposure revealed that at 125 and 250 mg/kg, *n*CeO_2 induced two proteins, *defensin* and *purple acid phosphatase*, responsible for stress response and metabolism, respectively. However, the number of downregulated proteins increased, with increasing *n*CeO_2 exposure concentration. At 500 mg/kg *n*CeO_2, eighteen proteins associated with protein storage, carbohydrate metabolism, and ATP/GTP binding activities were downregulated. Phase IV of this dissertation was accomplished by infesting plants exposed to 1000 and 2000 mg/kg *n*CeO_2 with Mexican bean beetles (*Epilachna varivestis*). The beetles were allowed to grow through their entire

life cycle, feeding on *n*CeO_2 exposed plants. Then they were analyzed for Ce accumulation at the various stages of development. Beetles were shown to accumulate Ce in tissues, depending on the exposure concentration, and their food assimilation habits at different developmental stages. Beetles at the pupal stage feeding on 2000 mg/kg *n*CeO_2 accumulated the highest concentration (1300 µg Ce/kg d wt), which decreased to 400 µg Ce/kg d wt in adult tissues. This dissertation thus provides a holistic understanding of the interaction of *n*CeO_2 with kidney beans at physiological, biochemical and molecular level, and their possible transfer along a terrestrial food chain.

Table of Contents

List of Tables

List of Figures

CHAPTER 1

Introduction

Since the onset of nanotechnology era about half a century ago, there has been a rapid progression in its development into a general purpose technology [1]. According to the American Society for Testing and Materials and the International Standard Organization [2,3], nanomaterials are defined as materials with at least one dimension at the size range of 1-100 nm. Engineered nanomaterials (ENMs) have unique properties like high surface to volume-ratio, high reactivity, and large accessibility to inorganic surfaces, compared to their bulk counterparts. They are being used in wide range of applications in the fields of medicine, agriculture, energy, electronics, chemical sensors, consumer products, environmental remediation and other industrial sectors, utilizing their physical, thermal, optical, and biological properties at the atomic scale [4]. Currently, there are no regulations implemented by federal governments or international organizations on the use of ENMs in commercial products or their release into the environment. Some of the nano-enabled consumer products already in the U.S. market includes fabric, cosmetics, sporting goods, food packaging, dietary supplements, and electronics [4,5]. Recently ENMs have been defined by the European Union as "*any intentionally manufactured material, containing particles, in an unbound state or as an aggregate or as an agglomerate and where, for 50% or more of the particles in the number size distribution, one or more external dimensions is in the size range 1 nm to 100 nm*" [6]. The margin of 50% passes most of the nano-enabled products, especially food additives, dietary supplements, and food packaging among others. It has been reported that there are more than 800 nano-based products in the market and recent estimates suggest an exponential increase in few years [7]. Unavailability of any real statistics on their usage and waste production, along with their unknown effects on the environment and human health, has led to increasing concern amongst environmental agencies and federal bodies. It is extremely urgent to employ precautionary principle and perform rapid life cycle and risk assessment of these "game changing" nanomaterials, before they become ubiquitous in our environment.

Numerous studies have been devoted towards estimating and evaluating the concentrations of the ENMs in different environmental media, and the probability and extent of human exposure [8,9]. The fate of the ENMs in the environment and their effects are varied and dependent on the test organism, exposure conditions as well as chemical properties of the ENM like size, shape, functionalization, and elemental composition. ENMs are primarily categorized into carbon based (single and multi-walled carbon nanotube, nanowires), metal based (metal and metal oxide nanoparticles), and quantum dots. Cerium oxide nanoparticle particles or *nanoceria* ($n$$CeO_2$) are one of the top ten important metal oxide nanoparticles, being widely used for various applications [8]. Due to their *bonafide* catalytic and redox properties, and enhanced surface defects at nanoscale, $n$$CeO_2$ are rapidly replacing micro-sized ceria particles in varied applications like fuel additives, catalytic converters, scratch resistant polishing agents, and electronic devices [9]. Studies have suggested that $n$$CeO_2$ have anti-oxidative properties, owing to the facile conversion between its redox states, Ce(IV)/ Ce(III) [10]. Due to these unique properties, they are being widely researched for biomedical purposes like treatment of neurodegenerative and ocular diseases, and for tissue regeneration [10]. Current market estimates suggest 10,000 metric tons of global annual production of $n$$CeO_2$, primarily from Asia, Australia and Europe [9]. This has simultaneously raised serious concern on their fate upon release in various environmental media [8], and corresponding exposure to ecological receptors, like plants and humans. Ecological modelling and mass balance studies suggests that a major fraction (80%) of $n$$CeO_2$ released to the environmental finally accumulate in the soils, sediments, and biosolids [8,9]. According to current prediction, the concentration of $n$$CeO_2$ in biosolids ranges from 0.5 to 10 mg/kg [9]. These estimates have placed plants grown naturally and in agricultural land in a vulnerable situation. This is also alarming for human health due to scarcity of information available on the possibility of transfer of $n$$CeO_2$ from plants to next level consumers [11].

Earlier studies on $n$$CeO_2$ exposure to plants have provided evidence on their uptake by roots and translocation to aerial tissues in different plant species [12-21], with contrasting

physiological and biochemical responses. Although they were reported to primarily retain their oxidation state and nanoparticulate form, a small fraction of Ce(IV) was found to biotransform to Ce(III) in soybeans [13], and cucumber [19]. Recent studies have detected Ce in edible tissues of soybeans [12,13], tomato [14], rice [15], cilantro [16], radish [17], and cucumber plants [20], exposed to *n*CeO_2 in soil. It has also been reported to increase the plant yield [12,14] and alter the mineral contents in edible tissues [22,23]. A recent study showed that upon feeding on *n*CeO_2 exposed zucchini plants, crickets accumulated Ce in their tissues [24].

Despite of increasing number of publications reporting the effects of *n*CeO_2 with plants [12-23], current literature lacks conclusive studies on plants grown for their complete life cycle. Also, there are only a few studies concerning the transfer of *n*CeO_2 to the edible tissues [12-17, 20], without any understanding of the molecular mechanisms responsible for observed disturbances in nutritional parameters. There is a major gap in understanding the mechanisms of *n*CeO_2 phytotoxicity and the influence of soil properties on their interactions at the nano-bio interface. There are no reports on the long term interaction of *n*CeO_2 with common beans plants, *Phaseolus vulgaris*, and their possible transfer to the primary consumers in a terrestrial food chain. Common bean is an annual leguminous crop, societally important due to the nutritional significance of the beans. It represents 50% of the grain legumes consumed worldwide, and produced nearly twice that of chickpeas, the second most consumed food legume [25]. Beans are highly rich in proteins and essential nutrients like folate, iron, zinc, molybdenum and magnesium [26]. It is the most common legume consumed due to its health benefits that includes reducing blood cholesterol and sugar levels, thereby preventing various degenerative diseases like diabetes, cancer and heart ailments [27]. Also, studies have shown that beans contain proteins responsible for inhibition of the HIV-1 reverse transcriptase [28]. Apart from the nutritional benefits, common bean is a very important agricultural crop that is beneficial for replenishing the nitrogen content in the soil, thereby maintaining soil fertility of agricultural land.

In this study, the interactions of *n*CeO_2 with kidney bean plants (*P. vulgaris var. red hawk kidney)* at physiological, biochemical and molecular levels were assessed. The impact of *n*CeO_2

on the nutritional quality of the harvested beans, and further transfer to primary consumer level in a food chain was explored. The broad scope of this research was divided into four major phases. In Phase I, the mechanism of root uptake and associated toxicity was investigated in hydroponics. Time dependent root uptake of Ce and further translocation to aerial tissues was analyzed using inductively coupled plasma spectroscopy (ICP-OES). Scanning electron microscopy and synchrotron μ-XRF mapping/ μ-XANES were performed for Ce localization and speciation in the root tissues. Primary indicators of stress like lipid peroxidation, antioxidant enzyme activities, soluble protein and chlorophyll content in the tissues were examined using biochemical assays. In Phase II, soil organic matter was tested as a factor for impact of *n*CeO_2 on Ce accumulation in the tissues, plant metabolism, physiology, yield, and bean quality. Effects on metabolic activities including photosynthesis, transpiration, and stomatal conductance were examined. Phase III was a follow up study from the previous phase. The beans harvested from the plants grown in *n*CeO_2 amended organic matter enriched soil, were subjected to proteomic analysis using LC-MS/MS tandem spectrometry, to identify proteins responsible for nutritional disturbances by comparing with untreated control beans. In the last phase, Phase IV, 22 days-old *n*CeO_2 exposed plants were infested with Mexican bean beetles (*Epilachna varivestis)*. Beetles were fed on the plants through the three major stages of development including larvae, pupae, and adult, and were analyzed for Ce accumulation in the tissues. Phase I and Phase II were performed under the working hypothesis that the *n*CeO_2 will be taken up by the plant roots and translocated to the aerial parts. It was hypothesized that the incorporation of *n*CeO_2 in the tissues will disturb the cellular homeostasis, expressed by variations at the biochemical level. Phase III and Phase IV were follow-up studies from Phase II. Phase III was performed under the working hypothesis that proteins responsible for regulation of cellular processes and protein storage will be affected in the beans, and in Phase IV, it was premised that trophic transfer to the next consumer level could be possible.

CHAPTER 2

Exposure of nanoceria to kidney bean shows disturbance in the plant defense mechanisms

2.1 Introduction

Over the last decade, globalization of nanomaterial research initiatives have progressed nanotechnology towards a general-purpose technology [1]. The unregulated usage and disposal of engineered nanoparticles (ENPs) has resulted in a dilemma among environmentalists, industrialists, and regulatory agencies on the possible sinks and associated environmental risks. Plants are at maximum risk due to the concentration build-up of ENPs in natural sediments, agricultural soils, and aquatic environments [2-4]. Nanoceria particles ($n$$CeO_2$) are one of the most produced metal oxide nanoparticles worldwide, accounting for around 10,000 metric tons/year [5]. They are used as catalysts for augmenting fossil fuel oxidation, scratch-resistant glass polishing, petrochemical processing, and UV radiation protectants [6,7]. Studies have confirmed that the reduction of Ce(IV) in $n$$CeO_2$ and $n$$Ce_{1-x}Zr_xO_2$ is easier than in bulk ceria [8]. Thus, nanoscale cerium compounds are expected to behave differently in environmental matrices and biological systems. Dissolution of ENPs and redox conditions at the nano-bio interface are critical parameters to determine their toxicity [9-11].

Previous reports suggest that $n$$CeO_2$ have positive effects in terms of growth and yield at low concentrations (10-125 ppm) [12, 13]; whereas, at higher concentrations, adversely affect the plant physiology [14], metabolism [15], and yield [15,16]. The available literature on the toxicity of $n$$CeO_2$ in edible plants is contradictory. For instance, in tomato (*Solanum lycopersicum*) seeds exposed to $n$$CeO_2$ at 2000 mg/L, Ma *et al.* reported no toxicity symptoms [17], whereas in another study, López-Moreno *et al.* reported decrease in germination rate and root length [14]. In soybeans (*Glycine max*), at similar exposure concentration, the plants were shown to experience genotoxicity [18], and at 1000 mg/kg soil the nitrogen assimilation, growth, and yield was negatively affected [15]. Thus, this area is still in its infancy and needs more standardized studies to conclude their effects depending on the exposure medium. Hydroponic studies are preferred

when precise information on the interaction of the ENPs with the plant is being explored. This is to avoid multitude of variables that come into play when the ENPs interact with a complex exposure medium like soil [3]. The impact of *n*CeO_2 on plant physiology and their defense mechanisms, as a function of time, has not been well explored. Also, there are very few studies on the protein rich edible crops which deserve special attention due to their contribution to our daily nutrition.

To the best of authors' knowledge, there are no studies on the interaction of *n*CeO_2 with kidney beans (*Phaseolus vulgaris*). Kidney bean is a very important leguminous crop and a major global source of proteins and micronutrients, especially zinc and iron [19]. In this study, kidney bean plants were exposed to *n*CeO_2 suspensions for 15 days to follow their uptake and transport to aerial tissues. To determine the probable route of *n*CeO_2 uptake through roots, scanning electron microscopy (SEM) and elemental mapping using synchrotron micro-X-ray fluorescence (μ-XRF) were performed followed by speciation studies using micro-X-ray absorption near-edge structure spectroscopy (μ-XANES). To shed light on the biochemical responses in the plant tissues, activities of major antioxidant enzymes, lipid peroxidation, and contents of chlorophylls and total soluble protein were determined.

2.2 Materials and methods

2.2.1 Preparation of nanoparticle suspensions

nCeO_2 (≈8 nm, Meliorum Technologies, Rochester, NY) were obtained from The University of California Center for Environmental Implications of Nanotechnology (UC-CEIN) [20]. A detailed characterization of *n*CeO_2 used, has been previously published by Keller *et al*. [21] and Lopez-Moreno *et al.*[18]. As previously reported, the *n*CeO_2 were rods, measuring (67 ± 8) × (8 ± 1), (≤10% polyhedra: 8 ± 1 nm) with 95.14% purity and surface area of 93.8 m^2g^{-1} [21].

Suspensions of *n*CeO_2 at concentrations of 62.5, 125, 250 and 500 mg/L were prepared in modified Hoagland nutrient solution (NS) (pH 5.8) upon 30 min bath sonication (Crest Ultrasonics, Trenton, NJ) at 25 °C. Bulk CeO_2 (*b*CeO_2, Sigma Aldrich) suspensions (125, 500 mg/L) were also

prepared similarly. The suspensions were immediately characterized after sonication for pH, size, and zeta-potential (ζ-potential). The size and ζ-potential of the particles in *n*CeO_2 and *b*CeO_2 suspensions were measured by dynamic light scattering (DLS) method using NanoSizer 90 (Malvern Instruments, Worcestershire, UK) at 25 °C. TEM image of the well-dispersed suspension was carried out using a 120 CX Transmission electron microscope (JEOL USA, Inc., MA, USA) at 80 kV.

2.2.2 Nanoparticle exposure

Phaseolus vulgaris var. red hawk kidney seeds were provided by Dr. James Kelly, Michigan State University. The seeds were disinfected with 2% hypochlorite solution and rinsed with sterilized MPW three times. Antimycotic - antibiotic solution, 50% (A5955, Sigma, St. Louis, MO) was used to prevent the growth of any fungal or bacterial infections. After germinating the seeds under moist and sterilized condition in dark for four days, the seedlings were exposed to light for three days until the emergence of plumule. Thereafter, the seedlings were transplanted to plastic jars with a polyurethane foam cover for support, containing 500 ml of Hoagland nutrient solutions [($Ca(NO_3)_2.4H_2O$, 0.35mM; $CaCl_2.2H_2O$, 2.1mM; $Mg(NO_3)_2.6H_2O$, 1.1mM; KH_2PO_4, 0.97 mM; KNO_3, 0.25mM; H_3BO_3, 23.13µM; $MnCl_2$, 3.9 µM; MoO_3, 0.07 µM; $CuSO_4.H_2O$, 0.44 µM; $Fe(NO_3)_3.9H_2O$, 10 µM; $Zn(NO_3).6H_2O$, 0.37 µM] to acclimatize with controlled conditions in a growth chamber (Environmental Growth Chamber, Chagrin Falls, OH) with 14 h photoperiod (340 µmole $m^{-2}s^{-1}$), 25/20 ºC day/night temperature and 65% relative humidity. After seven days, the plants were exposed to freshly prepared *n*CeO_2 and *b*CeO_2 suspensions for 15 days, using plastic pipettes supported through the foam so that only the roots were exposed to the suspensions. Pure NS served as the control. Quadruplicate sets of four plants per jar per treatment, aerated with aquarium pumps, were installed on magnetic stirrers to reduce the settling of *n*CeO_2 aggregates (Figure 2.1).

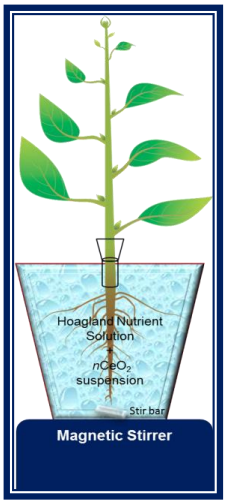

Figure 2.1. Hydroponic set up for nCeO$_2$ treatments with continuous magnetic stirring to maintain homogeneity

Preliminary experiments performed without continuous stirring showed settling of the aggregates within the first few hours. To determine dissolution of nCeO$_2$, Ce ions were quantified on the 1st, 7th and 15th day by centrifuging 50 ml of suspensions for 30 min at 4500 rcf (Eppendorf 5804R, Hamburg, DE). The water loss was replenished everyday using Millipore water (MPW). The experiment was run in three sets that were harvested after one, seven, and 15 days of exposure (DE). Plants exposed to bCeO$_2$ were harvested after 15 days. During sampling, the roots were washed three times with 0.01M HNO_3 and MPW to remove adhered particles prior to all the analyses [14,22].

2.2.3 Quantification of cerium in tissues

After one, seven, and 15 DE, one plant from each treatment replicate (n=4) was washed and severed into roots (including hypocotyl), stems and leaves (first true leaf including the petiole), and other aerial tissues, and dried at 70 °C for 96 h. The dry weight was recorded. The dried tissues were digested in microwave accelerated reaction system (CEM Mars$_x$, Mathews, NC) following the U.S. EPA 3051 method using plasma pure HNO_3 and 30% (w/v) H_2O_2 (1:4) mixture as described by Packer *et al.*[23]. Ce concentration in the tissues was determined using inductively coupled plasma-optical emission spectroscopy (ICP-OES) (Optima 4300 DV, Perkin Elmer) [14].

Ten blanks were used to calculate the detection limit of Ce. National Institute of Standards and Technology (NIST) certified standard reference material (peach leaves NIST-SRM 1547, Gaithersburg, MD) were analyzed to validate the digestion process, obtaining 90% recovery [16]. Also, 0.5 mg/L Ce standard was analyzed every 10 samples to monitor the matrix effect on the analyte and for quality assurance/quality control.

2.2.4 SEM analysis

After 15 DE to 500 mg *n*CeO_2/L, roots were frozen in liquid nitrogen, freeze dried for 24 h, sectioned, and then mounted on aluminum stubs. The samples were viewed at an accelerating potential of 20 kV under high vacuum mode with backscatter detector using a JSM-5400LV SEM (JEOL, Tokyo, Japan) equipped with IXRF-EDS system with a Moxtek AP3.3 light element entrance window.

2.2.5 Synchrotron µ-XRF and µ-XANES analysis

After 15 DE to 500 mg *n*CeO_2/L, a portion of the root was excised from the absorption zone, snap-frozen in liquid nitrogen and embedded in Tissue Tek resin (Sakura Finetek USA, Inc., Torrance, CA). The embedded samples were sectioned at 30 µm, mounted on ultralene window film, lyophilized at -53ºC and 0.140 mbar for 1h (Labcono FreeZone 4.5, Kansas City, MO) and stored in desiccant until analysis at beamline ID21 at the European Synchrotron Radiation Facility (ESRF, Grenoble France). Micro-XRF mapping for Ce distribution in the root was performed with incident energy at 5.8 keV using beamline ID21at the European Synchrotron Radiation Facility (ESRF, Grenoble, France) [24]. The storage ring current during data acquisition ranged between 180 and 200 mA (continuous) operating at 6.0 GeV. The beam was focused with the use of a Fresnel zone plate to a size of 0.2×0.8 μm^2 (V×H) and the fluorescence signal was detected with a Si drift detector in vacuum. Two photodiodes were used to measure the incident and transmitted beam intensities. Dwell time and distance of the detector was optimized for each image keeping the detector dead time below 15% [25]. The X-ray fluorescence data was fitted using PyMCA software. For µ-XANES data acquisition, the energy was selected using a (Si111) double crystal

monochromator and scanned from 5.69 to 5.79 keV and the zone plate was translated in the beam axis in order to maintain the beam focus.

The final Ce-L_{III} edge spectra were the sum of 10 individual scans with 0.5 eV resolution energy steps. In order to improve the data quality, four spots from the root epidermis were averaged for analysis by linear combination fitting. Micro- XANES data analysis was carried using the linear combination procedure in ATHENA software [26]. Reference materials (cerium (IV) hydroxide, cerium (III) acetate) were chemical grade reagents analyzed as fine powder pellets in transmission and fluorescence mode.

2.2.6 Analytical methods

Total chlorophyll in leaves were extracted in 80% acetone and measured as described by Lichtenthaler and Buschmann [27]. Soluble protein content in the fresh samples was analyzed according to Bradford using bovine serum albumin standard [28]. Lipid peroxidation was determined as described by Heath and Packer and expressed as μmol MDA (mg protein)$^{-1}$ [29].

2.2.7 Antioxidant enzyme assays

To investigate the oxidative stress response of kidney bean plants upon *n*CeO_2 and *b*CeO_2exposure, the specific activity of major antioxidant enzymes such as catalase, ascorbate peroxidase and guaiacol peroxidase was studied in the different parts of the plant. After 1 DE, the leaf biomass was not enough for performing biochemical analyses. Upon harvest on 7th and 15th DE to *n*CeO_2 and *b*CeO_2, the plants were washed and severed into roots, stems and the central leaflet from the second true leaf. The fresh tissues were ground in frozen condition (liquid nitrogen) and extracted in 50 mM potassium phosphate buffer containing 1 mM EDTA, 1 % PVP, and 0.5% (v/v) Triton X-100. The 10% homogenates were then centrifuged at 10,000 rcf for 20 min (Eppendorf 5417R centrifuge, Hamburg, DE) and the supernatant fractions were used to perform specific activity of antioxidant enzymes [30].

The activity of catalase (CAT; EC 1.11.1.6) was assayed according to Aebi (1974) by measuring the decomposition of H_2O_2 at 240 nm (coefficient of absorbance, ε = 39.4 $mM^{-1}cm^{-1}$)

in a reaction mixture containing 50 mM phosphate buffer (pH 7.4), 10 mM H_2O_2 for 3 min [31]. The enzyme activity is expressed as μmol of H_2O_2 decomposed mg^{-1}protein min^{-1}. The ascorbate peroxidase (APOX, EC1.11.1.11) activity was assayed by measuring the ascorbate oxidation at 290 nm for 2 minutes upon addition of H_2O_2 [32]. The reaction mixture (1.5 mL) contained 50mM phosphate buffer (pH7.4), 0.5mM ascorbate, 1.0mM H_2O_2 and 100μl of enzyme. APOX activity was quantified using the molar extinction coefficient for ascorbate ($2.8mM^{-1}cm^{-1}$) and the results were expressed in μmol of H_2O_2 decomposed mg^{-1}(protein) min^{-1}, taking into consideration that 2 mol ascorbate are required for reduction of 1 mol H_2O_2. Guaiacol peroxidase (GPOX, EC1.11.1.7) activity was determined as described by Urbanek *et al.* in a reaction mixture (2.0 mL) containing 100mM phosphate buffer (pH 7.0), 5.0mM guaiacol, 15.0mM H_2O_2 and 50μl enzyme extract [33]. Enzyme activity was quantified by the amount of tetraguaiacol ($\varepsilon=26.6mM^{-1}cm^{-1}$) formed at 470nm for 1 minute. The results were expressed as μmol H_2O_2 mg^{-1}(protein) min^{-1} taking into consideration that 4 mol H_2O_2 are reduced to produce 1 mol tetraguaiacol.

2.2.8 Statistical Analysis

The values for Ce content and biochemical analyses were reported as mean ± SE of four replicates. The data were analyzed using one-way ANOVA followed by Tukey's multiple comparisons test (IBM SPSS Statistics 19, Chicago, USA).

2.3 Results and discussion

2.3.1 Characterization of *n*CeO_2 suspensions

The exposure concentrations in this study were selected considering the future perspective of environmental build-up with elevating production and disposal of *n*CeO_2 [34-36]. The TEM image of the *n*CeO_2 suspension is shown in Figure 2.2A and the size, pH and ζ-potential of the *n*CeO_2 and *b*CeO_2 suspensions have been provided in Table 2.1. DLS measurements suggest that *n*CeO_2 suspended in NS aggregated to particles with average hydrodynamic diameters ranging between 1057 and 2547 nm.

DLS measurements are highly biased towards larger sizes in polydisperse suspensions as only few larger particles can produce a highly scattered light, thereby making it difficult to detect the smaller particles [37]. TEM image confirmed that the suspension consisted of many particles with a size ≤ 50 nm (Figure 2.2A). Due to the low dissolution of *n*CeO_2 in distilled water or soil solution, soluble cerium compounds were not tested [11,25]. The dissolution of *n*CeO_2 in NS in this study was found to be 0.15 ± 0.02 %. Figure 2.2B shows that the dissolution of Ce did not change significantly during the exposure period.

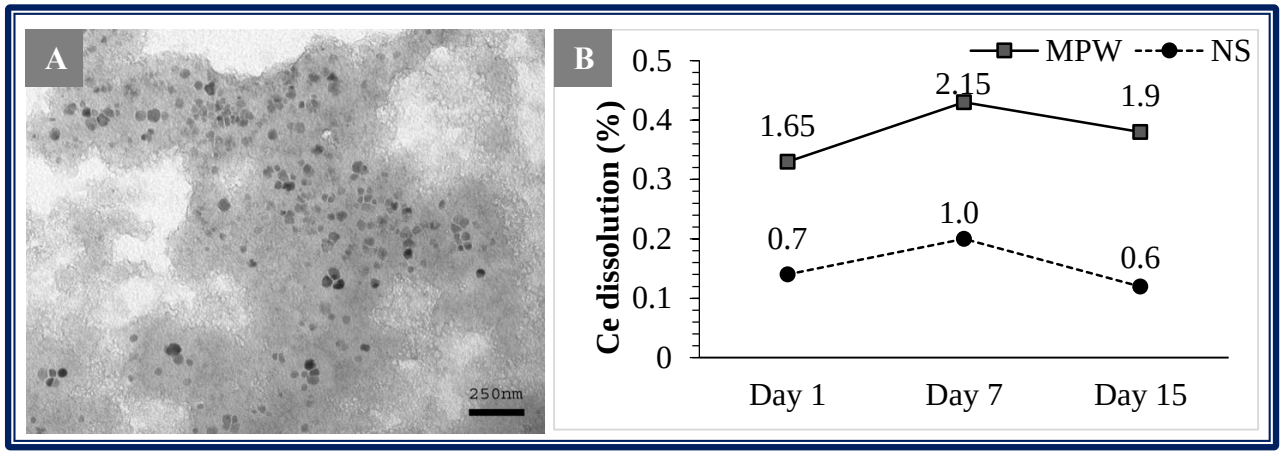

Figure 2.2. Characterization and stability of 500 mg *n*CeO_2/L suspension (A) TEM image of *n*CeO_2 suspension in Hoagland nutrient solution (pH 5.8), (B) Dissolution kinetics of *n*CeO_2 in MPW and NS. Data labels correspond to the Ce concentration (mg/L) upon dissolution in MPW and NS.

Table 2.1. Characterization of the *nano* and *bulk* CeO_2 suspensions prepared in Hoagland's nutrient solution.

Treatment concentration (mg/L)	**pH**	**Z-averaged hydrodynamic diameter (nm)**	**Zeta potential (mV)**
62.5 *n*CeO_2	5.77 ± 0.02	2547.2 ± 123	- 1.98 ± 0.55
125 *n*CeO_2	5.78 ± 0.02	2200.5 ± 148	- 1.19 ± 0.47
250 *n*CeO_2	5.78 ± 0.02	1653.7 ± 124	- 1.47 ± 0.53
500 *n*CeO_2	5.70 ± 0.02	1056.7 ± 145	- 0.39 ± 0.13
125 *b*CeO_2	5.78 ± 0.01	3114.7 ± 314	- 3.62 ± 0.36
500 *b*CeO_2	5.79 ± 0.02	2498.5 ± 171	- 0.22 ± 0.09

Values are expressed as mean ± SE (n=4).

2.3.2 Accumulation of cerium in roots

The accumulation of Ce in the roots and the uptake flux are shown in Figure 2.3. As seen in Figure 2.3A, Ce accumulation increased linearly with increasing exposure concentrations at all sampling times (r = 0.936, 0.924, and 0.959 for one, seven, and 15 DE, respectively). This corroborates with previous studies in other edible plants like tomato [12], rice [13], soybean [14], corn [25], and cucumber [38]. The concentration-dependent linear increase in Ce accumulation in roots suggests uptake through simple diffusion. Adsorption of nCeO$_2$ aggregates on the root surface was observed in the SEM images (Figure 2.4). Due to the negative ζ-potential of the nCeO$_2$ suspensions (Table 2.1), they are easily adhered non-specifically to the acidic surface of roots [39]. But the spectroscopic evidence of Ce in root vascular tissues (Figure 2.5) and the transport of Ce to the aerial tissues (Figure 2.6A) confirm that the Ce concentration in roots was not entirely due to adhered particles. The Ce concentration in roots reached 3596 mg/kg upon exposure to 500 mg nCeO$_2$/L for one day. However, after seven and 15 DE, Ce in roots decreased to 2771 and 2844 mg/kg, although the decrement was not statistically significant. Except at 62.5 mg/L, in all the treatments the Ce concentration in roots did not increase with increasing exposure duration. This stagnancy of Ce concentration in roots was attributed to an increase in aerial translocation with time.

Since cellular transport of nutrients is primarily dependent upon the binding and release of ions/molecules to the active site of the transport proteins, kinetic studies have been used to understand the regulation of transport [40]. Here, the flux for Ce accumulation in roots was calculated as follows:

$$\text{Uptake flux } ((\text{mg Ce/kg dwt})/\text{h}) = [[\text{Ce}]\text{in roots (mg Ce/kg dwt)}]/\text{ Exposure duration(h)}$$

As shown in Figure 2.3B, the uptake flux (mg/kg d wt/h) of Ce increased sharply with increasing nCeO$_2$ treatment upon one (primary Y-axis, left), seven, and 15 (secondary Y-axis, right) DE. But, the flux for each treatment decreased with increasing DE. For instance, in 500 mg nCeO$_2$/L treated plants, the Ce flux into the roots was 184.9 mg/kg d wt/h after one DE; however, it reduced to 16.1 and 7.9 mg/kg d wt/h after seven and 15 DE, respectively. This further supports

that the rate of Ce uptake is not entirely dependent on exposure duration, but guided by concentration gradient. The above accumulation trend suggests passive mode of transport, possibly through simple or facilitated diffusion. It is probable that the redox cycling behavior of Ce(IV) on the surface of nanocrystals in the aggregates, allows it to compete with other redox active elements like iron for transporters. The mechanism of passive uptake is also supported by the negative ζ-potential of the *n*CeO_2 in the suspension (Table 2.1). Patil *et al.* reported that *n*CeO_2 with negative ζ- potential does not significantly adsorb proteins [41], negating possibility of active carrier protein transport which requires binding to membrane proteins [40].

Cerium accumulation in the roots of *b*CeO_2 treated plants were significantly lower than the *n*CeO_2 treated plants (Figure 2.6B).This strongly suggests that the *n*CeO_2 are more active in crossing the biological barriers owing to their size and surface chemistry.

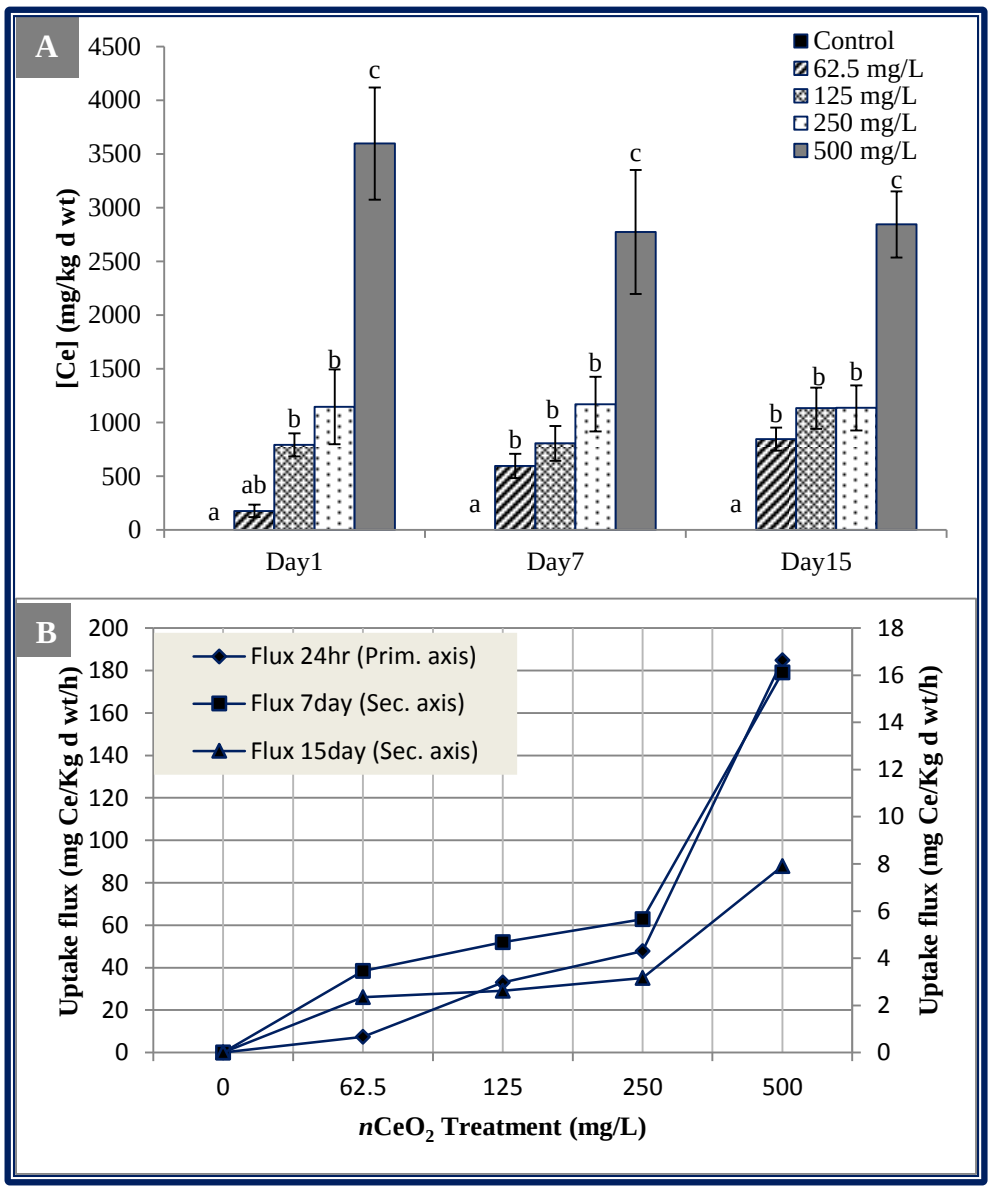

Figure 2.3.(A) Ce accumulation in the kidney bean roots exposed to 0 to 500 mg/L nCeO$_2$ for 1, 7 and 15 days. Values are mean ± SE (n=4). Different letters within each DE represent significant difference at $p \leq 0.05$, (B) Uptake flux of Ce for 24 h, 7d, and 15 d. Values are mean ± SE (n=4).

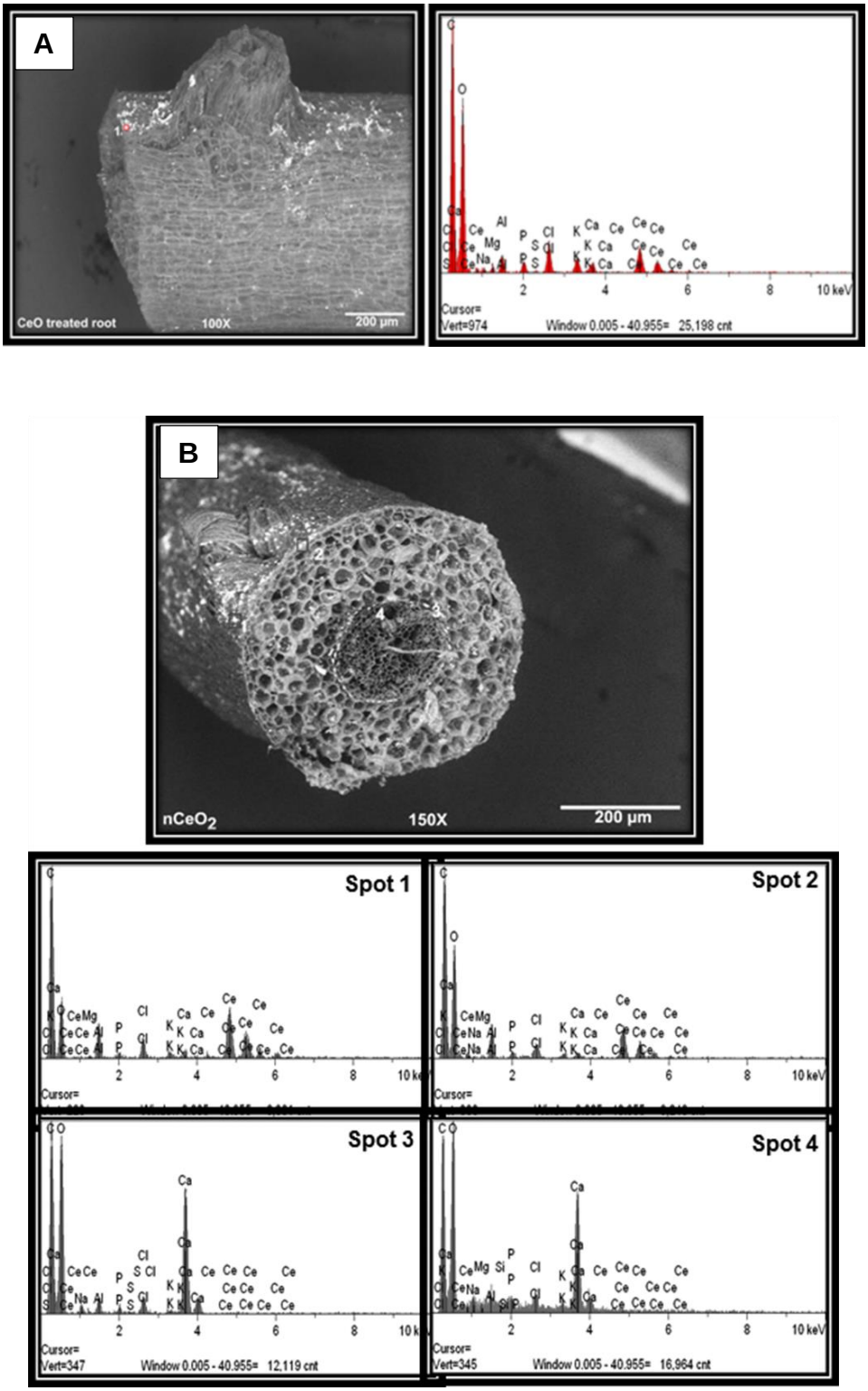

Figure 2.4. (A) SEM image of the root surface of a kidney bean plant exposed to 500 mg $n$$CeO_2$/L for 15 days, (B) SEM image of transverse section of the exposed root.

2.3.3 Localization and in situ speciation of *n*CeO_2

SEM-EDS was performed in the roots to localize Ce, but due to homogeneous distribution of Ce per unit area, strong detectable signals were not attained in the tissues. However, as seen in Figure 2.4, they were found to smear on root surface and in some sections inside the epidermal cells.

μ-XRF/μ-XANES are very powerful techniques for mapping elements and studying coordination chemistry, even at low concentrations (few mg/kg) due to the brilliance provided by the synchrotron source [42]. Recently, these techniques have been used to detect *n*CeO_2 in corn [25] and cucumber [43]. Figure 2.5A shows an optical image of a 500 mg *n*CeO_2/L exposed root cross-section and Figure 2.5B shows the trielemental μ-XRF map of a selected area from the cross-section. Figure 2.5C-E presents the temperature map of epidermal and vascular regions of Ce-L^{III} fluorescence line. As shown in Figure 2.5B-E, Ce was detected in the root hairs, epidermal cells, cortical cells, and the vascular region. The evidence of Ce in the vascular tissues (Figure 2.5B-D) supports the translocation of Ce to aerial tissues measured by using ICP-OES (Figure 2.6A). Zhao *et al.* previously reported that Ce follows an apoplastic movement in corn roots [25]. In Figure 2.5B-C, Ce signals were not detected in the root endodermis, corroborating previous studies and suggesting that Ce does not enter the root symplast. Any ion/molecule that reaches the endodermis either through apoplast or symplast, has to finally enter the symplast to reach the stele, as the Casparian strip in the endodermis restricts apoplastic transport [40]. Figure 2.5B indicates that Ce crosses or bypasses the waxy Casparian strip barrier and enters into the root xylem. Secondary roots develop anatomically from the layer of cells just inside the endodermis, called pericycle, and they are thus a direct route into the vascular tissues without entering the symplast [44]. As observed in Figure 2.5B-D, a strong Ce signal was obtained in the vascular tissues connecting the secondary root, demonstrating the transport of Ce through the region devoid of Casparian strip. This suggests that Ce diffuses through the gaps in the Casparian strip at the point of emergence of the secondary root.

To determine if nCeO$_2$ retained their chemical form, μ-XANES was performed on the root sections. Figure 2.5F shows the Ce L^{III} edge μ-XANES spectra acquired in the root epidermis. The Ce intensity in the vascular region was too low (650 cps) to perform μ-XANES. Spectra from several (n=4) spots on the root epidermis were averaged and analyzed by linear combination fitting (LCF). Fitting results showed that the oxidation state of Ce was slightly modified in the root epidermis. Typical double white line feature at 5729 and 5737 eV in the spectra from the analyzed spots in the epidermis represent a signature for Ce(IV) oxidation state and fits 88% as nCeO$_2$. However, the slight difference in the spectra was attributed to biotransformation of Ce(IV) to Ce(III), resulting in 12% fit with Ce(III) acetate. The reference compounds Ce(III) acetate and Ce(IV) hydroxide were used as a representative of respective oxidation states of Ce, identified by their characteristic white line features, and they do not necessarily represent the Ce compound(s) in the root sections. This indicates that a fraction of Ce(IV) in nCeO$_2$ or on the surface of their aggregates was reduced to Ce(III). This could be due to the reducing environment (pH 5.8) of the NS and the acidic nature of the root exudates (rich in organic acids, fatty acids, and carbonyl compounds) [45]. The redox modification at the surface of nCeO$_2$ lattice (Ce^{4+}/Ce^{3+}) at the nano-bio interface is a very interesting phenomenon. The standard reduction potential of nCeO$_2$ (Ce^{4+}/Ce^{3+}) (Eh= 1.15V, in water) is significantly higher than the biologically active redox couples (Eh= -0.38 to +0.34 V), which favors the reduction of Ce(IV) on the surface of nCeO$_2$ lattice [10]. Slight modifications of nCeO$_2$ has been previously reported in root tissues of cucumber [43] and corn [25], supporting our findings. In cucumber tissues, nCeO$_2$ was reported to exist in its original configuration as Ce(IV), but a small fraction was transformed to Ce(III), showing the best fit with CePO$_4$ and Ce(CH$_3$COO)$_3$ [43].

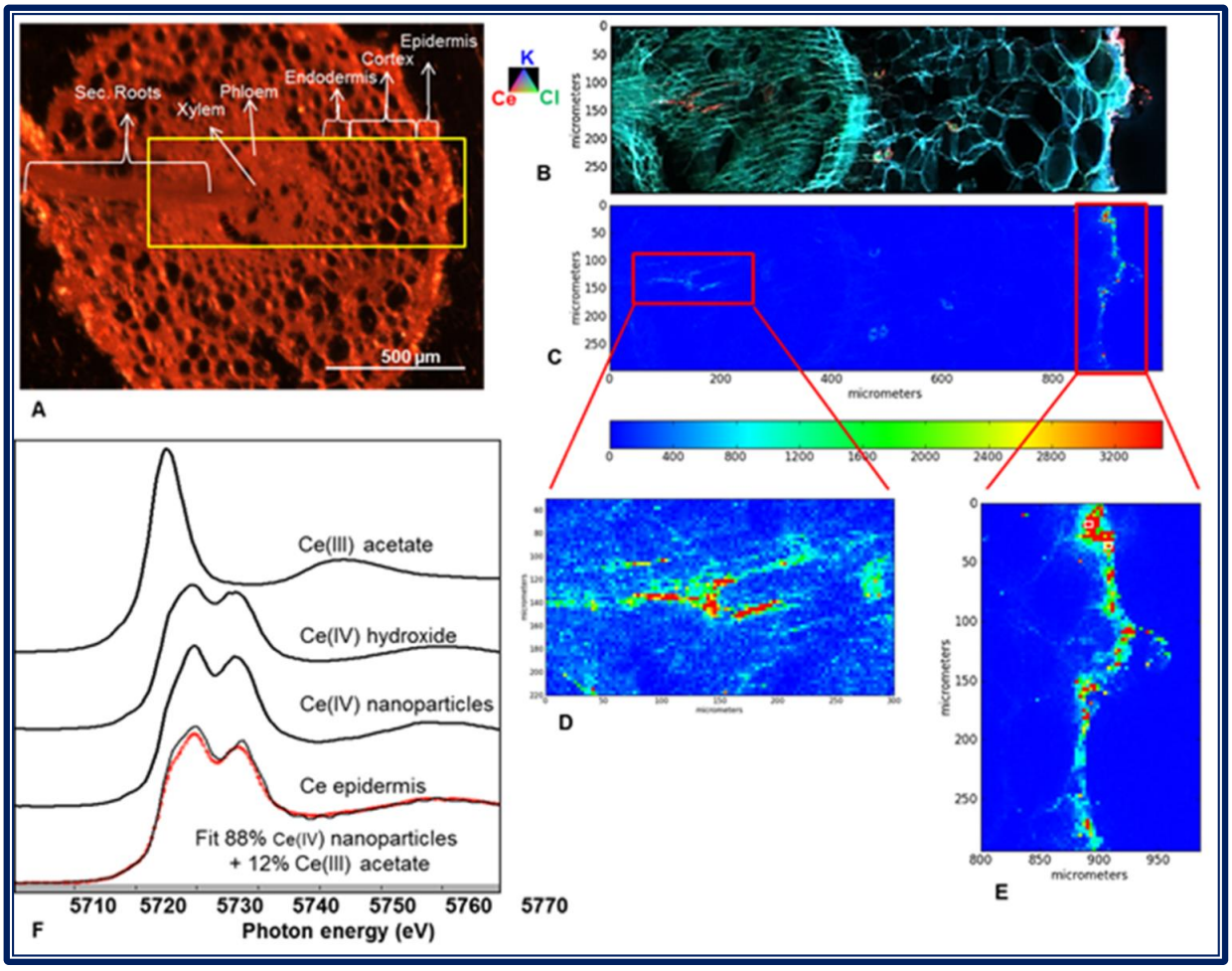

Figure 2.5. Synchrotron images of a transverse section of kidney bean roots exposed to 500 mg/L *n*CeO_2. (A) Optical image of the root cross section, (B) Tricolor µ-XRF map of the selected area from the cross section (red = Ce, green = Cl, blue = K, (C) µ-XRF temperature map of the selected region, showing normalized Ce intensity; red represents higher Ce intensity, and dark blue represents the absence of a Ce signal. (D) Temperature map of Area1 (vascular region), (E) Temperature map of Area 2 (epidermis). (F) Ce L(III) µ-XANES from root epidermis (solid, black) and the spectra from the linear combination fitting (dotted, red).

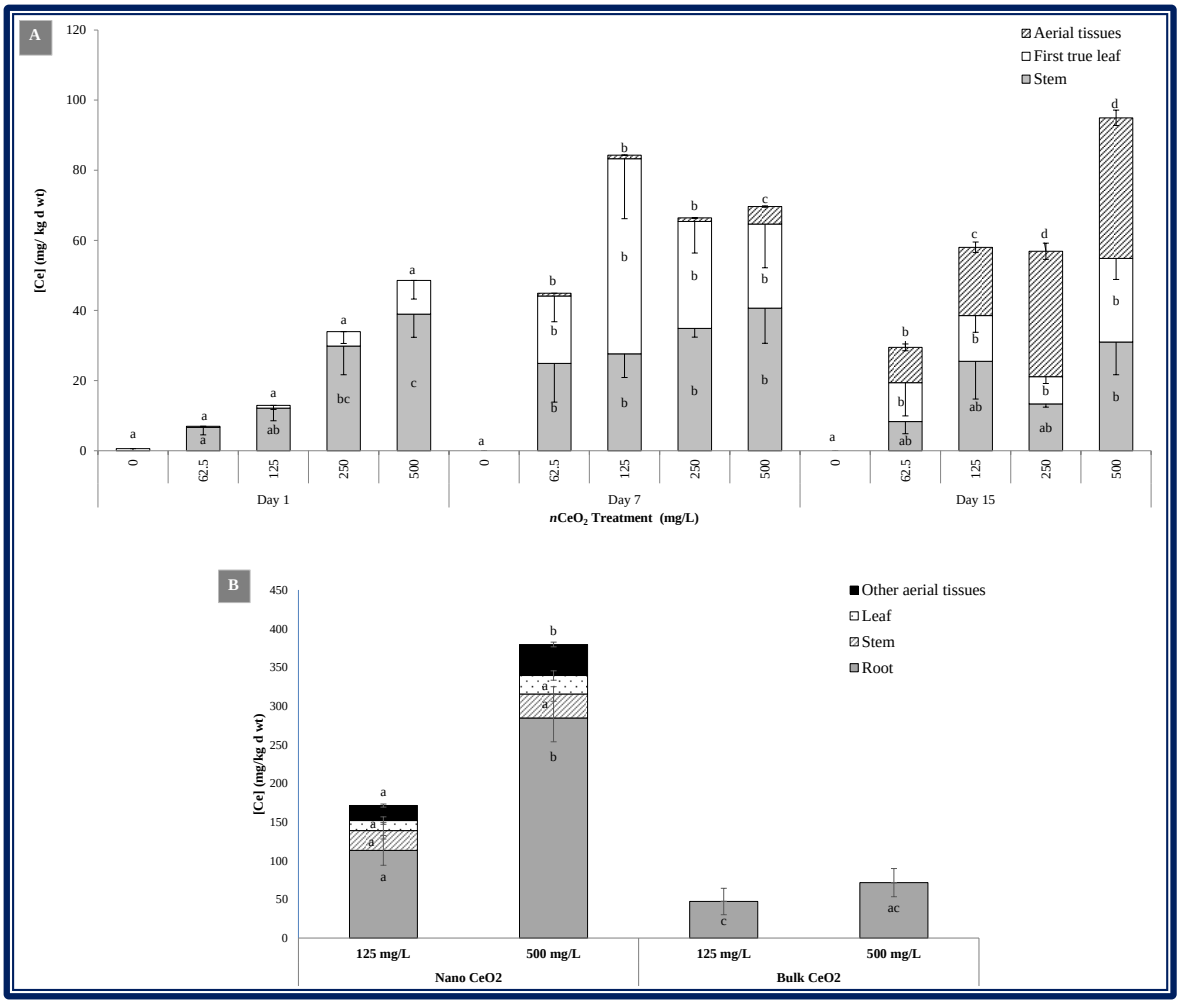

Figure 2.6 (A) Ce concentration in aerial parts of kidney bean plants exposed to 0- 500 mg/L *n*CeO_2 for 1, 7 and 15 days. (B) Comparison of Ce concentration in different parts of plants exposed to 125 and 500 mg/L of *nano* CeO_2 and *bulk* CeO_2 for 15 days. Values for roots are a tenth of actual concentration. Values are expressed as mean ± SE (n=4). Bars with different letters within same exposure duration represent significant difference at $p \leq 0.05$.

2.3.4 Translocation of cerium to aerial parts

The Ce concentrations in the aerial parts of *n*CeO_2 exposed kidney bean plants are shown in Figure 2.6A. Cerium was translocated to aerial parts in all the treatments, reaching up to 40.7 mg/kg in stems (500 mg *n*CeO_2/L) and 55.7 mg/kg in leaves (125 mg *n*CeO_2/L) after seven DE. Ce translocation corroborates with previous studies in cucumber [38,43] and corn [25]. For each exposure treatment, Ce concentration in roots and stems did not significantly increase with time. But, simultaneously the plants showed an increase in Ce accumulation in farther aerial tissues with

time. This may be due to the transfer of Ce from the lower tissues to the aerial parts with increasing growth. Upon prolonged exposure (15 days), the rate of translocation significantly increased. For example, at 500 mg *n*CeO_2/L, the aerial tissues accumulated significantly more Ce after 15 DE, compared to one ($p \leq 0.003$) and seven ($p \leq 0.005$) DE. This explains the decrease in Ce concentration in roots with exposure duration. Ce concentrations in the first true leaves harvested after seven DE, were significantly higher than at one DE in all the treatments (Figure 2.6A). However with longer exposure (15 days), the Ce accumulation in the first true leaves decreased significantly (125 mg/L, $p \leq 0.003$; 250 mg/L, $p \leq 0.001$). This trend in the decrease of Ce accumulation in first true leaf and increase in the farther aerial tissues suggests phloem transport. On an interesting note, Ce was not detected in any aerial tissues of the plants exposed to *b*CeO_2 for 15 days, which indicates immobility of the bulk forms inside the plant (Figure 2.6B).

2.3.5 Effects on plant biomass, leaf chlorophyll and soluble protein content

In this study, no apparent signs of toxicity such as stunted growth, mortality, chlorosis, or wilting were observed. Dry biomass of plant tissues exposed to *n*CeO_2 and *b*CeO_2 is shown in Table 2.2. After one DE, plants treated with 500 mg *n*CeO_2/L had significantly more biomass with respect to control, which demonstrates positive physiological response. Such positive response has also been reported in soybean, where the root growth was enhanced upon *n*CeO_2 exposure [18]. After seven DE, only the leaves of plants treated with 500 mg *n*CeO_2/L showed significant increase in biomass with respect to control and other treatments. However, after 15 DE, there were no significant effects on the biomass production. No prominent effects on biomass upon exposure to *n*CeO_2 for more than eight days have been previously reported in cucumber [38], tomato [14], and soybean [15]. Contrary to *n*CeO_2 treatments, 125 and 500 mg *b*CeO_2/L treatments significantly increased the root biomass (24 and 26%, respectively) and decreased the stem biomass (66 and 58%, respectively) (Table 2.2) compared to control. The decrease in stem biomass corroborates with the increase in oxidative stress in stems as discussed in the following section. No significant impact on the total chlorophyll content (chlorophyll *a* and *b*) in the leaves of plants exposed to

nCeO_2 for 15 days, with respect to control was observed (Figure 2.7). This corroborates with a previous study on corn exposed to 800 mg *n*CeO_2/kg [16]. However, in germinating rice, 125 and 250 mg *n*CeO_2/L significantly reduced the chlorophyll content. Lack of any prominent negative physiological response in kidney beans on exposure to *n*CeO_2 could be due to the chemical stability of *n*CeO_2, which prevents the dissolution of Ce(IV)/ Ce(III) species and their reactivity to the major metabolic processes.

In this study, *n*CeO_2 exposure for seven days did not affect the total soluble protein content in the tissues (Figure 2.8A). Interestingly, plants exposed to 500 mg *n*CeO_2/L for 15 days had significantly higher protein ($p \leq 0.014$) in roots (27.8 mg/g) as compared to control (9.2 mg/g). This may be due to expression of new stress proteins to counteract the effects of *n*CeO_2 residence in the tissues for longer period. Shyam *et al.* have reported that cerium nitrate [$Ce(NO_3)_3.6H_2O$, at 446.03µM Ce] increased the proline content in cowpea plants (*Vigna unguiculata*) [46]. Neto *et al.* reported increase in the corn root proline content in response to salt stress [47]. Expression of new stress protein isoenzymes in response to drought conditions has also been reported [48]. Conversely, the protein content in leaves of *b*CeO_2 exposed plants decreased significantly with respect to control and the *n*CeO_2 treatments (Figure 2.9). This can be due to increased oxidative stress expressed by increased GPOX activity in the leaves of 125 and 500 mg *b*CeO_2/L treated plants (Figure 2.11). Further studies on proteomics are required for a better understanding of the molecular mechanisms.

Table 2.2. Dry biomass weight (g) of different tissues of kidney bean plants exposed to *nano* and *bulk* CeO_2

Treatment (mg/L)	Roots			Stems			First true leaf		
	D1	D7	D15	D1	D7	D15	D1	D7	D15
Control	0.120 ± 0.01^{a}	0.259 ± 0.03^{a}	0.214 ± 0.00^{a}	0.045 ± 0.01^{a}	0.082 ± 0.01^{a}	0.154 ± 0.03^{a}	0.039 ± 0.01^{a}	0.175 ± 0.02^{a}	0.156 ± 0.02^{a}
62.5 *n*CeO_2	0.169 ± 0.02^{ab}	0.290 ± 0.03^{a}	0.210 ± 0.00^{a}	0.049 ± 0.00^{a}	0.119 ± 0.01^{a}	0.177 ± 0.02^{a}	0.029 ± 0.00^{a}	0.178 ± 0.02^{a}	0.219 ± 0.01^{a}
125 *n*CeO_2	0.121 ± 0.02^{a}	0.281 ± 0.04^{a}	0.215 ± 0.01^{a}	0.043 ± 0.00^{a}	0.116 ± 0.02^{a}	0.184 ± 0.01^{a}	0.026 ± 0.00^{a}	0.192 ± 0.03^{a}	0.211 ± 0.02^{a}
250 *n*CeO_2	0.136 ± 0.02^{ab}	0.272 ± 0.04^{a}	0.213 ± 0.00^{a}	0.054 ± 0.01^{a}	0.081 ± 0.00^{a}	0.181 ± 0.03^{a}	0.027 ± 0.01^{a}	0.171 ± 0.01^{a}	0.203 ± 0.03^{a}
500 *n*CeO_2	0.234 ± 0.03^{b}	0.355 ± 0.03^{a}	0.208 ± 0.00^{a}	0.126 ± 0.01^{b}	0.098 ± 0.02^{a}	0.154 ± 0.02^{a}	0.179 ± 0.04^{b}	0.232 ± 0.04^{b}	0.140 ± 0.04^{a}
125 *b*CeO_2			0.267 ± 0.09^{b}			0.052 ± 0.01^{b}			0.218 ± 0.06^{a}
500 *b*CeO_2			0.271 ± 0.06^{b}			0.064 ± 0.01^{b}			0.248 ± 0.02^{a}

Values are expressed as mean ± SE (n=4). The values superscripted with same letter within same exposure duration (each column) and similar plant parts are not significantly different at $p \leq 0.05$.

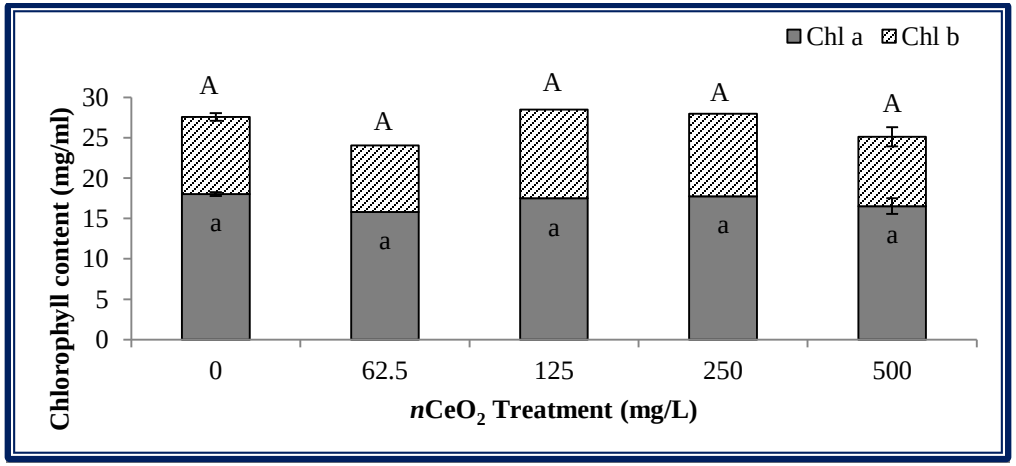

Figure 2.7. Chlorophyll content in the kidney bean leaves exposed to *n*CeO_2 for 15 days. Values are expressed as mean ± SE (n=4). Bars with different letters within same exposure duration represent significant difference at $p \leq 0.05$.

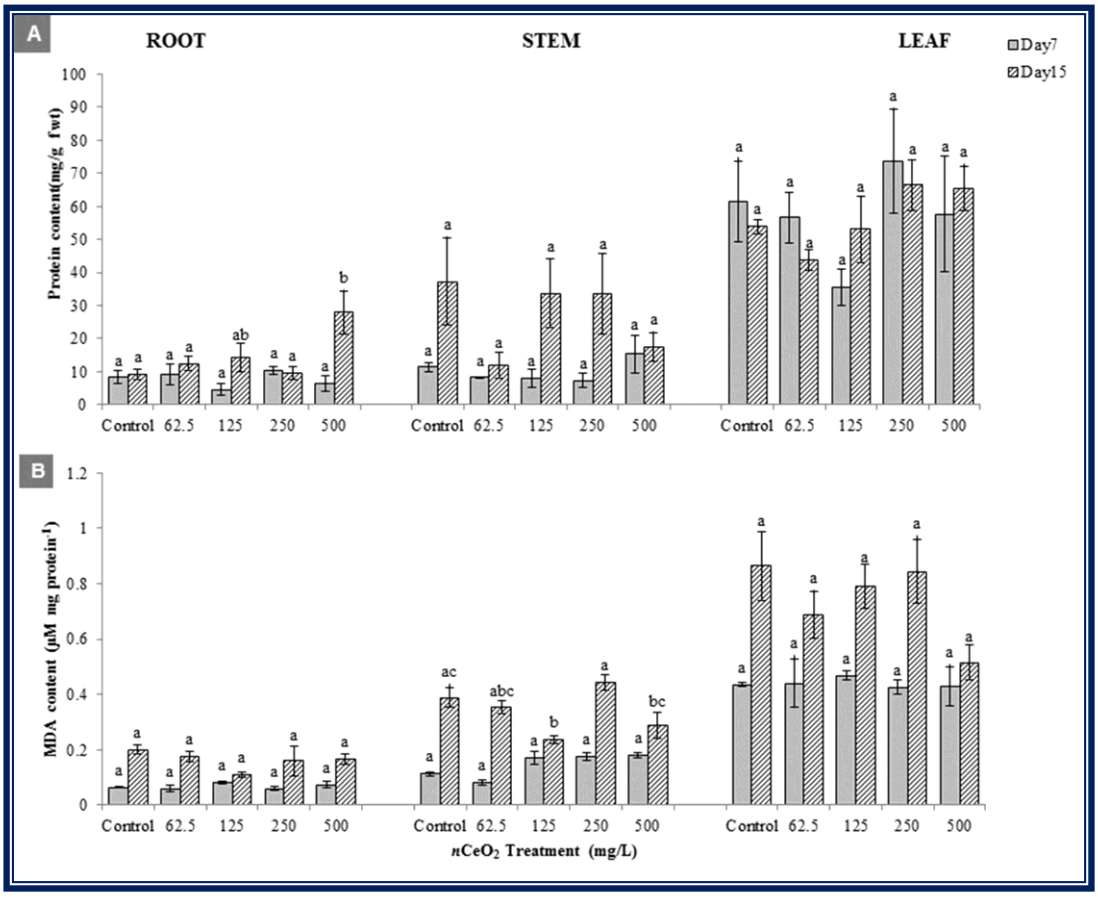

Figure 2.8. (A) Total soluble protein content in different parts of kidney bean plants exposed to *n*CeO_2 for 7 and 15 days, (B) Lipid peroxidation in different parts of kidney bean plants exposed to *n*CeO_2 for 7 and 15 days. Values are mean ± SE (n=4). Bars with different symbols within same exposure duration represent significant difference at $p \leq 0.1$.

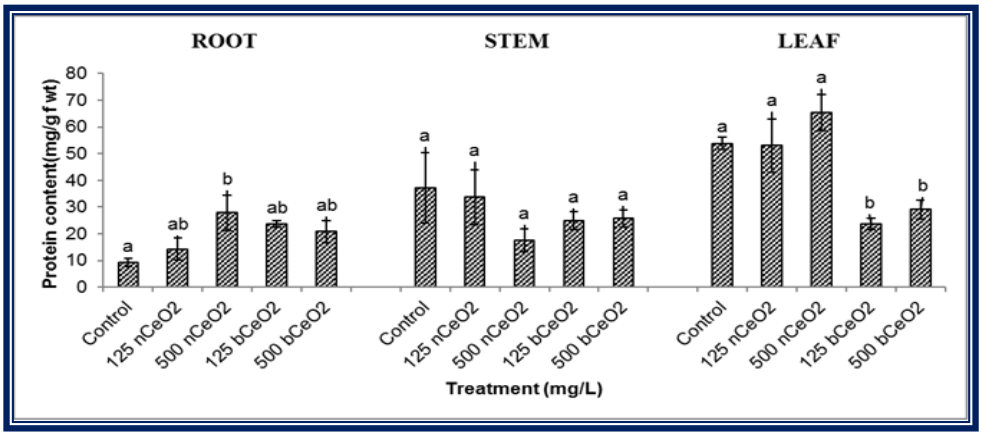

Figure 2.9. Total soluble protein content in different parts of kidney bean plants exposed to 125 and 500 mg/L of *nano* and *bulk* CeO_2 for 15 days. Values are expressed as mean ± SE (n=4).Bars with different letters within same exposure duration represent significant difference at $p \leq 0.1$.

2.3.6 Oxidative stress response

In plants, reactive oxygen species (ROS) are continuously produced in mitochondria, chloroplasts, and peroxisomes, due to aerobic metabolic processes [49]. Although plant cells are equipped with mechanisms to scavenge ROS, the equilibrium can be disturbed under oxidative burst caused by abiotic stress. Lipid peroxidation is considered as an indicator of over-production of ROS, as polysaturated fatty acids in membrane phospholipids are a preferred target for ROS [49]. Catalase, APOX, and GPOX play an important role to quench H_2O_2 in tissues by oxidizing their respective substrates.

The MDA content representing lipid peroxidation and the major antioxidant enzyme activities in the tissues of *n*CeO_2 exposed plants are shown in Figure 2.8B and 2.10, respectively. After seven DE, 250 mg *n*CeO_2/L treated roots showed a significant increase in APOX activity ($p \leq 0.079$) compared to control (Figure 2.10). In stems, the GPOX activity significantly increased at 125 mg *n*CeO_2/L with respect to control ($p \leq 0.03$), and none of the treatments affected the leaf enzyme activities after seven DE. As seen in Figure 5B, seven DE to *n*CeO_2 did not enhance lipid peroxidation, suggesting no oxidative burst in the tissues. Similar responses were reported in corn exposed to soil amended with *n*CeO_2 [50]. The results suggest that upon short-term exposure, APOX and GPOX in the plant tissues help to combat the oxidative stress by balancing the ROS production and scavenging processes. This is in contrast with Rico *et al.*, where a decrease in CAT, GPOX, APOX, and glutathione reductase (GR) activities in the shoots of rice seedlings treated with 125 mg *n*CeO_2/L was reported after ten days [13].

After 15 DE, the activity of CAT and GPOX in the roots showed a sharp decrease compared to control in all the treatments, except GPOX activity at 250 mg *n*CeO_2/L treatment. Although the APOX activity decreased in all the treatments with respect to control, it became significant only at 500 mg *n*CeO_2/L ($p \leq 0.078$). CAT activity has been reported to decrease in rice roots exposed to lower concentrations of *n*CeO_2 [13]. Decreased enzyme activities in mesquite (*Prosopis juliflora-velutina*) roots were also observed in response to *n*ZnO (500-4000 mg/L) exposure [22]. The decreased enzyme activities in the roots could be due to the ROS scavenging ability of *n*CeO_2

[15,51]. Due to the low redox potential of cerium oxide, the oxygen defects in *n*CeO_2 lattice structure are highly responsive to the surrounding pH [52]. The differential pH in the plant cellular environment (~7.5 in cytosol and ~ 5.5 in the extracellular and vacuolar spaces) allows the *n*CeO_2 to act as regenerative ROS quencher [53]. However, the decrease in the activities of all the major H_2O_2 quenching enzymes at 500 mg *n*CeO_2/L, with a simultaneous increase in the total soluble protein content, indicates a stress response to high concentrations of *n*CeO_2. Preliminary studies have shown that increasing *n*CeO_2 treatment resulted in decreasing iron content in the roots (data not shown). This suggests that *n*CeO_2 at higher exposure concentration may be competing with iron uptake, resulting in the down regulation of some major hemoproteins like CAT, APOX and GPOX. Further studies are being currently performed for a better understanding of the biochemical processes leading to such observations.

Unlike in roots, the enzyme activities in stems were not affected. On the other hand, the leaves' enzyme activities were affected by the *n*CeO_2 exposure. At 15 days, APOX activity was inhibited at 250 mg *n*CeO_2/L ($p \leq 0.057$), while GPOX was significantly higher at 62.5 mg/L ($p \leq 0.046$) and at 125 mg/L ($p \leq 0.077$), respect to control. At the same time, no significant changes were observed in lipid peroxidation, which suggests effective quenching of ROS by GPOX. Conversely, increased lipid peroxidation was reported in shoots of germinating rice exposed to 500 mg *n*CeO_2/L [13]. This variation could be due to the exposure conditions, plant species, or the stage of the plants. In the current study, 15 day-old plants were exposed to *n*CeO_2 unlike the more sensitive germination stage [54].

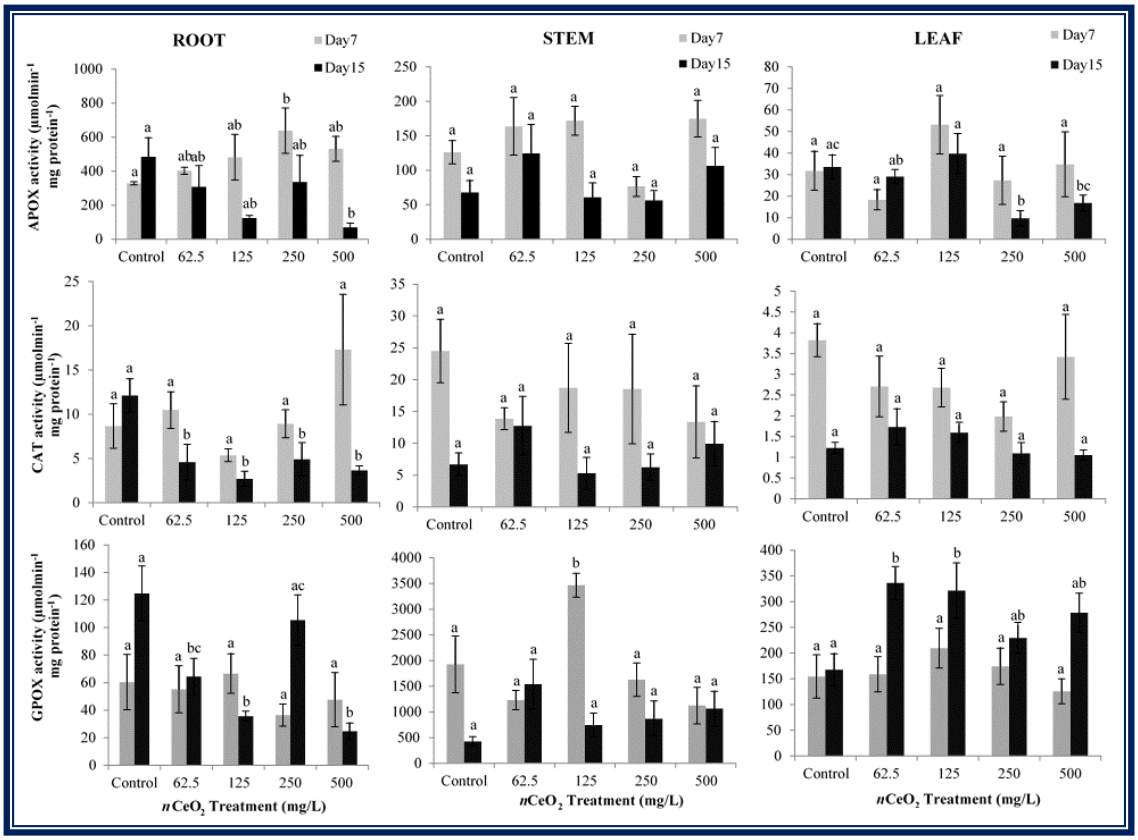

Figure 2.10. Specific activity of antioxidant enzymes, ascorbate peroxidase (APOX), catalase (CAT), and guaiacol peroxidase (GPOX) in different parts of kidney bean plants exposed to 0 to 500 mg nCeO$_2$/L. Values are mean ± SE (n=4). Bars with different symbols within same exposure duration represent significant difference at $p \leq 0.1$.

Contrary to the response to nCeO$_2$ treatments, in plants treated with 125 mg bCeO$_2$/L, APOX and CAT activities in the roots were unaffected, although root APOX activity significantly increased at 500 mg bCeO$_2$/L with respect to control ($p \leq 0.015$) as well as nCeO$_2$ treatments ($p \leq 0.001$), demonstrating oxidative stress (Figure 2.11). However, GPOX activity in the roots showed sharp decrease with respect to control, similar to nCeO$_2$ treatments. In stems, although nCeO$_2$ did not affect the enzyme activities, on exposure to bCeO$_2$, APOX, CAT, and GPOX experienced significant enhanced activities compared to control (Figure 2.11), which explains decreased biomass in those tissues (Table 2.2). In the leaves of bCeO$_2$ exposed plants, CAT and GPOX activities were significantly stimulated with respect to control and nCeO$_2$ treatments. This suggests that kidney bean plants are more tolerant to nCeO$_2$ compared to bCeO$_2$.

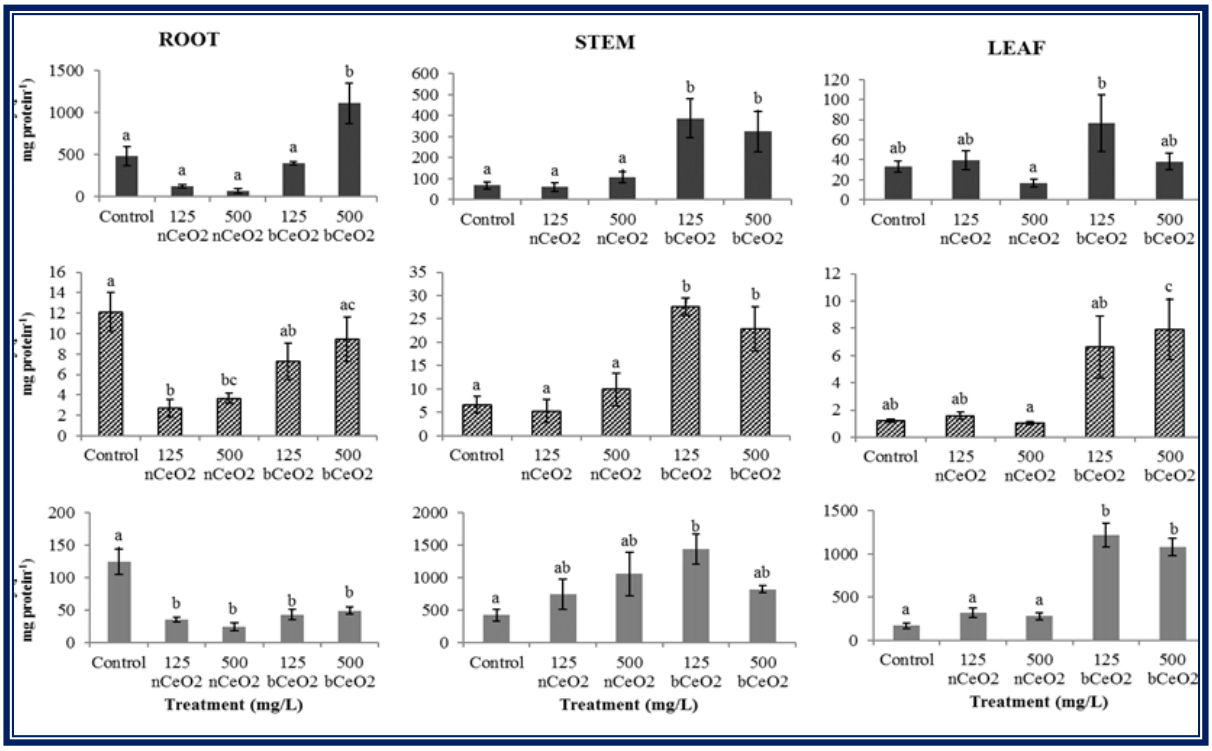

Figure 2.11. Comparative effects of *bulk* and *nano* CeO_2 on the specific activity of major antioxidant enzymes in the *P. vulgaris* roots, stems and leaves. Values are expressed as mean ± SE (n=4). Bars with different letters within same exposure duration represent significant difference at $p \leq 0.1$.

2.4 Conclusion

In this study, spectroscopic analyses suggest that *n*CeO_2 enter kidney bean roots passively, through the gaps in Casparian strip at the emergence of secondary roots. Transport of Ce through xylem and phloem to aerial tissues increased with exposure duration. Kidney bean plants were found to tolerate and effectively defend the oxidative stress imposed by *n*CeO_2 exposure, irrespective of the duration. The root enzyme activities were drastically reduced on prolonged *n*CeO_2 exposure; however, GPOX increased in leaves suggesting this enzyme is responsible for quenching the ROS. Upon prolonged exposure to high concentration (500 mg *n*CeO_2/L), the roots demonstrated stress response by increase in soluble protein content by 204% and subduing the antioxidant enzyme activities [55]. Further studies at molecular level are required to understand whether the decreased enzyme activity is attributed to the redox cycling of *n*CeO_2 or downregulation of genes associated with oxidative stress.

CHAPTER 3

Influence of soil organic matter on cerium translocation, physiology and metabolism of kidney bean plants upon nanoceria exposure

3.1 Introduction

The fate of engineered nanoparticles (ENPs) in the environment depends on their physicochemical properties as well as the mechanistic of the environmental matrices. Recent risk assessment modelling studies have assessed that a large fraction of the released ENPs during production, use, and disposal, finally accumulate in landfills, soils, sediments or biosolids [1,2]. This raises serious concern due to the possibility of translocation of ENPs from the soils to plants and eventually bioaccumulation in the food chain [3,4], or leaching to the groundwater [5]. However, the interaction between the ENPs and the soil matrix is largely dependent on the soil composition and nature, as they decide the aggregation, transformation, bioavailability and migration of nanoscale colloids in the porous media. In previous studies, presence of organic acids like humic and fulvic acids in aqueous solutions have been shown to stabilize the metal oxide ENPs [6,7] due to enhanced charge and/or steric effects [5]. This prevents aggregation of these ENPs, possibly leading to their prolonged dispersion in the soil pore water, which in turn may enhance the possibility of increased mobility of ENPs in groundwater and also through plant roots. Other properties like pH, ionic strength, porosity also affect the behavior of the ENPs in the soil. Despite of increasing research on the interaction of organic acids and ENMs, there have very few investigations addressing on how the variability in their content in the soil under natural conditions, may affect the interactions at the nano-bio interface. Recently, Collins *et al.* reported that humic acids coated nanoceria (*n*CeO_2) decreased Ce bioaccumulation and toxicity in a model soil organism, *Caenorhabditis elegans* [8]. Previous studies have shown that *n*CeO_2 is capable of being taken up by plant roots with minimal biotransformation into Ce(III) compounds [9,10]. In corn plant, lower Ce translocation to aerial tissues was observed in organic matter rich soil compared to natural unenriched soil amended with bare as well as alginate coated *n*CeO_2 [12]. In soil based

studies, *n*CeO_2 were found to be non-detrimental in terms of plant physiology [13,14], whereas negatively affected the yield [13,14] and nitrogen fixation in soybeans [14].

To the best of the authors' knowledge, there are no reports investigating the effects of soil properties on the toxicological effects of *n*CeO_2 on plants. In this study, response of *n*CeO_2 on the plant physiology and metabolism were examined upon exposure for 52 days in soils varying in physicochemical properties. Uptake of Ce and further translocation to aerial parts were analyzed using ICP-OES, with soil type and *n*CeO_2 concentrations as the factors. Leaf area and content of photosynthetic pigments were measured. Physiological and metabolic processes undergoing in leaves like photosynthesis, transpiration and stomatal conductance were assessed upon *n*CeO_2 exposure.

3.2 Materials and Methods

3.2.1 Soil characterization and nanoceria addition

Two types of soils were used in this study, low organic matter soil (LOMS) and organic matter enriched soil (OMES). Natural sandy loam soil (64% sand, 31% silt, 5% clay) collected from an agricultural field in Fabens, TX (N 31° 29' 02.1", W 106° 08' 27.2", elevation 1102 meters, mineral horizon, depth 55 cm) was considered as LOMS [15]. LOMS was enriched with Miracle-Gro potting mix at 2:1 (v/v) ratio to prepare OMES.

Previously characterized *n*CeO_2 (≈8 nm, Meliorum Technologies, Rochester, NY) were procured from The University of California Center for Environmental Implications of Nanotechnology (UC-CEIN). *n*CeO_2 were nanorods measuring (67 ± 8) nm × (8 ± 1) nm, (≤10% polyhedra: 8 ± 1 nm) with 95.14% purity and surface area of 93.8 m^2g^{-1}[16]. Suspensions of *n*CeO_2 were prepared in 250 mL of Millipore water (MPW) by 30 min bath sonication (Crest Ultrasonics, Trenton, NJ, USA) at 25°C. The suspensions were diluted to 600 ml and mixed homogeneously with the soils to prepare final concentrations of 62.5, 125, 250, 500 mg/kg *n*CeO_2 in 4 and 3 kg of LOMS and OMES, respectively. Soils mixed with MPW served as the untreated control. Homogenously

mixed soils were placed in 7 1/2" dia. x 6" H plastic pots and were allowed to equilibrate for 24 h. Treatments were performed in quadruplicates.

Untreated and treated LOMS and OMES were air-dried, homogenized and sieved through 2 mm mesh prior to characterization. Soil pH in water and $CaCl_2$, and electrical conductivity (EC) was measured using Hanna Instruments HI 9813-6 Portable pH/EC/TDS/Temperature Meter. Cation exchange capacity (CEC) was measured by EPA Method 9081[17]. Nitrogen content in the soils were determined using Kjeldahl method using a digestion and distillation unit (Labconco Co., Kansas city) Labconco, Kansas city, USA and expressed as % N (NTK) [18,19]. Organic matter content of LOMS and OMES was determined by loss on ignition method, and the Ce content in the aqua-regia digested soils were determined using ICP-OES. Characteristics of untreated and *n*CeO_2 treated soils have been provided in Table 3.1.

3.2.2 Exposure conditions

Kidney bean (*Phaseolus vulgaris* var. Red Hawk) seeds were provided by Dr. James Kelly, Michigan State University were washed with 2% sodium hypochlorite and MPW, and soaked in MPW for a day. A total of 15 kidney bean seeds were planted per pot at one inch depth from the surface, and the pots were placed in controlled condition in a growth chamber (Environmental Growth Chamber, Chagrin Falls, OH) with 14 h photoperiod (340 µmole $m^{-2}s^{-1}$), 25/20°C day/night temperature and 65-70% relative humidity for 7 days. Germination of the seeds was noted and the pots were transferred to greenhouse with similar conditions upon the appearance of the cotyledonous leaves for 45 days. The plants were watered with 200 mL MPW every day until the appearance of the first true leaves (15 days after planting, DAP). The watering was then increased to 400 mL throughout the life cycle of the plants.

3.2.3 Root uptake of Ce and aerial translocation

Composite of two plants from each replicate were used to determine Ce accumulation in the different tissues of the plant. The roots were carefully washed three times with 0.1% plasma

pure HNO_3 and MPW. The whole plant was then severed into roots, stems, and true leaves, which were dried at 70°C for 96 h. Dried roots and leaves were digested in a mixture of plasma pure HNO_3 and 30% (w/v) H_2O_2 (1:4) using microwave accelerated reaction system (CEM $Mars_x$, Mathews, NC) according to Packer *et al.*[20]. Accumulation of Ce was analyzed in the digested samples using ICP-OES. Blanks, spikes and certified standard reference material (NIST-SRM 1547, Gaithersburg, MD) were analyzed to validate the digestion process and spectroscopic analysis, obtaining 95% recovery. Also, 0.5 mg/L multi-elemental standard was analyzed every 10 samples to monitor the matrix effect on the analytes and for quality assurance/quality control [11].

3.2.4 Measurement of leaf area and photosynthetic pigments

After 52 DAP, area of the first true leaf of three plants per pot was determined using LI-3100C area meter (LI-COR® Biosciences, Lincoln, NE). Photosynthetic pigments in the leaves were extracted in 80% acetone and chlorophyll *a,b*, and total carotenoids were measured as described by Lichtenthaler and Buschmann [21].

3.2.5 Monitoring of plant gas exchange activities

Leaf net photosynthetic rate (Pn), stomatal conductance (g_s), and transpiration (E) of one plant per replicate treatment were monitored after 52 DAP, by placing the fully expanded leaf in the cuvette of a portable gas exchange system (CIRAS-2; PP Systems, Amesbury, MA). Environmental conditions in the cuvette were controlled at a leaf temperature of 25°C, photosynthetic photon flux (PPF) of 1000 $\mu mol \cdot m^{-2} \cdot s^{-1}$, and CO_2 concentration of 375 $\mu mol \cdot mol^{-1}$. The data was recorded when environmental conditions and gas exchange parameters in the cuvette were stable. The plants were well watered to avoid water stress, and measurements were taken between 1000 and 1400 h.

3.2.6 Statistical analysis

Statistical analysis of the data were performed using one-way ANOVA followed by Tukey's multiple comparisons test based on a probability of $p \leq 0.05$, unless stated otherwise (IBM SPSS Statistics 19, Chicago, USA). All analyses were performed in triplicates.

3.3 Results and Discussion

3.3.1 Effect of *n*CeO_2 on soil properties

Table 3.1 shows the characteristics of the untreated and *n*CeO_2 amended LOMS and OMES. The organic matter content of LOMS and OMES were 4.22 and 10.09 %, respectively. In the OMES, humic and fulvic acids tend to form a coat around the nanoparticles, and stabilize them in the soil solution by electrostatic repulsion. This restricts the nanoparticles from aggregating and increases their mobility in the soil solution [5,7]. Whereas, in LOMS, the surface charges of the heterogeneous soil colloids allows the nanoparticles to aggregate and thereby restricts their ability to pass through the soil pores [6]. Soil pH, CEC and NTK were not affected upon addition of *n*CeO_2. Soil EC and TDS were increased significantly ($p \leq 0.05$) at all the nanoparticle treatments. The measurement of EC and TDS in the soils gives an indirect measurement of the salt content [22]. Nanoparticles have been used in various applications due to its ability to increase electrical conductivity [23]. Increase in EC and TDS signify an increase in the soil salinity which alters the soil fertility. Increased EC leads to poor water filtration and drainage thereby affecting plant health. On contrary, *n*CeO_2 application did not alter the CEC which measure the capacity of the soil to exchange cations like Al^{3+}, Ca^{2+}, Mg^{2+}, K^{+}, NH^{4+}, Na^{+} [22]. CEC of the OMES and LOMS was 43% higher than the LOMS due to the enrichment with organic matter, which increases the number of sites for exchange of the cations [22]. The actual concentration of Ce in the LOMS and OMES amended with 0-500 mg *n*CeO_2/kg are provided in Table 3.2. Untreated soils contain traces of cerium as it is a rare earth element and is present in soils naturally.

Table 3.1. Characteristics of the low organic matter soil (LOMS) and organic matter enriched soil (OMES) exposed to 0 - 500 mg/kg *n*CeO_2. Values are expressed as mean ± SE (*n*=4). Values with different letters represent significant difference at $p \leq 0.05$.

	Low organic matter soil (LOMS)					Organic matter enriched soil (OMES)				
***n*CeO₂ (mg/kg)**	**0**	**62.5**	**125**	**250**	**500**	**0**	**62.5**	**125**	**250**	**500**
Organic matter, loss on ignition (%)	4.22		-	-	-	10.09	-	-	-	-
pH (water)	7.92 ± 0.08a	7.98 ± 0.20a	7.88 ± 0.05a	7.68 ± 0.02a	7.95 ± 0.03a	7.28 ± 0.05a	7.00 ± 0.07a	6.90 ± 0.04a	6.83 ± 0.02a	6.98 ± 0.02a
pH ($CaCl_2$)	7.53 ± 0.05a	7.60 ± 0.04a	7.68 ± 0.02a	7.65 ± 0.03a	7.70 ± 0.00	7.05 ± 0.03a	7.03 ± 0.05a	6.93 ± 0.02a	7.13 ± 0.05a	6.98 ± 0.03a
Electrical conductivity	207.5 ± 4.8a	395.0 ± 60.8b	472.5 ± 11.1c	545.0 ± 38.6d	470.0 ± 9.1c	485.0 ± 35.7a	947.5 ± 21.7b	992.5 ± 19.7c	972.5 ± 34.5bc	982.5 ± 32.2bc
Total dissolved solid (mg/l)	92.5 ± 2.5a	190 ± 31.9b	227.5 ± 4.8b	262.5 ± 18.9c	230.0 ± 4.1b	240.0 ± 19.2a	470.0 ± 10.8b	492.5 ± 9.5c	482.5 ± 17.0bc	497.5 ± 20.6c
Cation exchange capacity (meq/100g)	23.3 ± 1.8a	21.6 ± 1.3a	26.2 ± 3.2a	23.8 ± 0.9a	22.4 ± 1.0a	33.1 ± 1.3a	33.4 ± 0.8a	36.9 ± 1.9b	34.4 ± 0.9ab	34.1 ± 0.9ab
Total kjeldahl N (%)	0.06 ± 0.002	0.07 ± 0.001	0.07 ± 0.001	0.07 ± 0.000	0.07 ± 0.002	0.09 ± 0.004	0.10 ± 0.002	0.11 ± 0.001	0.11 ± 0.001	0.11 ± 0.002

Table 3.2. Cerium content in the low organic matter soil (LOMS) and organic matter enriched soil (OMES) exposed to 0 - 500 mg/kg *n*CeO_2. Values are expressed as mean ± SE (*n*=4).

***n*CeO₂ (mg/kg soil)**	**LOMS**	**OMES**
0	38.3 ± 0.9	33.9 ± 1.0
62.5	79.7 ± 0.6	74.5 ± 0.6
125	119.6 ± 2.3	124.9 ± 3.5
250	214.8 ± 4.3	193.6 ± 4.2
500	386.3 ± 9.6	350.8 ± 27.4

3.3.2 Accumulation of cerium in the roots

Uptake and accumulation of Ce by the kidney bean roots exposed to LOMS and OMES amended with 0 - 500 mg $n$$CeO_2$/kg are shown in Figure 3.1. In both soils, the Ce accumulation in the roots increased significantly ($p \leq 0.05$) with respect to control with increasing $n$$CeO_2$ exposure. At 500mg/kg $n$$CeO_2$, roots accumulated 25 and 23 mg Ce/kg d wt in LOMS and OMES, respectively. The Ce accumulation in the kidney bean roots were significantly lower than that reported in corn (~60 mg/kg dwt), cucumber (551 mg/kg), and soybeans (175 mg/kg dwt) at similar $n$$CeO_2$ exposure concentrations (400-500 mg/kg $n$$CeO_2$) [12-14] The accumulation of Ce in roots from LOMS amended with 62.5, 125, 250 and 500 mg/kg $n$$CeO_2$ was 78, 43, 93, 9% higher than those grown in OMES, significant ($p \leq 0.05$) at 62.5 and 250 mg/kg $n$$CeO_2$.

In LOMS, the soil colloids tend to bind to the $n$$CeO_2$, leading to aggregation and larger size [5], and thereby reducing the mobility in the pore spaces. Thus, the $n$$CeO_2$ might either remain primarily incorporated in the root epidermal layers [11] or bound to root exudates, leading to higher accumulation in the roots. On the other hand, in OMES, the organic matter stabilizes the $n$$CeO_2$ in the pore spaces and they remain dispersed maintaining their nanoparticulate size or small aggregates [6,7]. This enables the $n$$CeO_2$ to cross the barriers and reach the vascular tissues, enabling increased translocation (Figure 3.1B). In contrary, Zhao *et al.* reported lower root accumulation of Ce in the unenriched soil compared to enriched soil [12].

3.3.3 Translocation of cerium from roots to leaves

Concentration of Ce in the leaves of plants grown in LOMS and OMES amended with 0-500 mg/kg $n$$CeO_2$ has been provided in Figure 3.1B. In the control plants of LOMS and OMES, 0.16 and 0.13 mg/kg of Ce was detected in the leaves, respectively. With increasing $n$$CeO_2$ concentration (125-500 mg/kg $n$$CeO_2$) in LOMS and OMES, the accumulation of Ce in the leaves increased by 49, 134, 408 % and 101, 175, 608%, respectively, with respect to control. The Ce content in the leaves from plants grown in LOMS and OMES amended with 500 mg/kg $n$$CeO_2$ reached 0.66 and1.33 mg Ce/kg d wt. tissue. Unlike lower accumulation in the kidney bean roots,

the Ce content in the leaves of *n*CeO_2 exposed plants were higher or similar to reported values in soybean (0.000247 mg/kg) and cucumber (1.72 mg/kg) plant at 400-500 mg/kg *n*CeO_2. This shows that kidney bean plants are able to translocate Ce better than soybeans or cucumber [13,14]

Translocation of Ce to the kidney bean leaves was 65, 44, 71% higher in OMES, than LOMS at 125, 250 and 500 mg/kg *n*CeO_2 treatments. As noted in the previous section, Ce accumulation was higher in the *n*CeO_2 amended LOMS roots than OMES roots. This provided clear evidence that organic matter makes *n*CeO_2 more bioavailable and mobile to the plants due to better dispersion and stabilization of the particles in the porous media [7]. Several studies have shown that natural organic matter enables the disagglomeration of the metal oxide nanoparticles like *n*CeO_2 and titanium dioxide [6, 24]. The negative charges present due to the hydroxyl and carboxylate groups on the surface of organic matter tend to form a layer over the nanoparticles, leading to electrostatic repulsion between the individually coated particles due to similar surface charge. This explains the lower concentration of Ce in *n*CeO_2 amended OMES roots than LOMS. However, in corn, it has been suggested that the carboxylate and phenolate groups in the humus bind to the *n*CeO_2 leading to lower translocation in presence of higher organic matter [12]. In a soil organism, *C. elegans,* humic acid coated *n*CeO_2 also decreased Ce bioaccumulation in their tissues [8]. This disparity of previous reports with the current observations could be due to differential response by different organisms or species.

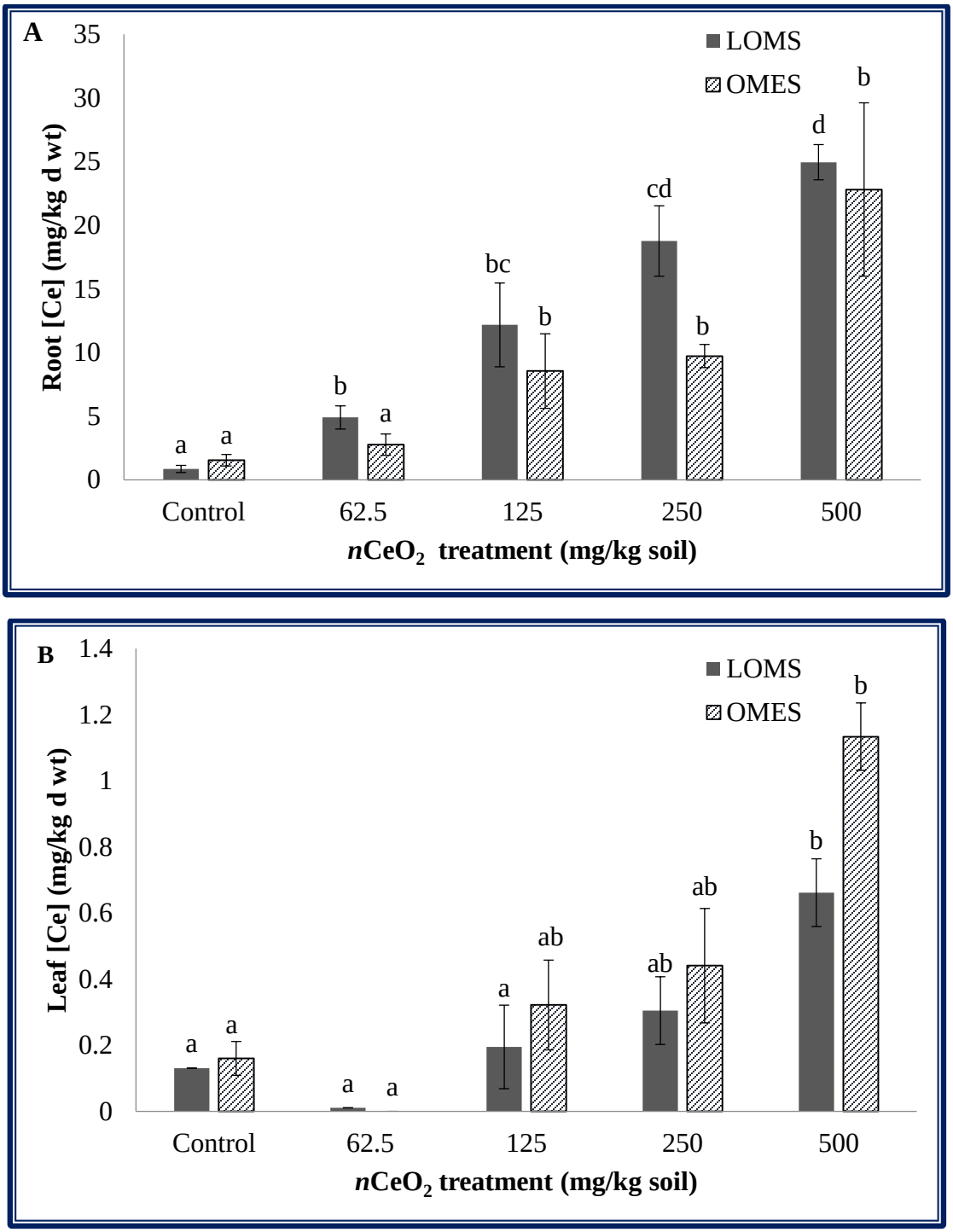

Figure 3.1. Cerium accumulation in kidney bean plant tissues (A) Roots, (B) Leaves, exposed to low organic matter soil (LOMS) and organic matter enriched soil (OMES) amended with 0 - 500 mg/kg *n*CeO_2. Values are expressed as mean ± SE (*n*=4). Values with different letters represent significant difference at $p \leq 0.05$ within a soil type.

3.3.4 Impact of *n*CeO_2 on plant metabolic activities

The effects of *n*CeO_2 exposure to plants grown in LOMS and OMES, concerning leaf area, photosynthetic pigment content, net photosynthesis and transpiration rate and stomatal conductance are shown in Figure 3.2 A-F. In LOMS, the leaf area was significantly increased at all *n*CeO_2 treatments with respect to control, however in OMES, no significant variations were observed (Figure 3.2A). The leaf photosynthetic pigments in the LOMS plants exposed to *n*CeO_2 showed no variations compared to control, whereas, was significantly ($p \leq 0.05$) reduced in OMES at 62.5 to 250 mg/kg *n*CeO_2 (Figure 3.2B). Chlorophyll a, b and carotenoid contents in the OMES leaves was dropped from 15.9, 7.5 and 3.2 µg/ml in control to 11.9, 6.1 and 2.3 µg/ml in the leaves of 125 mg/kg *n*CeO_2, which was affected to the greatest extent. This indicates that the higher translocation of *n*CeO_2 to the leaves in OMES (Figure 3.1B) leads to reduction in the photosynthetic pigments, which are responsible for absorption of light energy from the sunlight at certain wavelengths to carry out photosynthesis [25]. The net photosynthesis, stomatal conductance and transpiration rate increased significantly with respect to control, upon *n*CeO_2 exposure in both soils. In LOMS, all the three parameters showed a significant ($p \leq 0.05$) increase with respect to control at 62.5, 250 and 500 mg/kg *n*CeO_2 (Figure 3.2C). However, in OMES, 62.5, 125, and 250 mg *n*CeO_2/kg treatments showed adrastic and significant ($p \leq 0.05$) increase in stomatal conductance, net photosynthesis and transpiration rates. Interestingly, the increase in the photosynthetic and gas exchange activities were much higher in OMES than that in LOMS plants exposed to *n*CeO_2. Earlier studies, in corn showed no significant effects of *n*CeO_2 on photosynthetic activities and gas exchange in plants [12]. The effects on the photosynthetic pigment contents and the photosynthetic activities are contrasting, as these activities are dependent on these pigments to absorb and transfer the light energy. It could be possible that although the *n*CeO_2 decreases the photosynthetic pigments in the leaves, it simultaneously increases the photosynthetic efficiency of the plants, thereby increasing the metabolic activities of the kidney bean plant. Cerium oxide is used in many parts of the world as fertilizers to improve crop growth and yield [14]. For a comprehensive understanding of the effects on the photosynthetic apparatus

of kidney bean leaves, further studies on the different enzymes participating in the calvin cycle needs to be stuied.

3.4 Conclusion

Soil organic matter influences the behavior of the nanoparticles in the soils as well as their toxicity on the plants. This study clearly states that presence of high organic matter in the soil increases the mobility of the nanoceria within the plants. This leads to easier access of the nanoceria to the metabolic machinery of the plants, which alters the activities in the leaves pertaining to food and energy production and plant health. On the other hand, in natural sandy loam soil with low organic matter content, the nanoparticles are aggregated due to surface charge and restricted to the below ground biomass. This study suggests that fate, bioavailability and toxicity of nanoceria are highly dependent on the properties of the complex soil matrix. Further studies on the activity of photosynthetic enzymes and effects of nanoparticles on hormones responsible for different plant functions may help in a better understanding of the mechanisms by which the nanoparticles affect the metabolic functions.

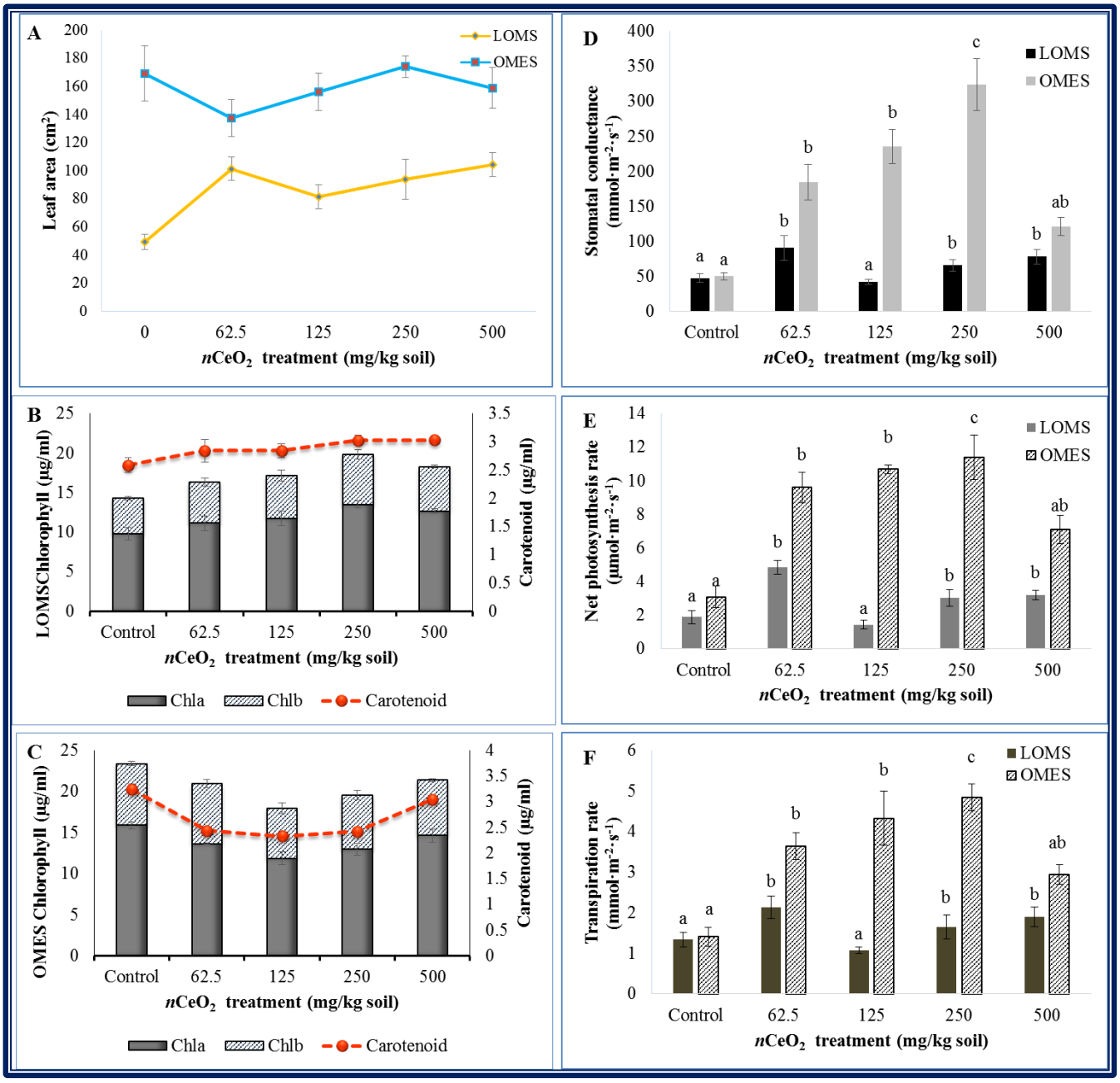

Figure 3.2. (A) Leaf area, (B) Photosynthetic pigment, (C) Stomatal conductance, (D) Net photosynthesis, (E) Transpiration rate in the plants, exposed to low organic matter soil (LOMS) and organic matter enriched soil (OMES) amended with 0 - 500 mg/kg *n*CeO_2. Values are expressed as mean ± SE (*n*=4). Values with different letters represent significant difference at $p \leq 0.05$ within a soil type.

CHAPTER 4

Soil organic matter modulates the effects of nanoceria on kidney bean production and bean quality

4.1 Introduction

In recent years, keen interest in nanoceria particles (*n*CeO_2) and associated applications have dramatically increased, mainly due to their *bonafide* catalytic and redox properties. Nanoceria are rapidly replacing micro-sized ceria particles in varied applications like fuel additives, catalytic converters, scratch resistant polishing agents, and electronic devices [1]. Due to their established antioxidative properties, they are being studied worldwide in a wide array of biomedical research for treating neurodegenerative and ocular diseases, and for tissue regeneration [2]. Current market estimates suggest 10,000 metric tons of global annual production of *n*CeO_2, primarily from Asia, Australia and Europe [1]. This has simultaneously raised serious concern on their fate upon release in various environmental media [3], and corresponding exposure to ecological receptors, including humans.

Previous studies on *n*CeO_2 exposure to plants have provided evidence on their uptake by roots and further translocation to aerial tissues in monocotyledonous [4,5], as well as dicotyledonous plants [6-10], with varying physiological and biochemical responses. Although they were reported to primarily retain their oxidation state and nanoparticulate form, a small fraction of Ce(IV) was found to biotransform to Ce(III) in soybeans [11], kidney beans [6], and cucumber [12]. Due to increasing concerns on reported bioaccumulation of engineered nanomaterials (ENMs) in the food chain [13], and resulting exposure to humans, research on their impact on plants grown to full maturity upon acute as well as chronic exposure is highly desired. It is imperative to assess the effects of the ENMs on the fruit/seed nutritional quality. Recent studies have reported the presence of Ce in edible tissues of rice [4], soybeans [7], tomato [8], cilantro [9], radish [10], and cucumber plants [14], exposed to *n*CeO_2 amended soil. Nanoceria has been reported to increase the plant yield in tomato and alter the mineral contents in cucumber fruits [14], rice grains [4], and soybeans [15], thereby altering the nutritional quality. Studies have also shown that *n*CeO_2 affected the

macromolecular compositions, especially carbohydrates, lipids, and amides in rice grains [4], but only carbohydrates in cucumber [14] and cilantro [9]. Soil quality and natural organic matter content are very critical factors that influence the extent of impact of ENMs on the plants [5,16]. Soil organic matter (SOM) can interact with ENMs and affect their chemical properties pertaining to aggregation, surface charge, and bioavailability. Low molecular weight humic substances, like fulvic and humic acids have been reported to increase the stability of ENMs in soil [17] and aquatic environments [16,18]. There is a major gap in research concerning how soil quality and the percentage of organic matter could influence the uptake of ENMs by plants grown to full maturity and, eventually, affect the nutritional quality of edible tissues.

Kidney beans are very important legumes produced and consumed worldwide due to its nutritional composition while supplying moderate calories. They are a major source of proteins, dietary fiber, folate, iron, zinc, magnesium, molybdenum, and potassium with no fats, sodium and cholesterol [19]. It is the most common legume consumed due to its health benefits that includes reducing blood cholesterol and sugar levels, thereby preventing various degenerative diseases like diabetes, cancer and heart ailments [20].

To the best of author's knowledge, there are no studies addressing the differential response of *n*CeO_2 on the plant yield and resulting seed nutritional quality, owing to difference in SOM content. In the current study, we explored the effect of *n*CeO_2 on the productivity of kidney bean plants grown in low-organic matter and organic matter-enriched soils. Cerium accumulation and micronutrient and macronutrient contents in the kidney bean's dried carpels and seeds were analyzed using inductively coupled plasma-based spectroscopic analyses. FTIR analysis was performed on the seeds to assess variations in their macromolecular composition. Quantitative analysis of crude protein, total sugar and starch in the seeds from control and *n*CeO_2 exposed plants were performed to determine their nutritional quality.

4.2 Materials and methods

4.2.1 Soil source and characteristics

In this study, two types of soils varying in their organic matter content were used. The low-organic matter soil (LOMS) was collected from Fabens, TX (N 31° 29’ 02.1”, W 106° 08’ 27.2”, elevation 1102 meters, mineral horizon, depth 55 cm) and air dried before use. The organic matter-enriched soil (OMES) was prepared by mixing the LOMS with Miracle-Gro potting mix at 2:1 (v/v) ratio. The organic matter content of LOMS and OMES was 4% and 10%, respectively, determined by loss on ignition method. The elemental contents in the aqua-regia digested soils were analyzed using inductively coupled plasma- optical emission spectroscopy (ICP-OES). Characteristics of LOMS and OMES are provided in Chapter 3.

4.2.2 Preparation of nanoparticle suspension and treatment

The *n*CeO_2 (≈8 nm, Meliorum Technologies, Rochester, NY) were provided by The University of California Center for Environmental Implications of Nanotechnology (UC-CEIN) and have been previously characterized [21]. According to Keller *et al.* [21], the *n*CeO_2 used were rods measuring (67 ± 8) nm × (8 ± 1) nm, (≤10% polyhedra: 8 ± 1 nm) with 95.14% purity and surface area of 93.8 m^2g^{-1}. Bulk CeO_2 (*b*CeO_2) was purchased from Sigma-Aldrich. Requisite amount of *n*CeO_2 and *b*CeO_2 were suspended in 250 mL of Millipore water (MPW) by bath sonication (Crest Ultrasonics, Trenton, NJ, USA) for 30 min at 25°C to prepare final concentrations of 62.5, 125, 250, 500 mg *n*CeO_2 /kg soil, and 125 and 500 mg *b*CeO_2 /kg soil in 4 and 3 kg of LOMS and OMES, respectively. The nanosuspensions were diluted to 600 mL and manually mixed homogenously with the soils and placed in plastic pots (7 1/2" dia. x 6" H) to equilibrate for 24 h, before planting 15 seeds per pot at a depth of 1 in. Only MPW mixed soil served as the control for the experiment.

4.2.3 Plant growth conditions

Kidney bean (*Phaseolus vulgaris* var. red hawk) seeds were obtained from Dr. James Kelly, Michigan State University. Each treatment and control was carried out in quadruplicates

and the pots were placed in growth chamber (Environmental Growth Chamber, Chagrin Falls, OH) with 14 h photoperiod (340 µmole $m^{-2}s^{-1}$), 25/20°C day/night temperature and 65-70% relative humidity for 7 days. After the appearance of the cotyledonous leaves, the pots were transferred to greenhouse with similar conditions. The plants were watered initially with 200 mL MPW for the first 15 days of planting, and then with appearance of leaves and increased transpiration, the volume was increased to 400 mL for the entire life cycle.

4.2.4 Assessment of yield-related parameters and harvest

After 50 days of plantation in control, *n*CeO_2, and *b*CeO_2 amended soil, ten plants from each treatment replicates were randomly selected to assess yield related parameters (number of pods per plant and pod length). For assessment of pod dimension, they were divided into two categories depending on their length (due to varying growth stages), < 7 (developing) and ≥ 7 cm (fully grown). The plants were considered matured when the pods dried and showed cracked openings to reveal the seeds inside. Plants were allowed to grow until maturity for 96-102 days, and the pods were cracked open and separated into dried carpels and seeds. Number of seeds per pod was counted and stored for further nutritive analyses. Fresh weight of the matured seeds was recorded as seed size (g/10 seeds). The moisture content of whole seeds were measured by low constant temperature oven method in batch of 4 seeds per replicate, weighing between 0.9 to1.5 g and expressed as a percentage of fresh weight of the seeds.

4.2.5 Analytical methods for assessment of nutritional quality

The seeds collected from each treatment were stored at 4°C. Prior to the following analyses, they were dried at 70 °C for 24 hours, finely ground and passed through 2 mm sieve. The nutritional analyses were performed in triplicates, except elemental analyses which were done in quadruplicates.

4.2.6 Quantification of cerium, micro- and macro-nutrients in carpels and seeds

Carpels and seeds from each pod were separated and dried separately at 70 °C for 96 h. Dried carpels and whole seeds were digested in a mixture of plasma pure HNO_3 and 30% (w/v)

H_2O_2 (1:4) using microwave accelerated reaction system (CEM $Mars_x$, Mathews, NC) [22]. Accumulation of Ce and most micronutrients (B, Co, Cu, Fe, Mn, Mo, Ni, Zn) was analyzed in the digested samples using inductively coupled plasma-mass spectrometry (ICP-MS) (Perkin Elmer ELAN DRC II, Shelton, CT). The macronutrients (Ca, Mg, P, S, K) and Na were quantified using inductively coupled plasma-optical emission spectroscopy (ICP-OES) (Optima 4300 DV, Perkin Elmer, Waltham, MA). Blanks, spikes and certified standard reference material (peach leaves NIST-SRM 1547, Gaithersburg, MD) were analyzed to validate the digestion process and spectroscopic analysis, obtaining 90% recovery. Also, 0.5 mg/L multi-elemental standard was analyzed every 10 samples to monitor the matrix effect on the analytes and for quality assurance/quality control [6].

4.2.7 Nitrogen and crude protein content

Nitrogen content in the finely powdered seeds were determined using Kjeldahl method using a digestion and distillation unit (Labconco Co., Kansas city) Labconco, Kansas city, USA and expressed as % N [23,24]. Crude protein content was calculated as % N x 6.25 [23].

4.2.8 Sugar and starch content

Total soluble sugars (TSS) and starch in the finely powdered seed samples were extracted following the methods described by Verma and Dubey with slight modifications [25]. TSS from 100 mg of samples were extracted three times in 10ml of 80% ethanol and boiled for 45 min and centrifuged at 4500 x g for 20 min (Eppendorf 5804R, Hamburg, DE). The pooled supernatant was reduced to 5 ml and diluted to 25mL with MPW. Starch in the seeds was extracted from the dried residues obtained from TSS extraction. The residues were suspended in 2 mL MPW and boiled in water bath for 15 min. The suspensions were cooled to room temperature and 2mL of 9.2 M $HClO_4$ was added to hydrolyze starch to glucose, followed by 15 min stirring and dilution to 10 ml with MPW. The mixture was centrifuged at 3000 x g for 20 in. Extraction was repeated two more times with 4.6 M $HClO_4$, supernatants were pooled together and diluted to 40 mL with MPW. Starch was analyzed similar to TSS determination. TSS and starch content were determined using phenol-

sulfuric acid method with glucose as the standard [26]. Starch content was calculated in terms of glucose equivalent (Glucose x 0.9). TSS and starch content were expressed as mg g^{-1} dry weight of samples.

4.2.9 FT-IR/ATR data acquisition

The spectra for major macromolecules in the finely powdered seeds were obtained using Fourier Transform Infrared-Attenuated total reflectance (FT-IR/ATR) spectrometer Spectrum100 (Perkin-Elmer, Shelton, CT) in the frequency range of 650-4000 cm^{-1} (2 cm^{-1} resolution, 4 number of scans, and air as background. Three replicates of composite samples of powdered seeds were used for the analysis. Each spectra was displayed in the absorbance mode, baseline corrected, smoothed, and area normalized using Perkin Elmer Spectrum software (Version 6.0.2.0025, Perkin Elmer, Shelton, CT). Each spectra calculated was an average of spectra from three different replicates [4].

4.2.10 Statistical Analysis

Statistical analysis of the data were performed using one-way ANOVA followed by Tukey's multiple comparisons test based on a probability of $p \leq 0.05$, unless stated otherwise (IBM SPSS Statistics 19, Chicago, USA). Elemental composition of the carpels and seeds were performed in quadruplicates, and all other nutritional analyses were performed in triplicates.

4.3 Results and discussion

4.3.1 Effects of *nano* and *bulk* CeO_2 on plant yield depending on SOM content

Yield related parameters, in terms of number of pods, pod dimensions, seeds per pod, seed size (g/10 seeds), and seed moisture content, as a response to *n*CeO_2 exposure in LOMS and OMES are shown in Figure 4.1 and Table 4.1. As seen in Table 4.1, the number of pods/plant or the pod length were not significantly affected by *n*CeO_2 treatments in either soil types; however, bulk CeO_2 (*b*CeO_2) at 125 and 500 mg/kg reduced the yield compared to control by 33 and 38 %, respectively in LOMS ($p \leq 0.1$), and 76 and 66% in OMES ($p \leq 0.001$). The reduction in yield may be attributed

to the difference in particle size. The micron-sized *b*CeO_2 may block the aquaporins and the ion transport channels on the root surface [6], thereby affecting the mineral imbalance responsible for ovule fertilization processes. Elaborate microscopy and spectroscopy studies are needed to better understand the difference in the mechanism by which nanoparticles and their respective bulk particles interact at root surface. Previous reports on cucumber [27] and soybeans [7] reported decrease in yield (number of fruits/pods) in response to 800 and 100 mg *n*CeO_2 /kg, respectively. However at 500 and 1000 *n*CeO_2/kg, the soybean yield resumed to normal [7].

The number of seeds per pod increased significantly with respect to control at 250 and 500 mg *n*CeO_2 /kg LOMS at $p \leq 0.1$ and $p \leq 0.078$, respectively, and at 125 mg *n*CeO_2 /kg OMES ($p \leq 0.029$), unlike bulk treatments (Figure 4.1A). Previous studies with soybeans, reported that the number of pods or seeds per pod were not affected even at very high *n*CeO_2 treatment of 1000 mg/kg.[7] However, in another chronic exposure study on tomato plants, Wang *et al.*[8] reported enhanced fruit production at 10 mg/L *n*CeO_2. The seed size, expressed as g/10 seeds was unaffected by *n*CeO_2 exposure in OMES. This is in accordance with previous reports on tomato, where fruit size and weight was not affected in OMES amended with *n*CeO_2 [8]. However, in LOMS at 250 mg/kg *n*CeO_2 and 500 mg/kg *b*CeO_2 treatments, the seed size was significantly increased at $p \leq 0.05$ with respect to control (Fig. 1B). Figure 1C shows the percent moisture content in the seeds harvested in LOMS and OMES amended with *n*CeO_2. The seed moisture content was significantly ($p \leq 0.01$) affected by *n*CeO_2 exposure at 62.5 and 250 mg/kg LOMS and at 125 mg/kg OMES. *b*CeO_2 at 500 mg/kg LOMS significantly enhanced the water content of the seeds with respect to control. This was an interesting observation, as previous studies on soybeans do not suggest any effects of *n*CeO_2 on the water storage by the pods.[7] Thus, in LOMS, at 250 mg *n*CeO_2 /kg, enhancement in seed production, weight and water storage with respect to control was consistent, whereas in OMES, 125 mg *n*CeO_2 /kg treatment was significantly affected with respect to number of seeds per pod and water storage, indicating hormesis. No effects on the pod appearance but increase in number of seeds per pod infer that *n*CeO_2 affects the embryo maturation rather than pod formation. In agricultural practices, cerium has been used as an additive in

fertilizers since 1980s in some parts of the world to enhance plant growth and yield [27]. But, the plant biochemistry responsible for such positive response has not been reported. Plant productivity is dependent on various factors like phytohormonal balance, mineral assimilation, and cell differentiation, elongation and synthesis of stored reserves in the endosperm [28]. Abscissic acid-induced genes have been reported to be associated with seed maturation and seed desiccation, during which the developmental processes are terminated. Thus to understand the effect of *n*CeO_2 on the seed development, biochemical, proteomic and metabolomic response on plant hormones especially abscissic acid, ethylene and gibberellin needs to be well explored [28,29].

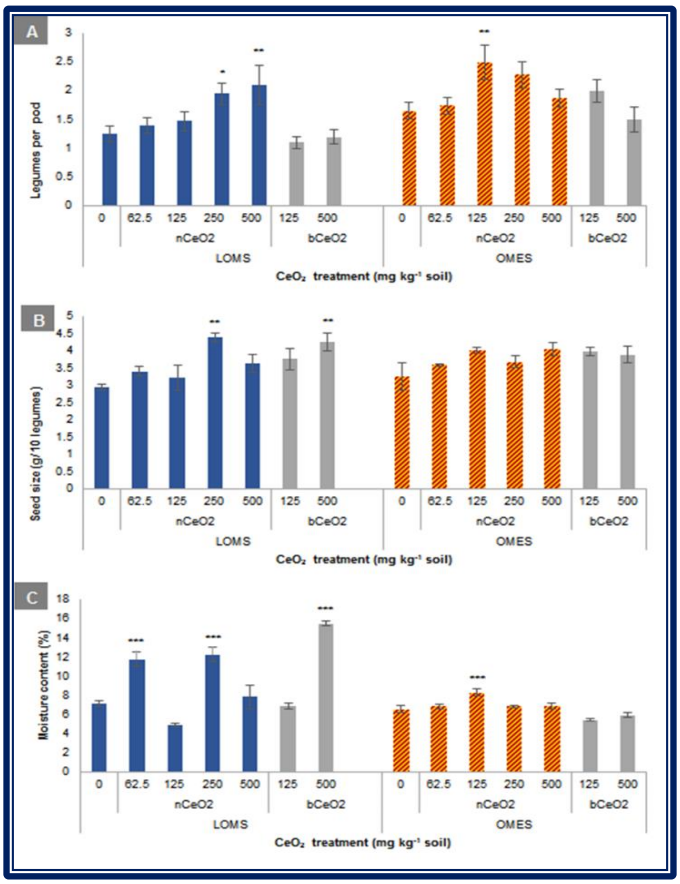

Figure 4.1. Seeds per pod, seed size and percent moisture content in the seeds harvested from plants exposed to 0 to 500 mg/kg *n*CeO_2 and 125, 500 mg/kg *b*CeO_2 treatments in Low organic matter soil (LOMS) and Organic matter enriched soil (OMES). Values are expressed as mean ± SE (n=4). Bars with *, ** and *** within same soil type, represent significant difference at $p \leq$ 0.1, 0.05 and 0.01, respectively.

Table 4.1. Yield related parameters for the plants exposed to 0 to 500 mg/kg *n*CeO_2 and 125, 500 mg/kg *b*CeO_2 treatments in Low organic matter soil (LOMS) and Organic matter enriched soil (OMES). Values are expressed as mean ± SE (n=4). The values with different letters within each soil type represent significant difference at $p \leq 0.05$.

Yield related parameters		**LOMS**							**OMES**						
		***n*CeO₂ treatment (mg/kg soil)**					***b*CeO₂ treatment (mg/kg soil)**		***n*CeO₂ treatment (mg/kg soil)**					***b*CeO₂ treatment (mg/kg soil)**	
		0	**62.5**	**125**	**250**	**500**	**125**	**500**	**0**	**62.5**	**125**	**250**	**500**	**125**	**500**
Number of pods per plant		2.9 ± 0.3a b	3.4 ± 0.3a	3.6 ± 0.1a	3.6 ± 0.4a	3.8 ± 0.2a	1.9 ± 0.1b	1.8 ± 0.1b	6.3 ± 0.4ab	5.6 ± 0.3a	6.9 ± 0.1b	6.3 ± 0.2ab	6.3 ± 0.2ab	1.5 ± 0.1c	2.1 ± 0.2c
Pod length (cm)	**Longest size**	10.1	11.3	12.4	11	11.7	12.4	10	13.2	12.7	14.8	14.2	14.2	11.6	11.6
	≥7	8.8 ± 0.5	9.3 ± 0.3	10.1 ± 0.4	8.9 ± 0.3	9.0 ± 0.3	9.1 ± 0.4	8.7 ± 0.2	10.2 ± 0.3	10.15 ± 0.3	10.7 ± 0.2	10.61 ± 0.27	10.4 ± 0.2	9.9 ± 0.2	10.1 ± 0.3
	<7	4.5 ± 1.6	4.3 ± 0.4	4.4 ± 0.5	4.4 ± 0.3	4.6 ± 0.5	5.1 ± 0.3	4.3 ± 0.3	5.5 ± 0.2	5.15 ± 0.3	5.5 ± 0.3	5.76 ± 0.2	5.87 ± 0.2	4.8 ± 0.3	4.3 ± 0.4

4.3.2 Ce accumulation in carpels and seeds

Cerium accumulation in the carpels and seeds of plants grown in LOMS and OMES amended with 0 to 500 mg/kg *n*CeO_2 are given in Figure 4.2. Cerium concentrations in the carpels and seeds obtained from the plants exposed to 125 and 500 mg *b*CeO_2/kg LOMS and OMES, were below the detection limit of inductively coupled plasma- mass spectrometry (ICP-MS), indicating very low translocation. In both the soils, traces of Ce were detected in the carpels and seeds from the control (Chapter 3), as current study was performed using natural soil from the agricultural field. Since Ce is a rare earth element, it is naturally present in soil. Although OMES was a mixture of LOMS and potting mix, Ce content in the potting mix was very low (2.1 mg kg^{-1}), thus diluting Ce concentration in OMES. In LOMS, all *n*CeO_2 treatments showed statistically similar Ce accumulation in the carpels (110 µg/kg d wt at control to 231 µg/kg d wt at 500 mg *n*CeO_2/kg). On the other hand, in OMES, Ce accumulation in the carpels from 250 and 500 mg/kg *n*CeO_2 treatments (160 and 188 mg/kg d wt) was significantly higher ($p \leq 0.023$ and $p \leq 0.003$, respectively) with respect to control (71 µg/kg d wt). Priester *et al.*[7] reported 133 µg Ce/kg d wt in the carpels of soybean exposed to 500 mg *n*CeO_2 /kg soil, which is in accordance with the accumulation levels we found in the kidney bean carpels.

Concentrations of Ce in carpel tissues were more than five times than that accumulated in the seeds. This is because the vascular connection between the parent plant and the fruit ends in the fruit seed coat, which is the pod coat in case of leguminous fruits. The nutrients are transferred to the legume seeds via the filial tissue of the endosperm or embryo by passive, facilitated membrane transport process [28]. Ce concentrations in the seeds from LOMS did not increase significantly with increasing *n*CeO_2 treatment. In OMES grown seeds, Ce accumulation at 250 and 500 mg/kg *n*CeO_2 treatments reached 27 and 23 µg/kg d wt respectively, which were significantly higher than the control ($p \leq 0.013$ and $p \leq 0.057$, respectively). Around 80% of the soil organic matter primarily comprises of an amorphous and colloidal mixture of materials known as soil humus (humic acid, fulvic acid and humin) [30]. The colloidal surface of humus is negatively charged due to carboxylic and phenolic groups which carry a pool of various cations like Ca^{2+},

Mg^2, K^+,Na^{2+}, Zn^+ in easily exchangeable forms [30]. *n*CeO_2 suspension prepared in millipore water (MPW) had positive zeta potential (37 ± 2 mV), which when mixed with soil, enables them to bind or chelate with the negatively charged organic moieties present in the soil matrix. The association of the *n*CeO_2 with organic matter increases its stability and bioavailability in the OMES. It may also enhance the possibility of Ce uptake through the metal ion transporters due to the enrichment of readily available exchangeable cations near the rhizophere [30,31]. Since the soils used in these studies were alkaline soils, the Ce on the surface of *n*CeO_2 lattice do not tend to reduce or biotransform, but should remain as Ce(IV), as reported in soybeans and cucumber [11,12]. Accumulation of Ce in the edible parts has been previously reported in rice [4], corn [5], tomato [8], and cilantro [9]. Compared to kidney beans, rice grains have been reported to bioconcentrate considerably higher (224 to 1912 µg/kg d wt) amount of Ce in the tissues upon 500 mg *n*CeO_2 /kg soil exposure. This could be attributed to the tremendous water volume required for rice irrigation, thereby promoting aerial translocation. Although, Ce accumulation in whole soybean pods has been reported previously [7], this is the first report to determine Ce accumulation in legume seeds that are directly consumed by humans, and correlated with soil quality.

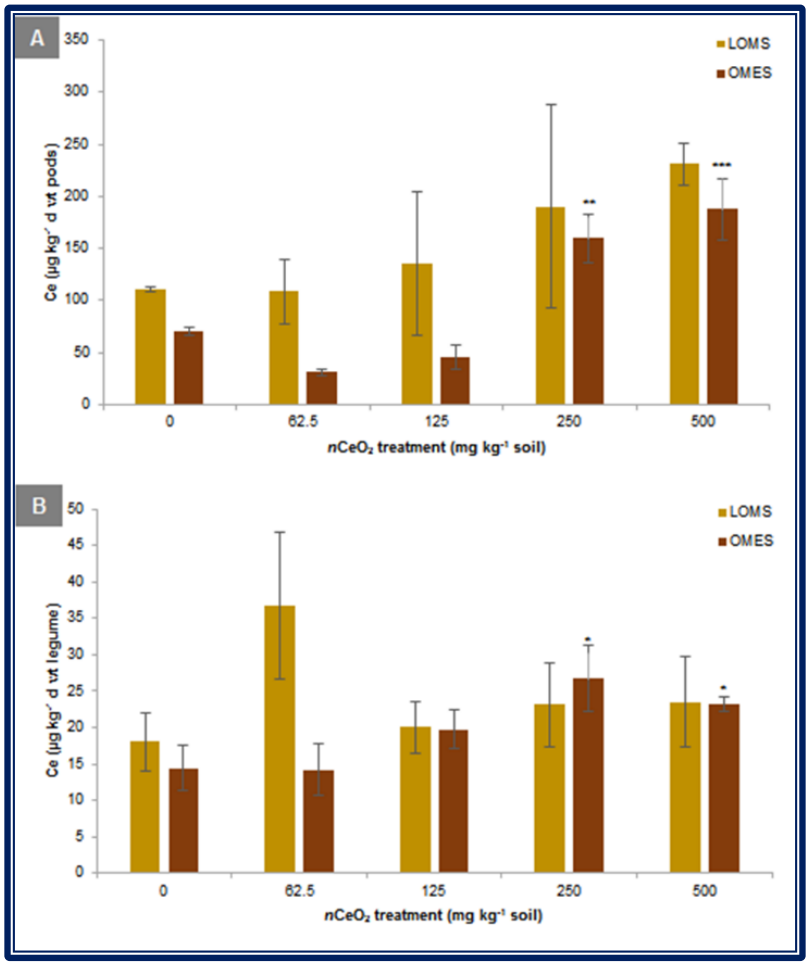

Figure 4.2 Ce accumulation in carpels and seeds harvested from plants exposed to 0 to 500 mg nCeO$_2$ kg^{-1} treatments in Low organic matter soil (LOMS) and Organic matter enriched soil (OMES). Values are expressed as mean ± SE (n=4). Bars with *, ** and *** within same soil type, represent significant difference at $p \leq 0.1$, 0.05 and 0.01, respectively.

4.3.3 Effects on legume ionome and nutrition quality

Elemental composition in the carpels

Kidney beans are very important source of essential minerals like iron, zinc, molybdenum, copper, magnesium and potassium. In this study, the macronutrients (Ca, Mg, P, N, K, and S) and micronutrients (B, Cu, Fe, Mn, Mo, Ni, Zn, and Na) were analyzed in the carpels and seeds to understand how nCeO$_2$ uptake and translocation affect the ion mobility in the plants and thereby impact the legume ionome. It is imperative to understand if the soil quality also serves as a factor

in the nutrient mobility to the seeds. Figure 4.3 and Table 4.2 present the micronutrients and macronutrients, respectively, in the carpels and seeds obtained from *n*CeO_2 exposure in LOMS and OMES. Nutrient analyses were not performed in seeds from *b*CeO_2 plant because they showed no traces of cerium in the tissues.

Macronutrients in the carpels harvested from the plants exposed to 62.5 to 500 mg *n*CeO_2 /kg LOMS were unaffected with respect to control, except Ca and Mg (Table 4.2). In LOMS, Ca content in the carpels increased 30 % at 250 mg/kg *n*CeO_2, whereas Mg decreased 17% at 125 mg/kg *n*CeO_2. On the other hand, in the carpels collected from the plants exposed to *n*CeO_2 in OMES, phosphorus content increased at 62.5, 125 and 250 mg *n*CeO_2 /kg OMES by 50 %, 33%, and 26 %, respectively with respect to control. Sulfur was also significantly ($p \leq 0.05$) increased at 62.5, 125 and 250 mg *n*CeO_2/ kg OMES compared to control. Both P and S contents reflected hormetic trend on exposure to *n*CeO_2 in OMES (Table 4.2). Phosphorus enhances various growth and development processes in the plant including seed number and size [32]. This clearly explains the observed increase in the number of seeds at 62.5 to 250 mg *n*CeO_2/ kg OMES treatments, particularly significant at 125 mg *n*CeO_2/ kg OMES ($p \leq 0.05$). Sulfur is an important macronutrient which is associated with different amino acids and proteins. It is also constituent of coenzyme A, thiamine pyrophosphate, glutathione, biotin and many other organic components of the plant [29]. Sulfur in soils is primarily released from the organic matter decomposition in the soils [30]. Thus, it is possible that *n*CeO_2 interacts with the sulfur released for the organic matter, leading to S enrichment in the carpel tissues. Thus plants grown in OMES, were found to be affected more in terms of macronutrient composition, demonstrating low *n*CeO_2 dose stimulation at 125 mg *n*CeO_2 kg^{-1}. This is in accordance to similar trend observed in the plant productivity in OMES, with respect to number of seeds per pod and water storage (Figure 4.1). As explained in previous section, the nutrient supply to the legume seeds is not directly connected to the parent plant but is passively transported from the carpel (pod coat) to the embryo. Thus, the hormetic trend in the macronutrient enrichment in the *n*CeO_2 exposed OMES pods explains the similar trend in the seed development and maturity. Micronutrients are equally essential to plants as the

macronutrients, but are required in trace amounts. These elements play crucial roles in various metabolic processes, electron transfer, growth and development of a plant [30]. The micronutrient composition in carpels and seeds is shown in Figure 4.3. Among all the micronutrients, B, Na, Mn, and Zn contents were not affected in the carpel from LOMS or OMES. However, Cu content in carpels decreased significantly ($p \leq 0.01$) compared to control in all the *n*CeO_2 treatments in LOMS and at 500 mg *n*CeO_2 /kg OMES ($p \leq 0.003$). Kidney beans are a good source of copper in dietary intake. Copper plays a very important role in plants as cofactor in enzymes participating in photosynthesis [29]. It also plays essential role in formation of chlorophyll, seed development, oxidative stress protection, among many other functions [33]. Nickel and iron content in the carpels decreased significantly ($p \leq 0.009$, and $p \leq 0.038$, respectively) at 125 mg *n*CeO_2 /kg LOMS with respect to control, however Ni showed reverse trend in *n*CeO_2 amended OMES, where it increased ($p \leq 0.117$) at 62.5 mg/kg *n*CeO_2 with respect to control. In plants, plasma membrane transporters are responsible in uptake, translocation, and homeostasis of metal ions at the cellular level. Some of the major transporters belong to ZIP and RAMP transporter families, which are involved in transport of metals like Cu^{2+}, Mn^{2+}, Zn^{2+}, Fe^{2+}, Cd^{2+}, Ni^{2+}, and Co^{2+} across plasma membrane and tonoplast [31].The copper transporters family (CTF) in plants have been reported to be involved in copper transport in the plants [31]. In the LOMS, the *n*CeO_2 might interact with, or block ZIP, NRAMP or CTF transporters, leading to reduced uptake or translocation of copper and iron. However, in OMES, at low *n*CeO_2 treatments, the particles are stabilized due to presence of organic acids in excess, but at high concentration (500 mg/kg *n*CeO_2), it quenches the Cu uptake or translocation. Molybdenum in the pods increased at 62.5 mg *n*CeO_2/ kg OMES ($p \leq 0.048$) with respect to control, but resumed to normal levels at higher concentrations.

Elemental composition in the seeds

Most of the macronutrients were unaffected in the seeds collected from the *n*CeO_2 exposed plants in LOMS or OMES. Although the nitrogen content in the seeds was not affected with *n*CeO_2 exposure in the OMES, it was increased at 125 mg *n*CeO_2/ kg LOMS ($p \leq 0.113$) with respect to

control. While studying food quality, some elemental ratios need special attention for balanced absorption of all the elements by human body. This is because some elements show synergistic or antagonistic properties in presence of some others. For efficient absorption of dietary phosphorus by the intestinal walls, calcium at similar amounts or higher ($\geq$ 1:1) must be present, or it may affect the bone integrity on consumption [34]. As shown in Table 4.2, the Ca:P ratio was well above normal and showed slight increase in the seeds from *n*CeO_2 treatments compared to control. Soils varying in their organic content influenced the impact of *n*CeO_2 on the seed quality differentially. As shown in Figure 4.3, in *n*CeO_2 amended LOMS, among all other micronutrients, only molybdenum and boron accumulation was affected. On the other hand, in *n*CeO_2 amended OMES, boron, iron and sodium were primarily affected. Molybdenum content in the LOMS grown seeds were significantly reduced ($p \leq 0.001$) on *n*CeO_2 exposure at all treatments, with respect to control. Molybdenum ions (Mo^{4+}) are cofactors of enzymes like nitrogenase and nitrate reductase that play critical role in nitrogen assimilation by the plants. However, nitrogen content of the seeds was not reduced corresponding to molybdenum. Molybdenum is also constituent of sulfite oxidase enzymes, which detoxifies sulfite present in food products [35]. Thus, decreased Mo content in the seeds can directly and indirectly affect human health. Boron in the seeds significantly increased at 62.5 mg *n*CeO_2/ kg LOMS ($p \leq 0.104$) and at 125 mg *n*CeO_2/ kg OMES ($p \leq 0.053$). At 125 mg *n*CeO_2/ kg OMES, iron content in the seeds decreased significantly ($p = 0.016$) with respect to control. Sodium was reduced significantly at 62.5 to 500 mg/kg *n*CeO_2 ($p \leq 0.01$). Apart from Ca:P as discussed before, another elemental ratio of significance is Na:K [36]. Balance between dietary Na and K is required for maintaining optimum pH and osmotic balance of the body fluids, enhanced protein retention for proper growth, and regulating blood pressure. The recommended ratio of Na:K is less than 1. Although the Na in OMES grown seeds decreased significantly with respect to control *n*CeO_2 exposure, the Na:K in the seeds were within recommended levels, and *n*CeO_2 exposure did not affect their balance (Table 4.2). This shows that OMES affects the nutrient mobility and accumulation in presence of *n*CeO_2 differently than LOMS.

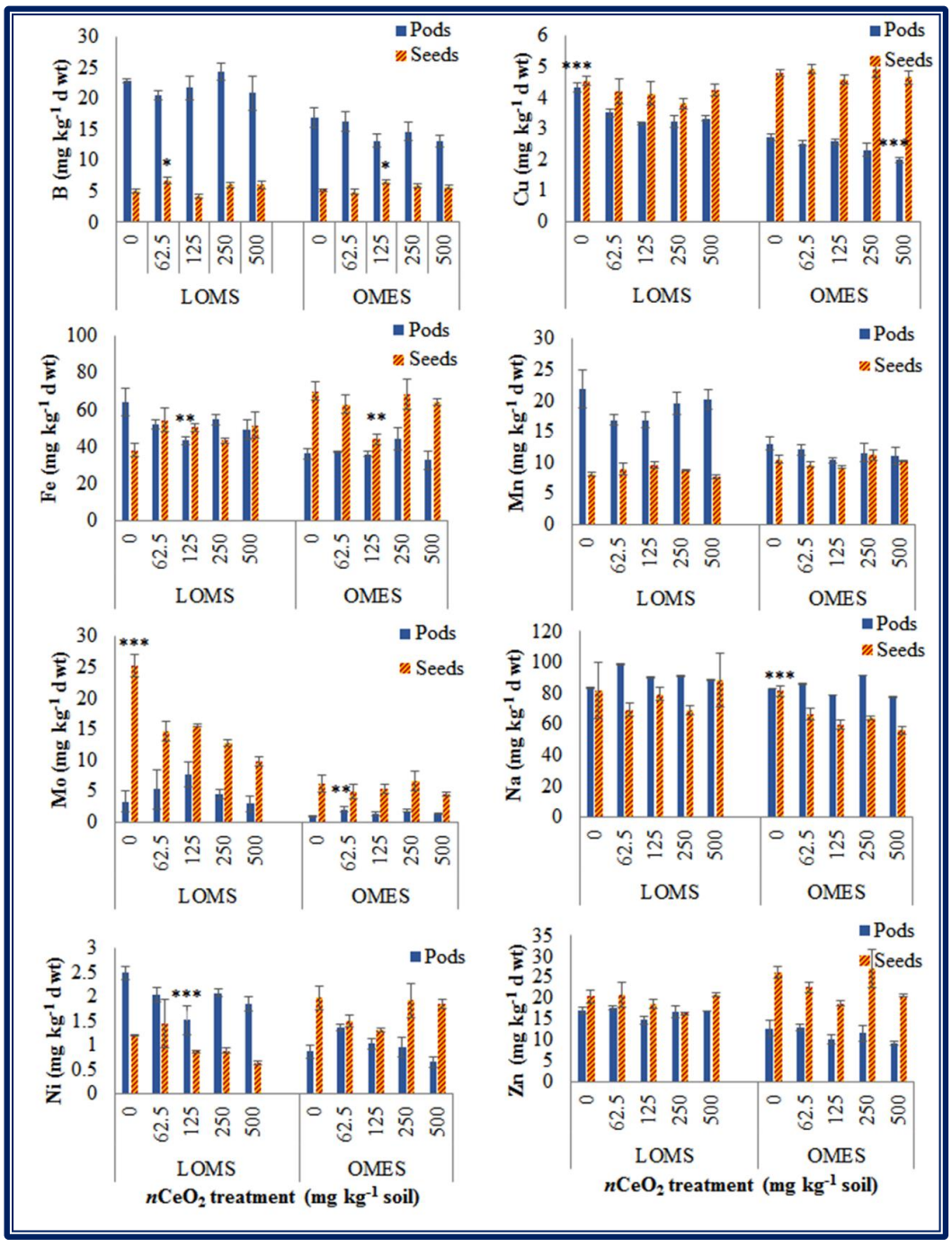

Figure 4.3. Micronutrients in carpels and seeds harvested from plants exposed to 0 to 500 mg/kg *n*CeO_2 treatments in Low organic matter soil (LOMS) and Organic matter enriched soil (OMES). Values are expressed as mean ± SE (*n*=4). Bars with *, ** and *** within same soil type, represent significant difference at $p \leq 0.1$, 0.05 and 0.01, respectively.

Table 4.2. Macronutrient composition (mg/kg d wt) in the carpels and seeds collected from plants exposed to 0 to 500 mg/kg *n*CeO_2 in Low organic matter soil (LOMS) and Organic matter enriched soil (OMES). Values are expressed as mean ± SE (n=4). The values with different letters within each soil type represent significant difference at $p \leq 0.05$.

		Carpels					Seeds							
		Ca	K	Mg	P	S	Ca	K	Mg	P	S	N	Ca/P	Na/K
	0	8640 ±	24645 ±	3757 ±	3613 ±	1646 ±	1230 ±	15218 ±	1880 ±	6757 ±	2783 ±	3.7 ±	0.18 ±	0.0055 ±
LOW		632 ab	1544 a	130 a	309 a	140 a	149 a	983 a	74 a	475 a	143 a	0.1 a	0.01 a	0.0013 a
ORGANIC	62.5	8264 ±	25359 ±	3727 ±	4168 ±	1771 ±	1451 ±	15019 ±	1815 ±	5930 ±	2399 ±	3.4 ±	0.25 ±	0.0047 ±
MATTER SOIL		157 a	678 a	120 a	148 a	93 a	286 a	1065 a	188 a	937 a	270 a	0.2 a	0.05 a	0.0007 a
	125	6890 ±	23574 ±	3103 ±	3299 ±	1635 ±	1067 ±	13746 ±	1752 ±	5313 ±	2601 ±	4.2 ±	0.20 ±	0.0058 ±
		390 a	1355 a	64 a	254 a	172 a	58 a	706 a	122 a	151 a	50 a	0.1 b	0.02 a	0.0003 a
	250	11152 ±	27185 ±	3806 ±	3992 ±	1983 ±	1487 ±	16641 ±	1944 ±	5432 ±	2606 ±	3.8 ±	0.27 ±	0.0042 ±
		639 b	1031 a	184 a	276 a	92 a	230 a	504 a	65 a	184 a	88 a	0.2 a	0.04 a	0.0002 a
	500	8571 ±	23711 ±	3446 ±	3831 ±	1748 ±	1586 ±	16880 ±	1963 ±	7380 ±	2674 ±	3.6 ±	0.22 ±	0.0053 ±
		979 ab	2039 a	312 a	507 a	173 a	103 a	406 a	33 a	165 a	29 a	0.1 a	0.01 a	0.0011 a
ORGANIC	0	6904 ±	21385 ±	2996 ±	3230 ±	1415 ±	1513 ±	16449 ±	1905 ±	8293 ±	3028 ±	3.5 ±	0.19 ±	0.0050 ±
MATTER		458 a	1915 a	130 a	302 a	159 a	205 a	836 a	66 a	512 a	100 a	0.1 a	0.03 a	0.0004 a
ENRICHED	62.5	7221 ±	24017 ±	3162 ±	4819 ±	2353 ±	1450 ±	15473 ±	1782 ±	7966 ±	2755 ±	3.5 ±	0.18 ±	0.0045 ±
SOIL		769 a	0 a	80 a	210 b	223 b	159 a	1389 a	135 a	780 a	228 a	0.2 a	0.01 a	0.0007 a
	125	5876 ±	24070 ±	2785 ±	4294 ±	2190 ±	1818 ±	17641 ±	1930 ±	7374 ±	2587 ±	3.0 ±	0.24 ±	0.0034 ±
		270 a	962 a	56 a	250 ab	160 b	266 a	571 a	41 a	231 a	57 a	0.1 a	0.03 a	0.0001 a
		6687 ±	23217 ±	3067 ±	4068 ±	2338 ±	1910 ±	17801 ±	1973 ±	9646 ±	3095 ±	3.1 ±	0.20 ±	0.0045 ±
	250	1233 a	545 a	338 a	534 ab	161 b	312 a	641 a	103 a	860 a	301 a	0.2 a	0.03 a	0.0008 a
		4799 ±	20646 ±	2696 ±	3082 ±	1640 ±	2104 ±	17634 ±	2042 ±	9263 ±	2945 ±	3.2 ±	0.23 ±	0.0032 ±
	500	441 a	363 a	150 a	274 a	109 b	78 a	165 a	26 a	394 a	77 a	0.1 a	0.02 a	0.0001 a

Effect of *n*CeO_2 exposure on macromolecules in the seeds

Kidney beans are a major source of proteins with minimal calorie intake. Thus, it is extremely important to understand if the *n*CeO_2 exposure to bean plants may affect the protein quality. In the food industry, the protein estimation is done on the basis of crude protein content in the food, which is estimated from the total kjeldahl nitrogen content. Here, the crude protein content in the seeds from the plant exposed to 0 to 500 mg/kg *n*CeO_2 is shown in Figure 4.4. *n*CeO_2 exposure did not affect the crude protein content in the seeds from plants grown in OMES, however in LOMS, at 125 mg/kg *n*CeO_2, the protein content was significantly increased ($p \leq 0.1$) by 14%, with respect to control. It is premature to predict if the increase in protein content is a positive or a negative effect as changes in macromolecular composition affects the overall machinery of seed metabolism, growth and development. Rico *et al.* showed that various fractions of proteins show differential response to 500 mg/kg *n*CeO_2 depending on the amylose content of the rice [4].

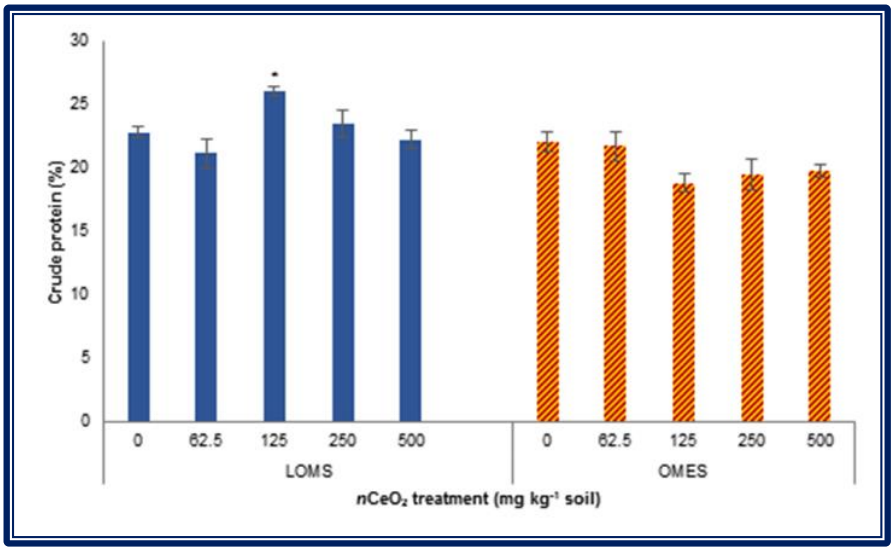

Figure 4.4. Crude protein content (%) of the seeds harvested from plants exposed to 0 to 500 mg/kg *n*CeO_2 treatments in Low organic matter soil (LOMS) and Organic matter enriched soil (OMES). Values are expressed as mean ± SE (n=3). Bars with * within same soil type, represent significant difference at $p \leq 0.1$.

Figure 3.5A and 3.5B presents the total soluble sugar (TSS) and starch content in the seeds obtained from the 96 days exposure to *n*CeO_2 in LOMS and OMES. Results suggest that in LOMS and OMES grown plants, varying SOM or *n*CeO_2 exposure do not affect the TSS content in the legume seeds. However, seed starch content was reduced ($p \leq 0.1$) at 125 mg *n*CeO_2/ kg LOMS, but significantly increased at 125 mg *n*CeO_2/ kg OMES with respect to control. Previous studies in rice suggest similar observation in TSS, but the starch content was decreased at 500 mg/kg *n*CeO_2 [4]. On contrary, in corn, only TSS was increased significantly with *n*CeO_2 treatment at 800 mg/kg soil [14]. The decrease in starch content in the 125 mg *n*CeO_2/ kg LOMS, could be due to breakdown of starch to glucose, as is apparent from the simultaneous increase TSS content, although statistically insignificant (Fig. 3.5A). Thus, seeds from plants exposed to 125 mg *n*CeO_2/ kg LOMS was found to store more protein and less starch, compared to control, thereby affecting their nutritional quality. 125 mg *n*CeO_2/ kg OMES seeds showed consistent positive response with respect to control in terms of sugar content, mineral composition and yield, as discussed in previous sections.

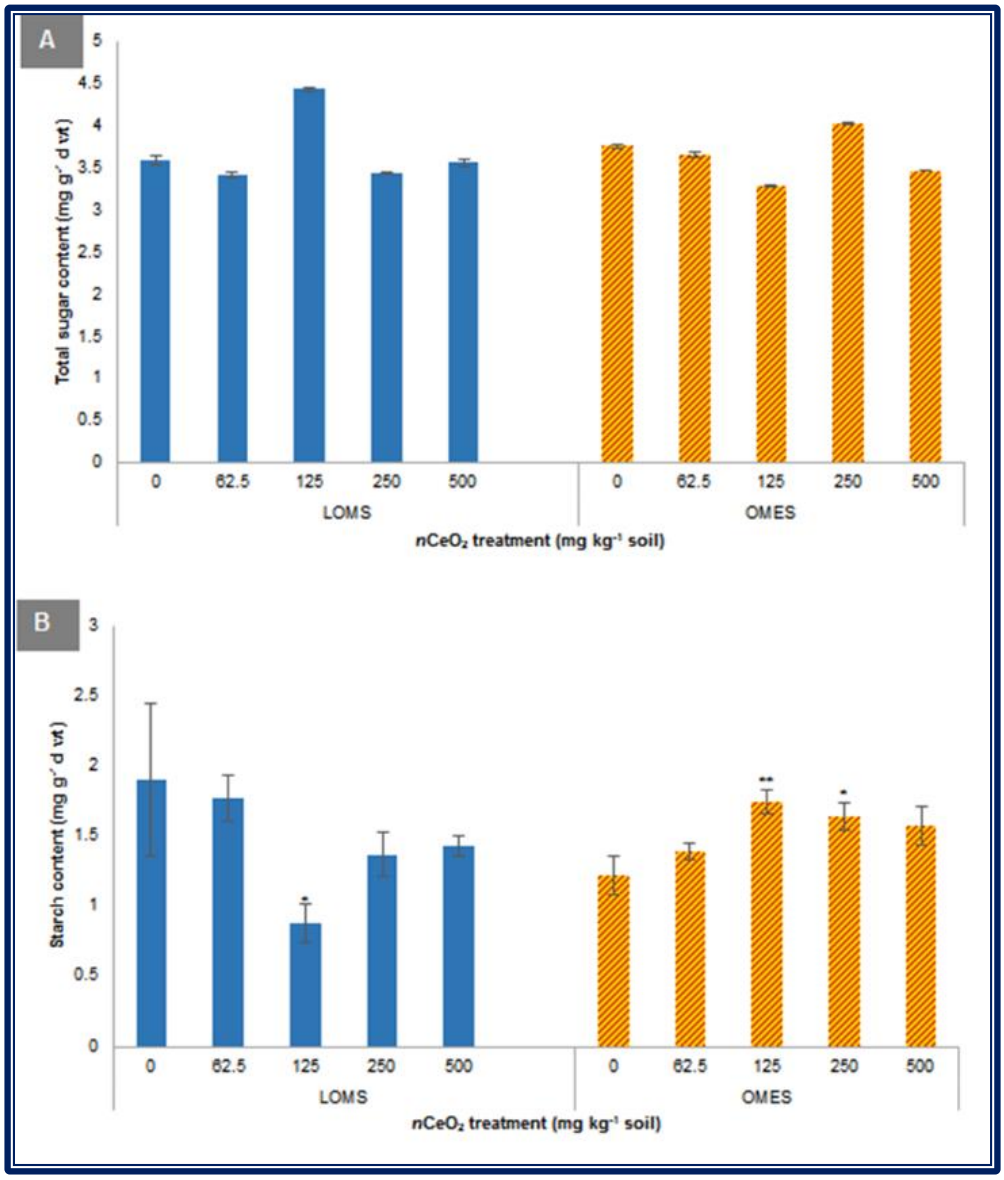

Figure 4.5. (A) Total soluble sugar content, and (B) Starch content in seeds harvested from plants exposed to 0 to 500 mg/kg nCeO$_2$ treatments in Low organic matter soil (LOMS) and Organic matter enriched soil (OMES). Values are expressed as mean ± SE (n=3). Bars with * and ** within same soil type, represent significant difference at $p \leq 0.1$ and 0.05, respectively.

4.3.4 FTIR analysis of the seeds

Fourier transform infrared spectroscopy is a well-established, simple and non-destructive technique used to study the variation in functional groups in plants in response to abiotic and biotic stress [37,38]. Recent studies have employed attenuated total reflectance FTIR (ATR-FTIR) as

well as FTIR- infrared microspectroscopy for bulk and *in situ* chemical composition in plant tissues exposed to various nanoparticles [4,5,9], or for detection upon *in situ* nanoparticle biosynthesis [39]. Figure 6 shows the ATR-FTIR spectral analysis of the seeds obtained after 96 days of *n*CeO_2 exposure to plants grown in LOMS and OMES. The assignment of peaks and the comparison between the major peaks of the treatments in LOMS and OMES have been provided in Table 4.3. As shown in Table 4.3, the FTIR spectra of the seeds obtained from *n*CeO_2 treatments in LOMS, showed slight shifting (<10 cm^{-1})in the peaks assigned for lipids (≈ 2800-3200, 1720-1740 cm^{-1}), in the overlapping band region (1500-1800 cm^{-1}) signifying amide II, lignin, phenol and polyphenols, and in the amide I region (≈ 1550) [32,34]. However, in OMES seeds, vibrational shifting of the band region signifying the polysachharides and carbohydrates was observed at 500 mg/kg *n*CeO_2 (900-1200 cm^{-1}). Previous studies with *n*CeO_2 in rice and cilantro have also reported changes in peaks denoting functional groups associated with carbohydrates [4,9]. The IR intensities in Figure 4.6A suggests that in *n*CeO_2 exposed plants grown in LOMS produced seeds that were affected primarily in the amide region, especially at 62.5 mg/kg *n*CeO_2. The seeds obtained after *n*CeO_2 exposure in OMES were affected to a higher extent in terms of IR intensities in the lipids, amide I and amide II regions. This can be attributed to significant increase in Ce accumulation in the seeds with increasing *n*CeO_2 concentration in the OMES. Sulfur, which plays role in formation of amino acids, proteins, and lipids, was also increased significantly with *n*CeO_2 exposure in OMES. This might have led to changes in the IR intensities in the amide regions, more than that in LOMS seeds.

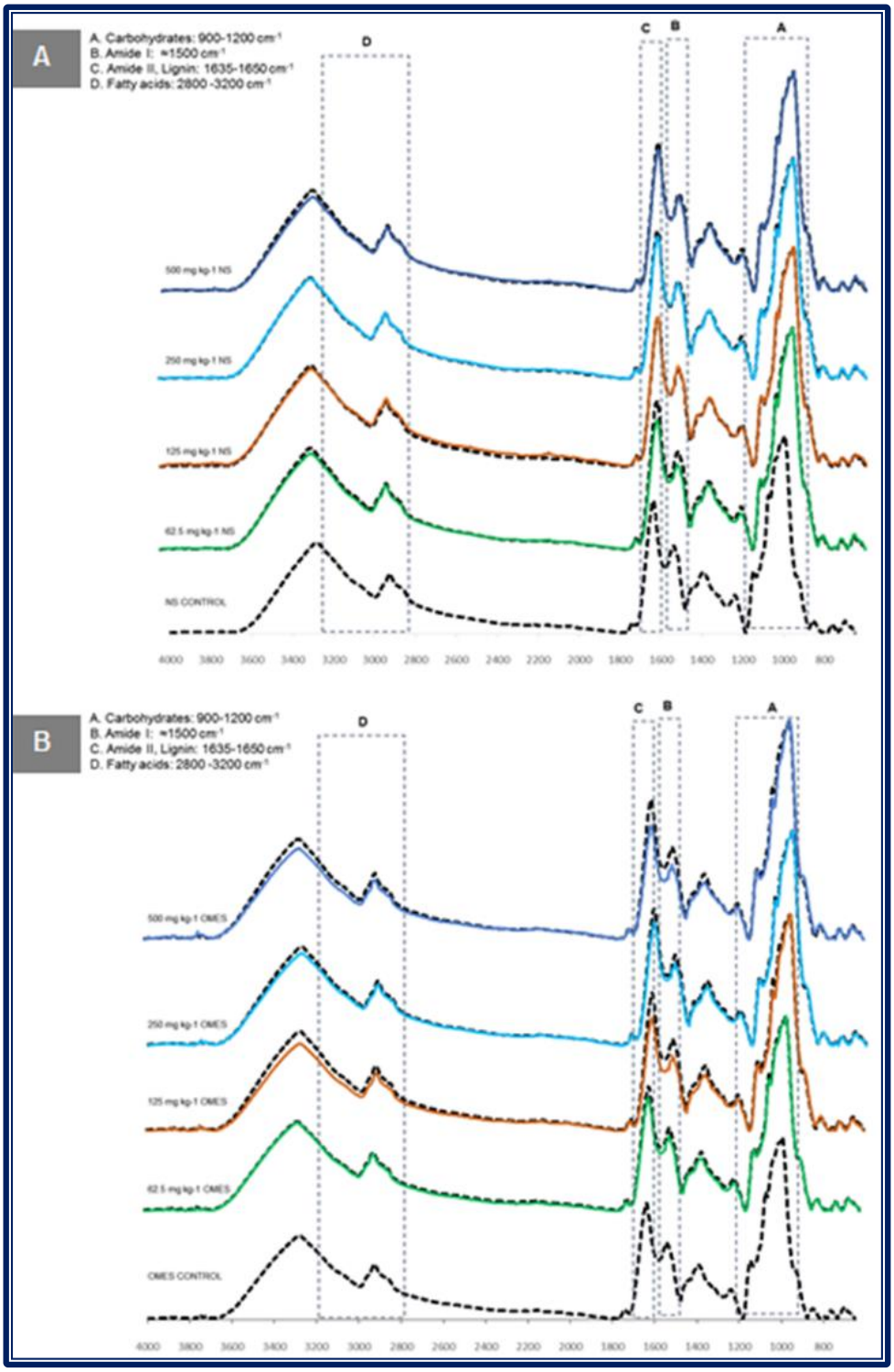

Figure 4.6. (A) Low organic matter soil (LOMS), (B) Organic matter enriched soil (OMES), FTIR spectra of seeds harvested from plants exposed to 0 to 500 mg/kg *n*CeO_2 treatments. Assignment of spectra region was adapted from Dokken *et al.* Black Dotted lines indicate the controls in respective soils.

Table 4.3. FTIR vibrational shifts corresponding to band regions in the seeds obtained from plants exposed to 0 to 500 mg/kg *n*CeO_2. The band regions have been referred from Dokken *et al.*[34] and Taoutaou *et al.* [32].

Low organic matter soil									
nCeO_2 (mg/kg soil)	Vibrational shifts								
	Lipids		Lipids	Lignin/ Amide II	Amide I	Carbohydrate			Lignin
Control	3284	2925	1739	1635	1539	1242	1146	1074	853
62.5	3277	2926	1736	1640	1542	1242	1146	1074	851
125	3275	2925	1735	1640	1542	1242	1145	1074	853
250	3276	2926	1735	1635	1542	1242	1147	1074	852
500	3285	2926	1735	1640	1542	1241	1145	1074	852

Organic matter enriched soil									
nCeO_2 (mg/kg soil)	Vibrational shifts								
	Lipids		Lipids	Lignin/ Amide II	Amide I	Carbohydrate			Lignin
Control	3285	2925	1735	1640	1542	1239	1147	1074	853
62.5	3277	2926	1735	1640	1542	1238	1147	1074	853
125	3276	2925	1735	1640	1542	1238	1146	1074	852
250	3275	2925	1735	1640	1542	1238	1146	1074	851
500	3276	2924	1734	1640	1542	1242	1147	1075	853

4.4 Conclusion

In this report, for the first time we prove that SOM content serves as a factor for the impact of nanoceria on nutritional quality of the edible tissues of a plant. Under natural conditions, soil quality may vary significantly, thereby affecting the fate of nanoparticles in the plant system. This is an important factor for consideration while performing fate and transport studies of nanoparticles. In this study we establish that the two different soils varying in their organic matter content differentially affected the legume yield, health and nutrition. The organic matter in the soil associates with the nanoparticles and the minerals in the soil, thereby affecting the overall health of the plant.

CHAPTER 5

Quantitative proteomic analysis provides evidence of nanoceria affecting bean quality

5.1. Introduction

Compared to microsized bulk-ceria particles, at the nanoscale, the surface defects pertaining to oxygen vacancies increases drastically due to enhanced surface area [1]. This allows facile transition between the two oxidation states (Ce(III)/Ce(IV)) on the lattice surface, depending on the partial oxygen pressure in its surrounding [2]. Owing to these unique properties, nanoceria ($n$$CeO_2$) are widely being researched for their applications in fuel cells, industrial catalysis, glass and metal polishing, agriculture, planarization, and biomedicine [3]. Applications of $n$$CeO_2$ in the field of biomedicine is rapidly expanding due to some groundbreaking research showing their antioxidant properties, mimicking H_2O_2 scavenging enzymes like catalase and superoxide dismutase in near neutral buffered solutions [2,4]. However, in *in vitro* studies with human cells, nanoceria has demonstrated contrasting effects depending on the particles size and cell type [5,6]. Prior to commercializing $n$$CeO_2$ in products with human as the end-user, complete life cycle and risk assessment studies must be performed.

With increasing applications of $n$$CeO_2$, the possibility of their exposure to plants, animals, beneficial microbes and humans, and concern regarding their fate in various environmental milieu has escalated [7]. The major routes of human exposure to $n$$CeO_2$ might be either through direct contact with these nanoparticles (NPs), by inhalation from the ambient air or dust particles, or indirectly through consumption of food, deliberately or accidentally contaminated during production, storage or packaging. Studies have shown that $n$$CeO_2$ when present in soil media, can reach the edible parts of the plants [8-14]. Simultaneously, studies have also reported that $n$$CeO_2$ modulates the nutrient content, antioxidant properties and macromolecular composition in the edible tissues [8,11,12,14,15]. However, there is a major knowledge gap in the understanding of the molecular mechanisms behind the morphological, physiological and biochemical changes in the plant tissues in response to $n$$CeO_2$ exposure. Thus, it is of high significance to understand the

mechanisms at the cellular and molecular level, as it will help us to comprehend if the modification in the nutrient quality is beneficial or if the *n*CeO_2 is negatively affecting the food quality. This will also enable us to identify biomarkers of xenotoxicity and also expand scope in the field of crop improvement and nanomaterial safety.

Omic technologies are extremely instrumental in the understanding of responses to abiotic or biotic stress at the cellular and molecular level in living organisms. Proteomic analysis aids the understanding of the information flow within cells through protein pathways and their relevant functions in physiological processes [16]. Previously, proteomic analysis in plant tissues have been mostly performed to study the diversity among species and for uncovering protein identification and function [17,18]. Very recently, proteomic analysis has been used to explore the impact of silver nanoparticles (Ag NPs) on plants grown in petri dishes for short-term exposure studies [19,20]. In rocket (*Eruca sativa*) roots, Ag NPs were found to cause changes in the proteins involved in redox regulation and sulfur metabolism [19]. In rice (*Oryza sativa*), Ag NPs were found to upregulate the expression of ROS detoxification enzymes and affect Ca^{2+} regulation in the root tissues [20]. However, there have been no studies to the best of our knowledge, on the expression of proteins in the edible parts of plants obtained after a full life cycle study following NP exposure. To understand the interaction at the nano-bio interface or indirect responses from disturbances caused in the cells due to NP exposure, it is pertinent to adopt *omic* technologies for nanotoxicological studies. In quantitative proteomic analysis in plants, 2D Gel electrophoresis (2D GE) has been for long, the method of choice [17,19,20]. The most common approach employed the separation of proteins using 2D GE, followed by excision of the gel spots, identification and quantification of the peptides using mass spectrometry (MS). However, label free and gel free shotgun techniques coupled with MS are currently state-of-the-art tool as they allow sensitive, high throughput, unbiased profiling of the entire proteome with high accuracy of quantification [21]. In this study, we performed the first gel and label free, shotgun quantitative proteomic analysis of the seeds obtained upon full maturity of the kidney bean plants exposed to a range of

0 to 500 mg nCeO$_2$/kg soil. This study provides strong evidence that nanoceria affects the nutritional and metabolic processes in kidney beans.

5.2. Materials and Methods

5.2.1. Nanoceria exposure

The nCeO$_2$ (≈8 nm, Meliorum Technologies, Rochester, NY) used in this study were obtained from The University of California Center for Environmental Implications of Nanotechnology (UC-CEIN). As previously reported by Keller *et al.* [22], they were 100% cubic ceria, rod-shaped measuring (67 ± 8) nm × (8 ± 1) nm, (≤10% polyhedra: 8 ± 1 nm). The purity of the nCeO$_2$ was confirmed to be 95.14%, with a surface area of 93.8 m^2g^{-1} [22]. The nCeO$_2$ suspensions were prepared according to procedure described in Chapter 3. Briefly, requisite amount nCeO$_2$ were suspended in Millipore water (MPW) and sonicated for 30 min at 25°C, and mixed homogenously with the soil to prepare final concentrations of 62.5, 125, 250, 500 mg nCeO$_2$/kg soil. The detailed characteristics of the soil have been provided in Chapter 3. The nCeO$_2$ amended soils were placed in plastic pots (7 1/2" dia. x 6" H) and each treatment was performed in triplicates. After 24 h of equilibration time, fifteen kidney bean (*Phaseolus vulgaris* var. red hawk) seeds were equidistantly placed in each pot, at a depth of 1 in. Soil mixed with MPW only, soil served as the untreated control for the experiment.

5.2.2. Plant growth conditions.

The pots were initially placed in a growth chamber (Environmental Growth Chamber, Chagrin Falls, OH) with 14 h photoperiod (340 μmole $m^{-2}s^{-1}$), 25/20°C day/night temperature and 65-70% relative humidity. After 7 days they were transferred to greenhouse with similar photoperiod, temperature and humidity. The plants were watered every 24 h, with 200 mL MPW for the first 15 days of plantation. The irrigation water was then increased to 400 ml due to increased transpiration by the leaves until seeds started desiccating.

5.2.3. Harvesting and storage

The pods started appearing after 45-50 days of planting, but reached maturity in 96-102 days. The pods were considered matured when they cracked open to reveals the desiccated dark-red colored seeds within. The seeds from each treatment were collected and stored at 4°C for further analyses.

5.2.4. Protein extraction

The matured seeds from each treatment were freeze dried in set of three seeds per replicate to obtain a representative sample. The seeds were then pulverized into fine powder in liquid nitrogen using prechilled mortar and pestle, and stored immediately at -80°C until use. Proteins were extracted according to Lee and Koh, from three representative biological replicates, each composite of three seeds [18]. Briefly, 150 mg of the powder was suspended in extraction buffer (100 mM Tris-HCl pH 8.5, 5 mM DTT, 1 mM EDTA, 1% (m/v) dodecyl-b-maltoside, and 1% (v/v) Plant Proteinase Inhibition Cocktail; Sigma, St. Louis, MO, USA) using pulse sonication for 1 min. After 30 min of incubation at room temperature, the extracts were centrifuged at 14,000 xg for 15 min. To obtain sufficient amount of protein for proteomic analysis, we performed two distinct protein precipitation procedure. One set of extracted proteins were precipitated overnight with chilled acetone, and the other set with chilled 10% (v/v) TCA/Acetone, followed by three times acetone wash. The precipitated protein pellets were resolubilized in 400mM NH_4HCO_3 containing 8M Urea. Protein concentration in each sample was quantified using BCA kit.

5.2.5. Protein digestion and 1D nanoLC -MS/MS analysis

From each extracted protein sample, 600 µg of protein was obtained and subjected to trypsin digestion. Briefly, the aliquots were reduced with 5 mM DTT for 30 min at 55°C. Reduced thiol groups were alkylated with 10 mM iodoacetamide at room temperature for 30 min, and diluted 8 fold to a final concentration of 1M urea, 50mM NH_4HCO_3. 6 µg of sequencing grade trypsin (Sigma-Aldrich) was added and the samples were digested overnight at 37°C. The protein digestion was quenched with TFA to a final concentration of 0.05% TFA. Resulting tryptic

peptides were then desalted with 100mg C18 cartridges (Supelco) for LC–MS/MS analyses. The aliquots from two different precipitation procedures, were mixed and run as one sample. We analyzed 18 biological replicates, three from control seeds, three from each dose (62.5, 125, 250 and 500 mg *n*CeO_2 /kg soil), and three from untreated parental seeds (as a negative control). Each biological replicate was run in technical triplicate, thus, totaling 54 samples subjected to 1D LC-MS/MS analysis.

LC-MS/MS analyses were performed on an Ultimate 3000 RSLC nano system online coupled to a Q-exactive (Thermo Scientific). Peptides were introduced to the analytical column (Acclaim® PepMap RSLC, 75 μm × 15 cm, nanoViper, C18, 2 μm, 100 Å) and separated using a 90 min gradient from 5 to 40% solvent B at a flow rate of 300 nl/min (solvent A: 0.1% formic acid 5 % acetonitrile, solvent B: 0.1% FA 80% acetonitrile). The mass spectrometer was operated in a data-dependent mode. Full scan MS spectra were acquired at a mass resolution of 70,000 (mass range 400-1600 m/z and AGC target value of 1E6) in the Orbitrap analyzer. Tandem mass spectra of the 10 most abundant peaks of a full scan MS spectrum were acquired following peptide fragmentation using higher-energy collisional dissociation (HCD) at a mass resolution 17,500 (AGC target value of 2E5, NCE 28%, isolation width 4 m/z). The dynamic exclusion time was set at 15 sec.

5.2.6. Protein identification semi-quantification, and statistical analysis

For protein identification and quantification, MS/MS spectra were searched against the *Phaseolus vulgaris* and *Glycine max* UniProt sequence database (downloaded on November 21, 2013) using X! Tandem search engine. In the database search, mass tolerances were set to 10 ppm and 0.02 Da for precursor and fragment ions, respectively, and up to two missed cleavages were allowed. Carbamidomethylation of cysteine was included as fixed modifications, and oxidation of methionine and deamidation of asparagine, glutamine were allowed as variable modifications. To control the overall false discovery rate (FDR) in the peptide identification and subsequent protein

assembly, the PeptideProphet and ProteinProphet algorithms implemented in the Trans-Proteomic Pipeline (TPP) were used to control the overall FDR at 1% at both levels [23,24].

For protein quantification, a semi-quantification method called spectral counting was employed, which tallies the number of MS/MS spectra assigned to any peptides belonging to each protein [25]. The Abacus tool was used to perform spectral counting [26], since the algorithm provides an automated spectral counting with robust treatment of ambiguity due to shared peptides in homologous proteins. The resulting spectral count data was analyzed using the QSPEC software [27], which performs model-based statistical analysis of differential protein expression for spectral count data. The software reports the statistical significance score (Z-statistics) and the associated local and global FDR, which was targeted to control the FDR at 10%. The rationale for using a rather large FDR is that, the total expected number of false positives is still low at 10% when only a moderate number of proteins are reported as differentially expressed, which was the case in all comparisons performed in this data.

5.3 Result and Discussion

5.3.1 Protein identification and grouping

Seeds harvested after 96 days of exposure to 62.5, 125, 250, 500 mg *n*CeO_2/kg soil were subject to proteomic analysis using LC MS/MS based shotgun technique. Seeds from the plants irrigated with Millipore water served as the control, and the parental seeds were used as negative control for reference. A total of 659 proteins were identified using X! Tandem, against the UniProtKB/Swiss-Prot databases for *Phaseolus vulgaris* and *Glycine max. G. max* database was used in this study along with *P. vulgaris* because it is better characterized than the latter. Also, these two genus plant species share extensive macrosyntentic relationships and a number of phenotypes, controlled by similar sets of genes [28]. Phylogentetically, these two species belong to the same group of papilionoid legumes, referred to as the core Phaseoleae [28]. The entire list of identified proteins in all the treatments along the three biological and three technical replicates have been provided in Appendix 1.

All the differentially expressed proteins at FDR ≤ 10 were identified with respect to untreated control, and categorized into upregulated and downregulated groups. Gene ontology analysis was performed only in differentially expressed proteins. The list of all differentially expressed proteins with their respective gene annotation in terms of cellular component, biological process and their molecular function, have been provided in Table 5.1. Twenty three proteins were differentially expressed at FDR ≤ 10%, out of which only two were upregulated at 125 and 250 mg *n*CeO_2/kg soil treatments. On the other hand, twenty one proteins were downregulated with respect to untreated control, combining all the proteins underexpressed in seeds from 62.5 to 500 mg *n*CeO_2/kg soil treatments. The differential expression of proteins in *P. vulgaris* seeds were dose-dependent as discussed in the following sections. The lowest dose of 62.5 mg *n*CeO_2/kg soil did not affect the proteome of the *P. vulgaris* seeds as seen in Table 5.1.

As shown in Figure 5.1, A hierarchical clustering analysis of the relative abundance of the 44 differentially expressed proteins (FDR ≤ 20%) was performed in the beans harvested from plants exposed to 0, 62.5, 125, 250 and 500 mg *n*CeO_2/kg soil. Spectral count data was transformed by log2 transform and the data was centered by the median of the three controls in each protein. The clustering was done with the agglomerative algorithm based on the Euclidean distance. In Figure 5.1, the colors in the heat map indicate the relative abundance of proteins in each dose level relative to the log2 transformed spectral count data in the controls (red = up-regulation, blue = down-regulation). The hierarchial clustering analysis between the untreated control and parental control has been provided in Appendix 2 for reference. It is apparent from Figure 5.1 that different proteins had different degree of regulation along the dose level; mostly being downregulated. There are no reports on the toxicity at the molecular level in the fruits obtained from plants exposed to NPs. However, there are some investigations at the proteomic or/and genetic level of the plant root tissue which were in direct contact with Au NPs [19,20] and *n*CeO_2 [29]. Vannini *et al.* [19] showed that 32% proteins were downregulated in the roots of rocket plants exposed to 10 mg/l for 5 days. In a similar study in rice roots exposed to 60 mg/l Ag NPs, abundance of proteins spots in 2D GE revealed upregulation of 18 and downregulation of 5 proteins [20].

5.3.2 Upregulation of seed proteins at low *n*CeO_2 doses

As seen in Table 5.1 and Figure 5.1, only defensin D1 and purple acid phosphatase were overexpressed in the seeds from 125 and 250 mg *n*CeO_2/kg soil. However, no proteins were upregulated at the highest treatment of 500 mg *n*CeO_2/kg soil. Defensin D1 is a stress response protein which was elevated at 125 and 250 mg *n*CeO_2/kg soil, indicating that *n*CeO_2 induced stress in the beans. Ag NPs and $AgNO_3$ have been shown to induce proteins related to redox regulations like glutathione S-transferase and superoxide distmutase, and universal stress proteins [19]. Overexpression of antioxidative enzyme isoforms has been previously reported in plants in response to heavy metals [30]. Sulfur is a very important constituent of antioxidative stress enzymes like glutathione S-transferase and stress related compounds like methionine and cysteine [19]. This corroborates our findings from the Phase II, where sulfur content in the bean carpels was significantly ($p \leq 0.05$) enhanced upon *n*CeO_2 exposure. Defensin has been shown previously to play role in tolerance to zinc in *Arabidopsis halleri*, a hyperaccumulator of zinc [31]. Thus, in this study at 125 and 250 mg *n*CeO_2/kg, defensin helps to combat stress. Purple acid phosphatases are a family of enzymes associated with phosphate acquisition and generation of reactive oxygen species in response to stress [32]. Phosphorus is an important macronutrient responsible for energy metabolism in the form of ATP, as well as biosynthesis of various biomolecules [32]. An upregulation of acid phosphatase indicate better phosphorus acquisition, which corroborates with high P content in the bean carpels of plants exposed to 125 and 250 mg *n*CeO_2/kg, as shown in Chapter 4. This indicates that at medium concentration of *n*CeO_2 (125-250 mg/kg), plant induced stress related proteins and enzymes related to macronutrient acquisition.

5.3.3 Dose dependent downregulation of seed proteins

Table 5.1 reveals that the number of downregulated proteins increased with respect to untreated control in a *n*CeO_2 dose-dependent fashion. In the seeds from 62.5 mg *n*CeO_2/kg soil treatments, only one protein (uncharacterized) responsible for cellulose biosynthetic activity, was suppressed. This protein was unaffected at other *n*CeO_2 treatments. Whereas at 125 and 250 mg

nCeO_2/kg soil, ten different proteins were negatively affected, and at 500 mg *n*CeO_2 /kg , eighteen proteins were downregulated with respect to untreated control at FDR ≤ 10%. The differentially expressed protein that were consistently affected at all three doses, 125, 250 and 500 mg *n*CeO_2/kg were phaseolin, antifungal lectin, mannose lectin, and an uncharacterized protein annotated for protein folding funtions. Phaseolin is the primary storage protein in kidney beans, and thus the name *Phaseolus* has been ascribed to this genus of leguminous crops. Phaseolin attributes for 50% of the total protein stored in bean cotyledons and 35-46% of total seed nitrogen [33]. Results from Phase II shows that N content in the seeds decreased from 3.5% in the untreated control seeds to 3% in the seeds from *n*CeO_2 exposure. The decrease was not significant, however the downregulation of phaseolin accounts for decrease observed in nitrogen and protein content. Thus, although many modification or disturbances that are not significant at physiological level, can be a serious factor towards the degradation of nutritional quality. This can only be comprehended using molecular level studies. Three other isoforms of phaseolin were downregulated in the seeds from 125 and 500 mg *n*CeO_2/kg treatments, including two alpha-type phaseolins, and one beta-type phaseolin. Among the storage proteins, legumin was also downregulated at 125 and 500 *n*CeO_2/kg soil treatments. Thus, downregulation of the expression of the major proteins of the seeds indicate depreciation in the seed quality. Downregulation of storage proteins have also been reported in germinating rice embryo in response to copper [34]. Mannose lectin belongs to a class of proteins, called "lectin" which agglutinate cells and bind to mannose, stereospecifically and reversibly [35]. Apart from mannose lectin, four proteins associated with carbohydrate metabolism were also significantly affected with respect to control. However, Peumans and van Damme have reported that they also play an important though indirect role in the plant defense mechanisms to biotic factors like bacteria and virus [36]. The downregulation of antifungal and mannose lectin indicate that *n*CeO_2 demotivates the ability of the seeds to fight against fungal or bacterial attack, thereby affecting their storage quality. Apart from these lectins, two isoforms of phytohemagglutinin, was also downregulated in the bean seeds at 250 and 500 mg *n*CeO_2/kg. Phytohemagglutinin is also responsible for defense response as well as mannose binding [37].

Thus, *n*CeO_2 exposure to kidney bean plants makes the seed more prone to biological attack, thereby reducing their storage life. Apart from proteins associated with nutrient reserve and mobilization, those associated with iron binding and ATP/GTP binding were downregulated primarily in the seeds from plants exposed to 500 mg *n*CeO_2/kg. Lipoxygenase and steroid binding protein, associated with Fe binding and fatty acid biosynthesis process were downregulated specifically at the highest exposure concentration (500 mg *n*CeO_2/kg). The downregulation of Fe binding proteins indicate that Fe mobilization to the seeds was affected, which was reflected in the reduced iron content in the seeds from 125 mg *n*CeO_2 /kg . Previous studies have shown that *n*CeO_2 affects Fe uptake by corn roots [14], as well as as accumulation in rice grains upon 500 mg *n*CeO_2/kg exposure [8]. Thus, *n*CeO_2 was shown to affect the plant metabolism pertaining to nutrient storage, micronutrient binding and accumulation as well as energy transfer.

5.4 Conclusion

To the best of our knowledge, this is the first study revealing the molecular mechanisms in the beans harvested from plants exposed to nanoparticles. Beans from 125 and 250 mg *n*CeO_2 /kg behaved alike with respect to upregulation of defense proteins. However, at high concentration, more proteins related to nutrient reserve, metabolism, and energy transfer were affected. This reveals the molecular mechanism by which *n*CeO_2 affects the micronutrient accumulation and nutrient quality. Further studies on the selected differentially expressed protein needs to be conducted to explore if such regulations also occur at the transcriptomic and genetic levels.

Table 5.1. Differential expression of proteins exposed to 62.5 to 500 mg/kg *n*CeO_2 soil with respect to untreated control. The green upward arrows indicate upregulation and the red downward arrows indicate downregulation.

Protein ID	Protein	Gene ontology			*n*CeO_2 (mg kg^{-1} soil)			
		Cellular component	Biological process	Molecular function	62.5	125	250	500
O24319	Purple acid phosphatase		dephosphorylation, metabolic processes	acid phosphatase activity, hydrolase activity, metal ion binding	-	↑	↑	-
F8QXP9	Defensin		defense response		-	↑	↑	-
Q43632	Phaseolin			nutrient reservoir activity	-	↓	↓	↓
P84869	Antifungal lectin PVAP		defense response		-	↓	↓	↓
I1MC31	Uncharacterized protein		protein folding	ATP binding	-	↓	↓	↓
Q9M7M4	Mannose lectin FRIL			carbohydrate binding	-	↓	↓	↓
P07219	Phaseolin, alpha-type			nutrient reservoir activity	-	↓	-	↓
Q41115	Alpha-phaseolin			nutrient reservoir activity	-	↓	-	↓
P24459	ATP synthase subunit alpha	Mitochondria	ATP synthesis coupled proton transport		-	↓	↓	-
P02853	Phaseolin, beta-type			nutrient reservoir activity	-	↓	-	↓
I1KPN3	Uncharacterized protein			ATP binding	-	↓	-	↓
F8QXP7	Legumin			nutrient reservoir activity	-	↓	-	↓
C6TGA8	Putative uncharacterized protein		carbohydrate metabolic process	hydrolase activity, hydrolyzing O-glycosyl compounds	-	-	↓	↓
Q41119	Peptidyl-prolyl cis-trans isomerase		protein folding	peptidyl-prolyl cis-trans isomerase activity	-	-	↓	↓
P05087	Leucoagglutinating phytohemagglutinin		defense response	mannose binding	-	-	↓	↓
Q43628	Phytohemagglutinin			carbohydrate binding	-	-	↓	↓
C6TAB7	Uncharacterized protein			intramolecular transferase activity; cellulose biosynthetic process	↓	-	-	-
I1L0N6	Uncharacterized protein				-	-	↓	-
Q9FQF9	Lipoxygenase		fatty acid biosynthetic process, oxidation reduction	iron ion binding, oxidoreductase activity	-	-	-	↓
T2DNN1	Steroid binding protein			heme binding	-	-	-	↓
B3TDK6	Lipoxygenase		fatty acid biosynthetic process, oxidation reduction	iron ion binding, oxidoreductase activity	-	-	-	↓
A7L3U9	Elongation factor 1-alpha		translation	GTP binding	-	-	-	↓
Q01899	Heat shock protein	protein folding	stress response	ATP binding	-	-	-	↓

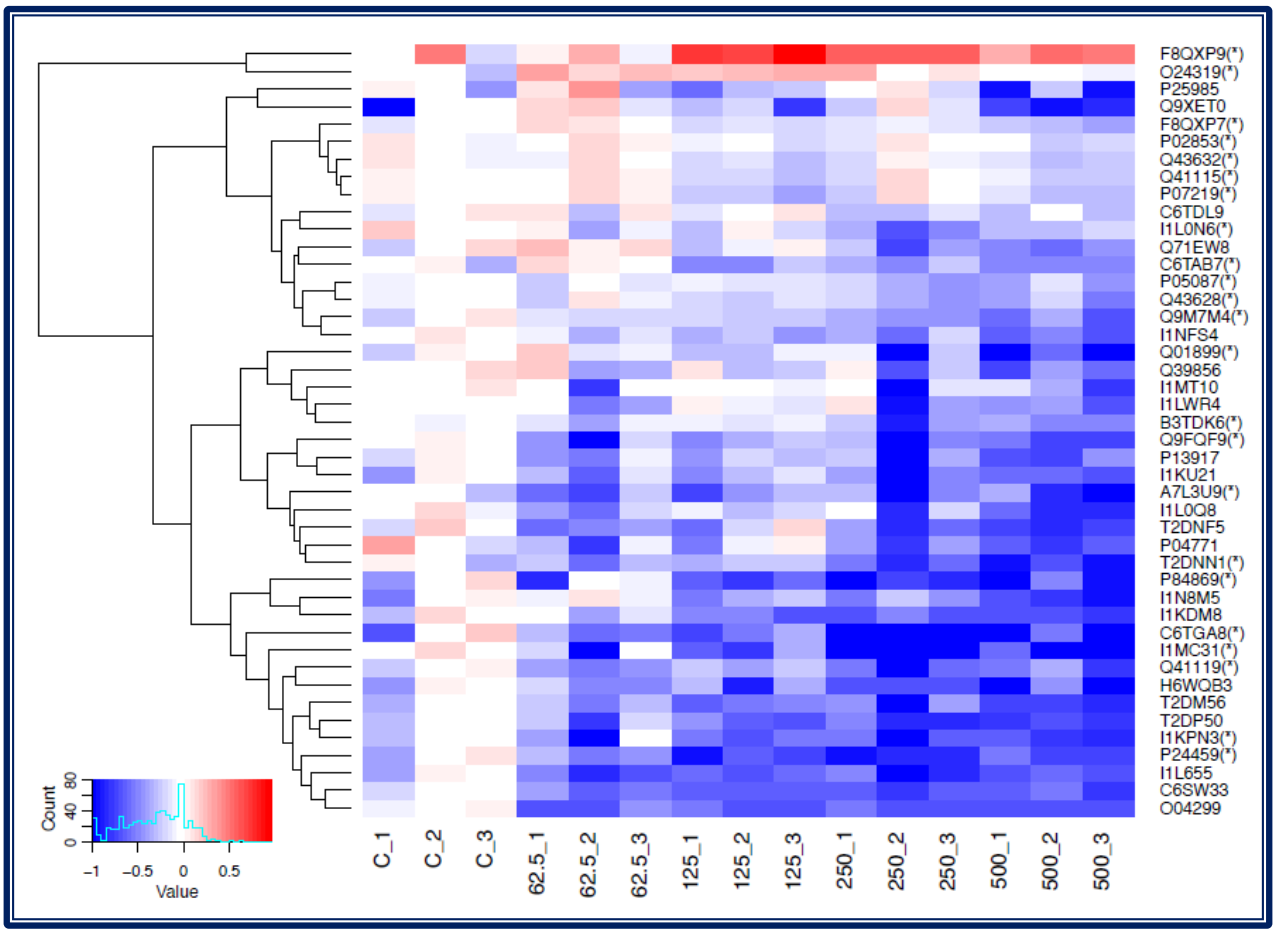

Figure 5.1 Hierarchial clustering analysis of the relative abundance of the 44 differentially expressed proteins at FDR ≤ 20% identified in the bean harvested from plants exposed to three biological replicates of 0,62.5, 125, 250 and 500 mg *n*CeO_2 /kg soil. 23 protein IDs with * indicate that the protein is differentially expressed at FDR ≤ 10%. Red = up-regulation, blue = down-regulation.

CHAPTER 6

Trophic transfer of nanoceria from Kidney bean plants to Mexican bean beetles

6.1 Introduction

With the advancement in the field of material science and microscopy, the ability to manipulate matter at the atomic scale has gained tremendous attention in scientific and engineering research. The unique properties of materials at the nanoscale have led to wide usage of the nanomaterials in multitude of applications related to energy, electronics, medicine, automotive, food and agriculture, personal care, and health and fitness [1]. Currently, fullerenes, carbon nanotubes, silver, titanium oxide, cerium oxide, zinc oxide, copper oxide and iron oxide nanoparticles are the most studied nanomaterials in terms of application as well as environmental fate and transport [2-5]. Due to no federal or international regulations on the use, release or product labeling of these nanomaterials, they are being increasingly incorporated into consumer products [1]. Compared to increasing release of these nanomaterials to the environment, studies on their fate and toxicity are lagging far behind. In the past five years, there have been numerous studies exploring acute and chronic toxicity of these materials on terrestrial and aquatic organisms as well as *in vitro* cell cultures [3,5,6]. Standardized procedures and risk assessment models are being deduced for better comparisons of the fate and toxicity of different nanomaterials varying in their size, surface charge, agglomeration properties, and dissolution rates, along a wide range of plant and animal test species [5,6].

Unfortunately, there is a huge gap in determining the routes of human exposure to these nanomaterials. Studies with plants have shown that the nanomaterials have the potential to bioaccumulate in plants tissues including their edible parts [7-12]. To address the issues of exposure routes and associated threats with the accumulation of nanomaterials in the consumers, studies related to trophic level transfers needs special attention. Several studies in aquatic systems have been performed on trophic level transfer of nanomaterials [13-20], however, studies on terrestrial ecosystem is seriously lacking. There have been two studies exploring bioaccumulation

of gold nanoparticles in tobacco [21] and tomato [22] plants, and their further transfer to tobacco hornworms. Judy *et al.* [21] provided evidences using synchrotron μ-XRF imaging and μ-XANES that gold nanoparticles were transferred to the hornworms, chemically untransformed, and were not stored in the gut region of the worms [22]. Biomagnification of these particles along the food chain was also reported [21]. In a recent study, particle-size dependent trophic transfer of cerium oxide was reported in crickets that were fed on zucchini plants grown in soil, as Ce was accumulated more in the insect tissues from the cerium oxide nanoparticles (nanoceria, *n*CeO_2) exposure than from the bulk particles [23].

In this study, kidney beans plants grown in *n*CeO_2 amended soils, were infested with larvae of Mexican bean beetles (MBB) which were allowed to feed until their adult stage. *n*CeO_2 was selected as the nanoparticle of choice, due to its increasing scope of applications in agriculture and medicine, and also due to lack of enough information on their trophic transfer. Ce accumulation in the MBB tissues at different stages of their development was studied in order to determine the potential trophic transfer of *n*CeO_2 from plants to the primary level consumers.

6.2 Materials and Methods

6.2.1 Selection of test species

Plant species

Kidney bean (*Phaseolus vulgaris* var. red hawk) plants, obtained from Michigan State University, were selected as the primary consumer, because they are fast growing plants and produce enough leaf biomass to feed the primary level consumers. They were rinsed with NaOCl and Millipore water (MPW), and soaked in MPW for 24 h before planting in soil.

Primary consumer species

Mexican bean beetles (*Epilachna varivestis*) (MBB) were selected as the primary consumer, because they are voracious predators that feed on leaves and soft tissues of kidney bean plants at their larval and adult stages [24]. They were procured from The Department of

Agriculture, State of New Jersey and the culture was maintained in a growth chamber (Environmental Growth Chamber, Chagrin Falls, OH) with 14 h photoperiod (340 μmole $m^{-2}s^{-1}$), 25/20°C day/night temperature and 65-70% relative humidity.

6.2.2 Nanoparticle exposure scenario

Previously characterized *n*CeO_2 (≈8 nm, Meliorum Technologies, Rochester, NY) obtained from The University of California Center for Environmental Implications of Nanotechnology (UC-CEIN) were used for this study [25,26]. Dissolution and stability of these particles in water has been reported in previous publications [26]. The particles were suspended in 100 mL of Millipore water (MPW) by bath sonication (Crest Ultrasonics, Trenton, NJ, USA) for 30 min at 25°C to prepare final concentrations of 1000 and 2000 mg *n*CeO_2/kg soil. The soil used in this study was prepared by mixing natural soil with Miracle Gro potting mix at a ratio of 2:1. The enrichment of soil with organic matter at this ratio was done for better plant growth and to achieve higher concentration of Ce in the aerial tissues, as observed in our previous study in Phase II (Chapter 3). The suspensions were homogeneously mixed with the soil. Soil wetted with MPW was regarded as the untreated control. After 24 h of equilibration, 4 seeds were equidistantly placed at an inch depth in the potted soils amended with *n*CeO_2 and MPW. Each treatment and control was carried out in quadruplicates and the pots were placed in the growth chamber. For each replicate, four pots containing four plants in each were prepared to replenish food for the MBBs every 5-7 days. The plants were watered with 80-100 ml MPW. Four replications of the experiment were done at two different times within four months, avoiding any chances of pseudo-replication [27]. A separate set of plantation with the same treatments was carried out to perform Ce accumulation in root, stem and leaf biomass after 22, 29 and 36 days of seeding. These days are relevant to the exposure of MBBs at different stages of their development, as discussed below.

After 22 days of growth, the leaves of the kidney plants were infested with 30 second-instar MBB larvae. The plants with the MBBs on its aboveground parts were enclosed in rearing and observation insect cages measuring 14 x 14 x 24" (Bioquip Products, CA). The replicates in each

cage were separated with cardboard sheets. The experimental set up has been demonstrated in Figure 6.1. The soil was covered along the rim of the pot with a net to avoid contamination by direct contact of MBBs with *n*CeO_2 amended soil. The second-instar larvae developed into pupae in 8-10 days, and the pupae metamorphosed into adult form in about 5-7 days. A total of 7 MBBs at different stages of their development per replicate were sampled every 7 days, starved for 24 h and finally euthanized by liquid nitrogen. Thus, the different MBB stages sampled after 7, 14 and 21 days of feeding were MBB larvae, MBB pupae and MBB adults. The feces collected from the adults during the starvation period were also collected for further analysis. Feces from all the replicates were composited into one sample to have sufficient biomass for elemental analyses.

6.2.3 Quantification of cerium in leaves and MBB tissues

After 22 days of *n*CeO_2 exposure, the leaves were severed from the plants that were grown separately for determining Ce accumulation in the leaves, and the fresh weight was recorded. The severed leaves, MBBs collected after 7, 14, and 21 days, and adult feces were oven-dried at 70 °C for 96 h. The dried tissues were then digested using plasma pure HNO_3 and 30% (w/v) H_2O_2 (1:4) mixture in a microwave accelerated reaction system (CEM $Mars_x$, Mathews, NC) according to Packer *et. al.* [28]. Ce concentration in the leaf and MBB tissues was determined using inductively coupled plasma-optical emission spectroscopy (ICP-OES) (Optima 4300 DV, Perkin Elmer) and inductively coupled plasma-mass spectrometry (ICP-MS) (Perkin Elmer ELAN DRC II, Shelton, CT), respectively. National Institute of Standards and Technology (NIST) certified standard reference material (peach leaves NIST-SRM 1547, Gaithersburg, MD) was analyzed to validate the digestion process, obtaining 90% recovery. For quality assurance/quality control, 0.5 mg/L and 10 µg/L Ce standards were analyzed every 20 samples in ICP-OES and ICP-MS, respectively.

6.2.4 Statistical Analysis

All the analyses were carried out in replicates of four, except in feces, and were reported as mean ± SE. One-way ANOVA was performed, followed by Tukey's multiple comparisons test (IBM SPSS Statistics 19, Chicago, USA).

Figure 6.1. Experimental set up for the trophic transfer experiment

6.3 Results and Discussion

6.3.1 Effect of *n*CeO_2 on plant biomass

Figure 6.2 shows the dry and wet biomass of kidney plant tissues exposed to 0, 1000 and 2000 mg/kg *n*CeO_2 soil for 22, 29 and 36 days. No significant difference in the shoot biomass

(including stems and leaves) of the plants exposed to *n*CeO_2 was observed with respect to control, throughout the exposure period. On the other hand, root fresh biomass after 29 days was significantly reduced with 1000 and 2000 mg/kg *n*CeO_2 exposure with respect to control by 48 and 66 %, respectively. Interestingly, the root dry weight was not affected, which indicates reduction in the water content of the roots. The moisture content in the roots of 29 days-old plants decreased from 91% in the control to 86 and 79% in 1000 and 2000 mg/kg *n*CeO_2 exposures, respectively. Similar reduction in root moisture content, without affecting the plant dry biomass was noted in soybeans exposed to 1000 mg/kg *n*CeO_2 for a complete life cycle of 48 days [29]. Zuchhini roots were also negatively affected in terms of biomass when exposed to 1228 mg/kg *n*CeO_2 [23]. Earlier reports on the interaction of *n*CeO_2 (0-1000 mg/kg) with different plants have shown that they have no significant detrimental or enhancement effect on the plant biomass [9,10,29]. This is in accordance with the minimal effects of *n*CeO_2 at 1000 and 2000 mg/kg on kidney bean plants' biomass observed in this study. As seen in other studies, *n*CeO_2 doesn't cause apparent injury at physiological level, but the toxicity symptoms are observed at biochemical and molecular level [9,26,30,31].

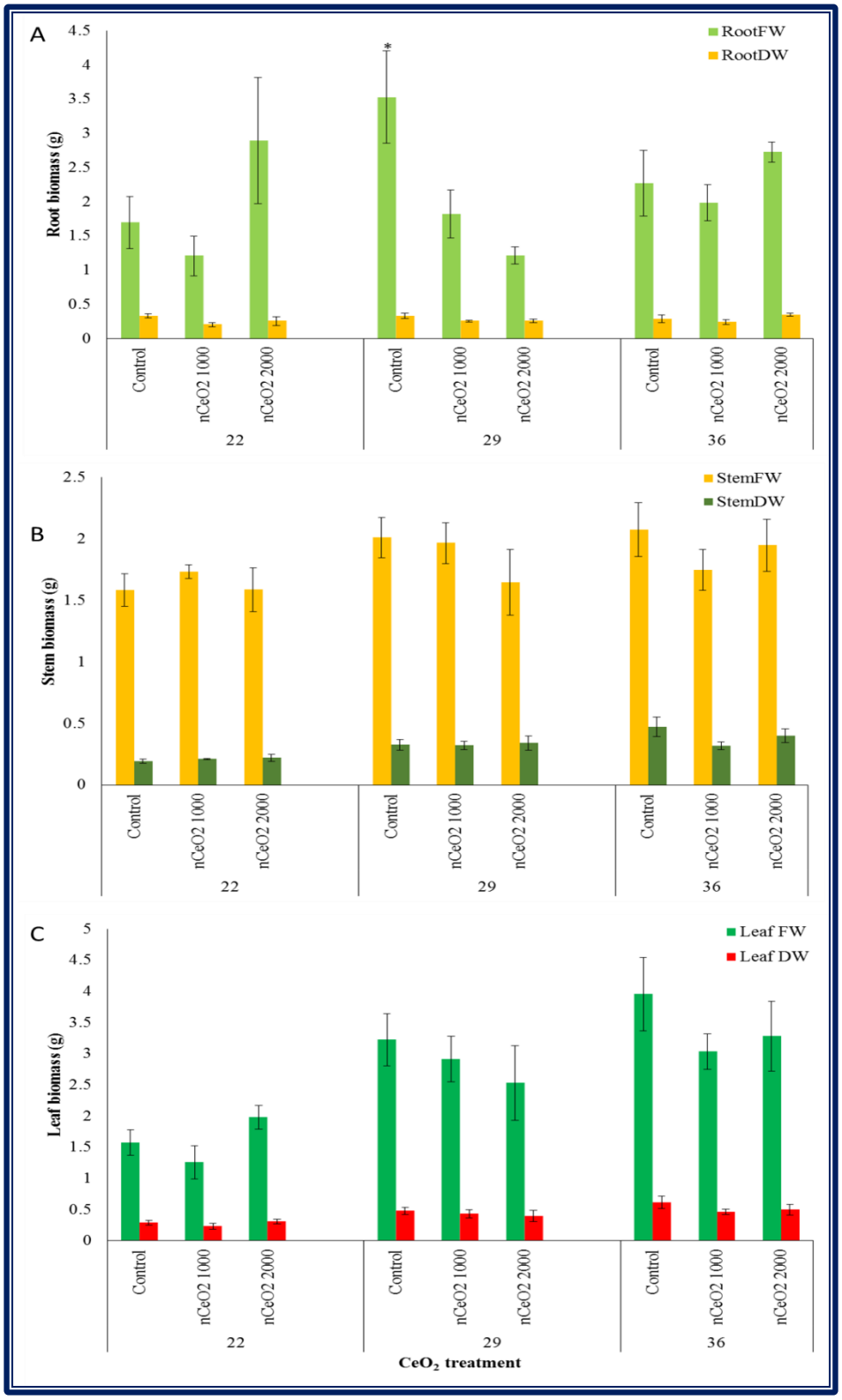

Figure 6.2. Fresh and dry biomass of (A) Root, (B) Stem, and (C) Leaf of kidney bean plants exposed to 0, 1000 and 2000 mg/kg $n$$CeO_2$ for 22, 29 and 36 days. Values are expressed as mean ± SE (n=4). Bars with * represent significant difference at $p \leq 0.05$.

6.3.2 Cerium accumulation in kidney bean plant tissues

Accumulation of cerium in different tissues of the kidney bean plants exposed to 0, 1000 and 2000 mg *n*CeO_2/kg soil for 22 days has been shown in Figure 6.3. All the plant tissues showed significant Ce accumulation ($p \leq 0.05$) with respect to control. Kidney bean roots accumulated 23 ± 2.6 and 26.5 ± 3.0 mg Ce/kg d wt tissue at 1000 and 2000 mg/kg *n*CeO_2, respectively, which was significantly higher compared to 2.1 ± 0.1 mg Ce/kg in control (Figure 6.2 A). Soil based *n*CeO_2 exposure studies in soybean and zuchhini have showed higher concentration of Ce in root tissues (210 and 567 mg/kg d wt) on exposure to 1000 *n*CeO_2/ kg soil compared to that accumulated in the kidney bean roots in this study [23,29]. This could be due to the duration of exposure for soybeans [29], which was twice that of current study. However, when compared to zuchhini [23], this variation might result from species dependent response. Morales *et al.* reported similar accumulation of Ce (40 mg/kg) in cilantro roots as in the kidney bean plants [9].

Cerium accumulation in the stems and leaves of kidney bean plant exposed to 0, 1000 and 2000 mg/kg *n*CeO_2 is shown in Figure 6.2 B and C, respectively. The Ce accumulation in the above ground biomass, especially the leaves, was of higher significance in this study due to the relevance of trophic transfer to the next consumer, through consumption of the leaves accumulating Ce. Kidney bean stems accumulated significantly ($p \leq 0.05$) higher amount of Ce in the 1000 and 2000 mg/kg *n*CeO_2 treatments (277 and 348 % higher, respectively), compared to control. The Ce concentration in the leaves of plants grown in 1000 and 2000 mg/kg *n*CeO_2 was 103 and 115% higher ($p \leq 0.05$) compared to control. The stems accumulated 2.1 ± 0.3 and 2.5 ± 0.3 mg Ce/kg d wt at 1000 and 2000 mg/kg *n*CeO_2. The leaves from both *n*CeO_2 treatments accumulated 1.1 ± 0.3 mg Ce/kg d wt. Despite of enormously higher (10-30 times) root Ce concentration in soybeans and zucchini compared to the kidney bean roots, Ce translocation to the stems were considerably lower (0.5 and 0.1 mg/kg, respectively). The kidney bean leaves accumulated similar amount of Ce as in zucchini leaves (1.5 mg/kg), but Ce accumulation in soybean was very low (0.0003 mg/kg) [23,29]. This indicates that in the kidney bean plants, Ce was effectively translocated to aerial parts, unlike in soybeans and zucchini. Translocation factor

(TF) from kidney bean roots to stems (TF_{sr} = [Ce]stem/[Ce]root) and roots to leaves (TF_{lr} = [Ce]leaf/[Ce]root) was calculated to be 0.09 and 0.04. However, in zucchini and soybeans TF_{sr} was 0.0009 and 0.003, respectively and TF_{lr} was 0.0005, 0.000001, respectively.

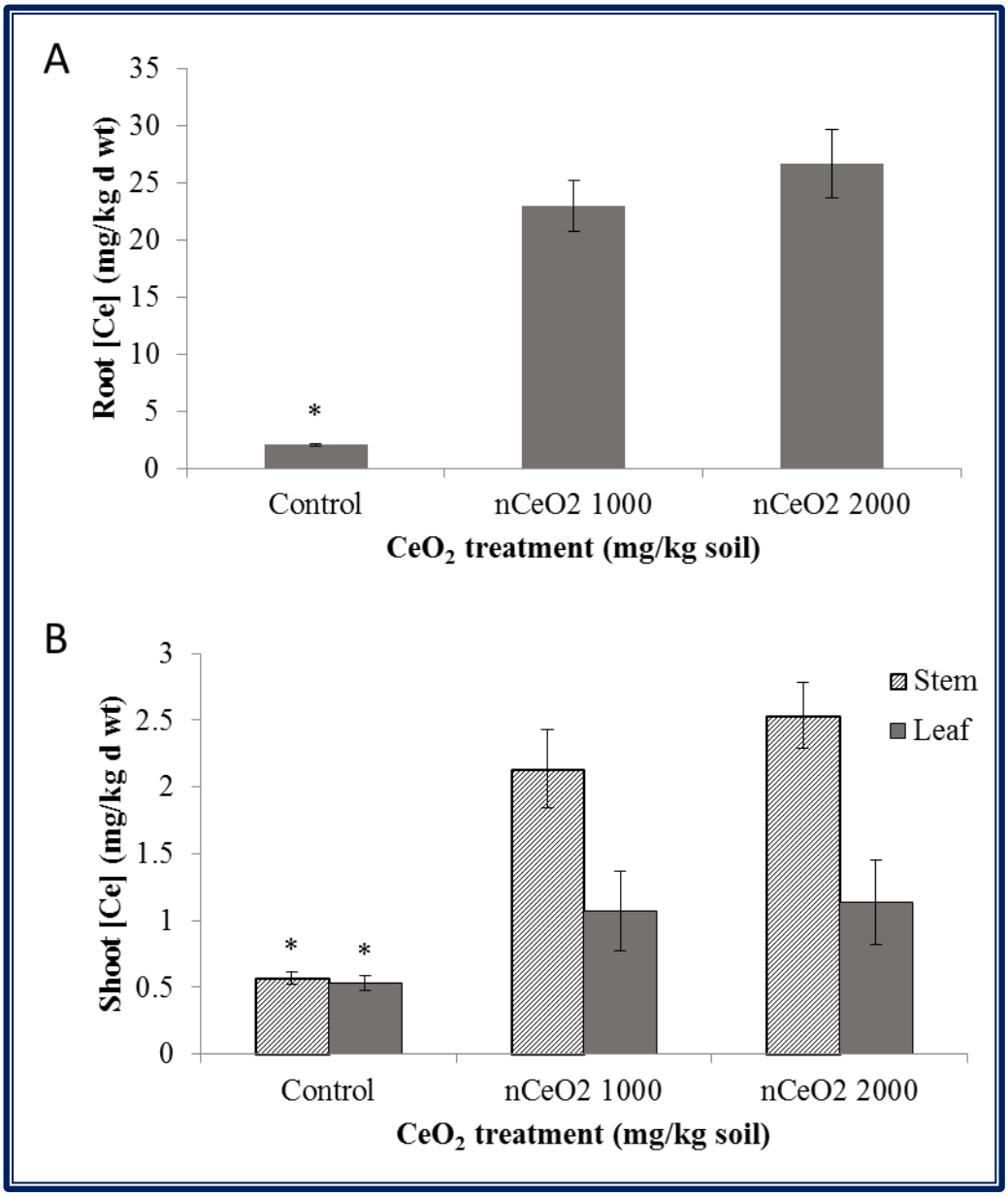

Figure 6.3. Ce accumulation in different tissues (A) Root, (B) Shoot including stem and leaf, of kidney bean plants exposed to 0, 1000 and 2000 mg/kg nCeO$_2$. Values are expressed as mean ± SE (n=4). Bars with * represent significant difference at $p \leq 0.05$.

6.3.3 Transfer of cerium from kidney bean leaves to MBBs

The accumulation of Ce in the MBB tissues at different developmental stages and adult feces are shown in Figure 6.4. Ce was detected in all the treatments including control using ICP-MS. Since Ce is a rare earth element, it is naturally present in the soil, according to the soil analysis in Chapter 3. The MBBs at the larval, pupal and adult stages were collected after 7, 14 and 21 days of feeding. Figure 6.4 reveals that the Ce concentration in the MBB larvae (499, 380, and 407 µg Ce/kg d wt) did not change within treatments. This could be due to low duration of exposure and feeding period. Also, at this stage the metabolism in the larvae is rapid, indicating that there is no accumulation of Ce in the MBB at larval stage exposed for 7 days to plants grown in 1000 and 2000 mg/kg *n*CeO_2. However, in the pupal stage, Ce detected in the tissues at 1000 and 2000 mg/kg *n*CeO_2 (523 and 1302 µg/kg d wt tissue, respectively) was significantly higher ($p \leq 0.05$) by 125 and 461%, with respect to control (232 µg/kg d wt tissue). When the MBB larva transforms into an adult, it passes through a sedentary and transitional phase called pupa. At this stage, the feeding is stopped and metabolic activities are lowered [24]. This explains the high concentration of Ce in the pupae from the *n*CeO_2 treatments. Probably, the dietary intake at larval stage just before it turns into pupa is not metabolized and excreted, thereby leading to transfer and accumulation of Ce present in the leaves to the MBB pupae tissues. As the MBB further develops morphologically into adult forms, the feeding and metabolism increases. As seen in Figure 6.4, Ce content in the adults from 1000 mg/kg *n*CeO_2 treatment increases significantly ($p \leq 0.05$) with respect to control, unlike the MBB adults feeding on 2000 mg/kg *n*CeO_2 exposed plants. The Ce content in the MBB tissues increased significantly ($p \leq 0.05$) by 32% from the pupa (523 µg/kg d wt tissue) to the adult stage (693 µg/kg d wt) at 1000 mg *n*CeO_2/kg soil exposure. However, at 2000 mg/kg *n*CeO_2 exposure, the Ce accumulation reduced in the adult tissues (395 µg/kg d wt) by 67% from the pupa tissues (1302 µg/kg d wt). To explain this variation in Ce accumulation within the growth stages and treatments, the feces were collected from the adults and analyzed by ICP-MS. Interestingly, high amounts of Ce was detected in the MBB adult feces. MBB adult feces from 0, 1000, and 2000 mg *n*CeO_2/kg soil contained 100, 478 and 800 µg Ce/kg d wt. Upon adding

up MBB adult tissue and feces Ce concentration, total Ce transferred to the adults was found to be 561, 1171, and 1196 µg/kg d wt at 0, 1000, and 2000 mg/kg *n*CeO_2. At 1000 and 2000 mg/kg *n*CeO_2, 41 and 67 % Ce was excreted as feces, thereby reducing the dietary accumulation of Ce in the MBB adult tissues. This proves that a major fraction of the Ce was stored in the guts of the MBBs. On contrary, Judy *et al.*[22] reported that tobacco hornworm (*Manduca sexta*) bioaccumulate gold nanoparticles when exposed to surface contaminated tomato plants, but the nanoparticles were not stored in the midgut, when fed on surface contaminated plant, indicating an important route of entry into a terrestrial food web. At 1000 mg/kg *n*CeO_2, Ce transfer increased significantly from MBB larvae to adult (124 %), however at 2000 mg *n*CeO_2/kg soil, it decreased by 8%. This is a very significant observation as it explains that although the Ce is transferred over trophic levels, a major part of it is excreted, thereby reducing the possible risks associated with their accumulation in the insect tissues. Similar observations were reported in a recent study with crickets feeding on zucchini plants exposed to *n*CeO_2 in soil [23]. Currently, no information is available on the toxicity of *n*CeO_2 on terrestrial insect species; however, studies with *Daphnia* species in freshwater ecosystems have provided evidence of sublethal toxic effects associated with physiological functions [18]. A recent aquatic mesocosm study with snail (*Planorbarius corneus*) demonstrated that bare *n*CeO_2 induced oxidative stress in the organism, however coating of the *n*CeO_2 had no effects pertaining to stress [20].Several studies are currently exploring the trophic transfer of nanoparticles in terrestrial [21-23] as well as aquatic ecosystems [18,19]. Previous studies on trophic transfer of gold nanoparticles in a terrestrial food chain involving tobacco plant (*Nicotiana tabacum* L. cv Xanthi) and tobacco hornworm reported biomagnification of gold nanoparticles (5, 10, and 15 nm) along the food chain [21]. However, the effect on the different growth stages of the predator/ consumer has never been studied before.

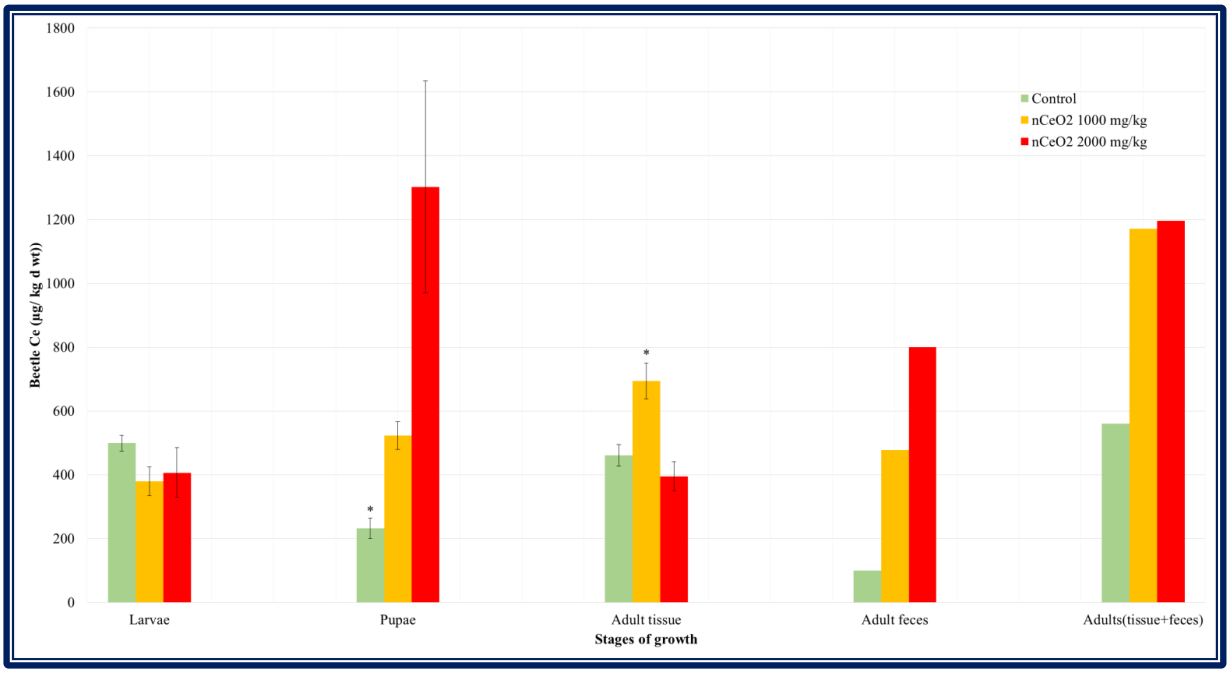

Figure 6.4. Accumulation of cerium in MBB tissues at different stages of growth. Values are expressed as mean ± SE (n=4). Bars with * represent significant difference at $p \leq 0.05$.

6.4 Conclusion

This study provides evidence of trophic transfer of nanoceria in a terrestrial food chain. It was observed that the duration of exposure as well as stages of beetle development were important factors contributing towards the accumulation in the tissues of primary level consumers. During the developmental stages with active metabolism, majority of Ce was discarded from the body in the form of feces. This is a positive sign that even though nanoparticles get transferred along the food chain, a large fraction may not be incorporated in the tissues of living organism. However, there is scarcity of information in case of chronic exposure. More studies are required on the localization and chemical speciation of the elements composing the nanoparticles in the tissues and feces of primary consumers are needed to be performed in future to conclude on the transfer of nanoparticles along the food chain.

CHAPTER 7

General Conclusions

This research was carried out to address critical gaps in the fate and toxicity of nanoceria in terrestrial ecosystems. Results provide comprehensive information on the short-term as well as long-term effects of *n*CeO_2 on kidney bean plants in regard to plant physiology, metabolism, mineral nutrition and oxidative stress response. In Phase I, synchrotron μ-XRF and μ-XANES analyses revealed that *n*CeO_2 adhered to the kidney bean roots enters the epidermis, and reaches the vascular tissues through the gaps in the Casparian strip at the emergence of lateral roots. Results from Phase I and II provided evidence of translocation of cerium to aerial tissues of plants grown in hydroponic as well as soil media. The response of the plants to *n*CeO_2 exposure, in terms of cerium translocation, metabolic activities, yield, and bean quality was significantly influenced by the soil organic matter content. Higher organic matter containing soil was found to augment cerium translocation to aerial tissues from the plant roots. This indicates increased bioavailability of *n*CeO_2 with increased organic matter content in the soil. Additionally, organic matter enrichment enhanced metabolic processes like photosynthesis and transpiration in the leaves of plants exposed to 62.5 to 250 mg/kg *n*CeO_2. Independent of the soil organic matter content, exposure to *n*CeO_2 at certain concentrations also improved bean productivity. This research was extended into molecular level studies in Phase III, where proteomic analysis of the beans harvested upon *n*CeO_2 exposure revealed that at 125 and 250 mg/kg treatments, two proteins, *defensin* and *purple acid phosphatase*, responsible for stress response and metabolism, respectively, were upregulated. However, the number of downregulated proteins increased with increasing *n*CeO_2 exposure concentration. At 125 and 250 mg/kg *n*CeO_2, 10 proteins associated with globular protein storage, carbohydrate metabolism and energy production were downregulated. Moreover, exposure to 500 mg/kg *n*CeO_2 resulted in downregulation of a total of eighteen proteins associated with protein storage, carbohydrate metabolism, ATP/GTP binding activities and iron binding activities. At the final step of this research, trophic transfer studies revealed that the Mexican bean beetle (*Epilachna*

varivestis) feeding on kidney plants cultivated in soil amended with *n*CeO_2 accumulate Ce in their tissues, depending on the exposure concentration, and their speed of feeding and metabolism, at different stages of their development. Unlike in the sedentary stage, non-feeding, and low metabolically active pupae, increased metabolism in the adults was responsible for flushing out a major fraction of Ce transferred to the beetles from the plants. In summary, interaction of *n*CeO_2 with kidney bean plants was dependent on the environmental conditions. Responses of beans to *n*CeO_2 which were insignificant at physiological level, were highly significant at the molecular level. This might affect the growth and health of the next generation of bean plants. The observed trophic transfer of *n*CeO_2 is a primary finding that entails more elaborate and long term studies in mammals to relate directly to humans.

References

CHAPTER 1

1. Roco, M. C. The long view of nanotechnology development: the national nanotechnology initiative at 10 years. In *Nanotechnology research directions for societal needs in 2020*; Roco, M. C., Hersham, M. C., Chad, A., Eds.; Science Policy Reports, Springerlink 2011; pp 1-28.
2. ASTM E2456-06. Standard Terminology Relating to Nanotechnology, Available at: http://www.astm.org/Standards/E2456.htm [accessed November 20, 2014]
3. ISO Concept Database. Nanotechnologies-Terminology and Definitions for Nano-objects-Nanoparticle, Nanofibre, and Nanoplate. Nanoscale, International Organization for Standardization, Available: http://tinyurl.com/6252dft [accessed November 20, 2014].
4. Kessler R. Engineered Nanoparticles in Consumer Products: Understanding a New Ingredient. *Environ. Health Perspect.* **2011**, *119*, A120-A125.
5. Project on Emerging Nanotechnologies, 2014. Consumer Products Inventory. Available: http://www.nanotechproject.org/cpi [accessed November 26, 2014].
6. Nanotechnology Industries Association News and alerts; Available: http://www.nanotechia.org/news/news-articles/new-definition-%E2%80%98engineered-nanomaterial%E2%80%99-eu-food-information-consumers-regulation [accessed November 26, 2014].
7. Aslani, F.; Bagheri, S.; Julkapli, N. M.; Juraimi, A. S.; Hashemi, F. S. G.; Baghdadi, A. Effects of Engineered Nanomaterials on Plants Growth: An Overview. *The Scientific World Journal*, **2014**, Article ID 641759.
8. Keller, A. A.; McFerran, S.; Lazareva, A.; Suh, S. Global life cycle releases of engineered nanomaterials. *J. Nanopart. Res.* **2013**, *15*, 1692.
9. Collin, B.; Auffan, M.; Johnson, A. C.; Kaur, I.; Keller, A. A.; Lazareva, A.; Lead, J. R.; Ma, X.; Merrifield, R.; Svendsen, C.; White, J.; Unrine, J. Environmental release, fate and ecotoxicological effects of manufactured ceria nanomaterials. *Environ. Sci. Nano*. **2014**, DOI 10.1039/C4EN00149D.
10. Walkey, C.; Das, S.; Seal, S.; Erlichman O.; Heckman, K.; Ghibelli, L.; Traversa, E.; McGinnisf, J. F.; Self, W. T. Catalytic properties and biomedical applications of cerium oxide nanoparticles. *Environ. Sci.: Nano* **2015**; DOI: 10.1039/c4en00138a.
11. Gardea-Torresdey, J. L.; Rico, C. M.; White, J.C. Trophic Transfer, Transformation, and Impact of Engineered Nanomaterials in Terrestrial. *Environ. Sci. Technol.***2014**, *48*, 2526-2540.
12. Priester, J. H.; Ge, Y.; Mielke, R. E.; Horst, A. M.; Moritz, S. C.; Espinosa, K.; Gelb, J.; Walker, S. L.; Nisbet, R. M.; An, Y. J.; Schimel, J. P.; Palmer, R. G.; Hernandez-Viezcas, J. A.; Zhao, L.; Gardea-Torresdey, J. L.; Holden, P. A. Soybean susceptibility to manufactured nanomaterials with evidence for food quality and soil fertility interruption. *Proc. Natl. Acad. Sci.* **2012**, *109,* 2451-2456.

13. Hernandez-Viezcas, J. A.; Castillo-Michel, H.; Andrews, J. C.; Cotte, M.; Rico, C.; Peralta-Videa, J. R.; Ge, Y.; Priester, J. H.; Holden, P. A.; Gardea-Torresdey, J. L. *In situ* synchrotron X-ray fluorescence mapping and speciation of CeO_2 and ZnO nanoparticles in soil cultivated soybean (*Glycine max*). *ACS Nano*, **2013**, *7*, 1415-1423.

14. Wang, Q.; Ma, X.; Zhang, W.; Pei, H.; Chen, Y. The impact of cerium oxide nanoparticles on tomato (*Solanum lycopersicum* L.) and its implications for food safety. *Metallomics* **2012**, *4*, 1105-1112.

15. Rico, C. M.; Morales, M. I.; Barrios, A. C.; McCreary, R.; Hong, J.; Lee, W. Y.; Nunez, J. Peralta-Videa, J. R.; Gardea-Torresdey, J. L. Effect of cerium oxide nanoparticles on the quality of rice (*Oryza sativa* L.) grains. *J. Agric. Food Chem.* **2013**, *61*, 11278-11285.

16. Morales, M. I.; Rico, C. M.; Hernandez-Viezcas, J. A.; Nunez, J. E.; Barrios, A. C.; Tafoya, A.; Flores-Marges, J. P.; Peralta-Videa, J. R.; Gardea-Torresdey, J. L.Toxicity assessment of cerium oxide nanoparticles in cilantro (*Coriandrum sativum* L.) plants grown in organic soil. *J. Agric. Food Chem.* **2013**, *61*, 6224-6230.

17. Corral-Diaz, B; Peralta-Videa, J. R.; Alvarez-Parrilla, E.; Rodrigo-García, J.; Morales, M. I.; Osuna-Avila, P.; Niu, G.; Hernandez-Viezcas, J. A.; Gardea-Torresdey, J. L. Cerium oxide nanoparticles alter the antioxidant capacity but do not impact tuber ionome in *Raphanus sativus* (L). *Plant Physiol. Biochem*. **2014**, *84*, 277-285.

18. Zhang, Z.; He, X.; Zhang, H.; Ma, Y.; Zhang, P.; Ding, Y.; Zhao, Y. Uptake and distribution of ceria nanoparticles in cucumber plants. *Metallomics,* **2011**, *3*, 816-822.

19. Zhang, P.; Yuhui, M.; Zhang, Z.; He, X.; Zhang, J.; Guo, Z.; Tai, R.; Zhao, Y.; Chai, Z. Biotransformation of ceria nanoparticles in cucumber plants. *ACS Nano* **2012,** *6*, 9943-9950.

20. Zhao, L.; Sun, Y.; Hernandez-Viezcas, J. A.; Servin, A. D.; Hong, J.; Niu, G.; Peralta-Videa, J. R.; Duarte-Gardea, M.; Gardea-Torresdey, J. L. Influence of CeO_2 and ZnO nanoparticles on cucumber physiological markers and bioaccumulation of Ce and Zn: a life cycle study. *J. Agric. Food Chem*. **2013**, *61*, 1945-11951.

21. Zhao, L.; Peralta-Videa, J. R.; Varela-Ramirez, A.; Castillo-Michel, H.; Li, C.; Zhang, J.; Aguilera, R. J.; Keller, A. A; Gardea-Torresdey, J. L. Effect of surface coating and organic matter on the uptake of CeO_2 NPs by corn plants grown in soil: Insight into the uptake mechanism. *J. Hazard. Mater.* **2012***, 225-226*, 131-138.

22. Zhao, L.; Peralta-Videa, J. R.; Rico, C.; Hernandez-Viezcas, J. A.; Sun, Y.; Niu, G.; Servin, A.; Nunez, J. E.; Duarte-Gardea, M.; Gardea-Torresdey, J. L. CeO_2 and ZnO nanoparticles change the nutritional qualities of cucumber (*Cucumis sativus*). *J. Agric. Food Chem*. **2014**, *62*, 2752-2759.

23. Peralta-Videa, J. R.; Hernandez-Viezcas, J. A.; Zhao, L.; Corral Diaz, B.; Ge, Y.; Priester, J. H.; Holden, P.A.; Gardea-Torresdey, J. L. Cerium dioxide and zinc oxide nanoparticles alter the nutritional value of soil cultivated soybean plants. *Plant Physiol. Biochem*. **2014**, *80*, 128-135.

24. Hawthorne, J.; De la Torre Roche, R.; Xing, B.; Newman, L. A.; Ma, X.; Majumdar, S.; Gardea-Torresdey, J.; White, J C. Particle-size dependent accumulation and trophic

transfer of cerium oxide through a terrestrial food chain. *Environ. Sci. Technol.***2014**, *48*, 13102-13109.

25. McClean, P. E.; Lavin, M.; Gepts, P.; Jackson, S. A. *Phaseolus vulgaris*: A Diploid Model for Soybean, Genetics and Genomics of Soybean Plant Genetics and Genomics: Crops and Models, Volume 2, 2008, pp 55-76.

26. Drewnowski, A. The nutrient rich foods index helps to identify healthy, affordable foods. *Am. J. Clin. Nutr.* **2010**, *91* (suppl), 1095S–1101S.

27. McClean, P.; Cannon, S.; Gepts, P.; Hudson, M.; Jackson, S.; Rokhsar, D.; Schmutz, J.; Vance, C. Towards a whole genome sequence of common bean, (*Phaseolus vulgaris*) Background, Approaches, Applications, USDA. http://www.csrees.usda.gov/business/reporting/stakeholder/pdfs/pl_common_bean.pdf.

28. Wong JH, Zhang XQ, Wang HX, Ng TB (2006) A mitogenic defensin from white cloud bean (*Phaseolus vulgaris*). Peptides 27, 2075-2081.

CHAPTER 2

1. Roco, M. C. The long view of nanotechnology development: the national nanotechnology initiative at 10 years. In *Nanotechnology research directions for societal needs in 2020*; Roco, M. C., Hersham, M. C., Chad, A., Eds.; Science Policy Reports, Springerlink 2011; pp 1-28.

2. Liu, H. H.; Cohen, Y. Multimedia environmental distribution of engineered nanomaterials. *Environ. Sci. Technol.* **2014**, *48*, 3281–3292.

3. Rico, C. M.; Majumdar, S.; Duarte-Gardea, M.; Peralta-Videa, J. R.; Gardea-Torresdey, J. L. Interaction of nanoparticles with edible plants and their possible implications in the food chain. *J. Agric. Food Chem.* **2011**, *59*, 3485-3498.

4. Miralles, P.; Church, T. L.; Harris, A. T. Toxicity, uptake, and translocation of engineered nanomaterials in vascular plants. *Environ. Sci. Technol*. **2012**, *46*, 9224-9239.

5. Future_Markets (2012), The global market for nanomaterials 2002-2006: production volumes, revenues and end use markets. Future Markets Inc., Available:

http://www.futuremarketsinc.com/index.php?option=com_content&view=article&id=176&Itemid=73.

6. Piccino, F.; Gottschalk, F.; Seeger, S.; Nowack, B. Industrial production quantities and uses of ten engineered nanomaterials in Europe and the world. *J. Nanopart. Res.* **2012**, *14*, 1109.

7. Trovarelli, A., Eds. *Catalysis by ceria and related materials*. Imperial College Press: London, 2002, 15-50.

8. Rodriguez, J. A.; Hanson, J. C.; Kim, J. Y.; Liu, G.; Iglesias-Juez, A.; Fernandez Garcia, M. Properties of CeO_2 and $Ce_{1-x}Zr_xO_2$ nanoparticles: XANES, density functional, and time-resolved XRD studies. *J. Phys. Chem. B*. **2003**, *107*, 3535-3543.

9. Nel, A. E.; Madler, L.; Velegol, D.; Xia, T.; Hoek, E. M. V.; Somasundaran, P.; Klaessig, F.; Castranova, V.; Thompson, M. Understanding biophysicochemical interactions at the nano-bio interface. *Nat. Mater.* **2009**, *8*, 543-557.

10. Auffan, M.; Rose, J.; Wiesner, M. R.; Bottero, J. Y. Chemical stability of metallic nanoparticles: a parameter controlling their potential cellular toxicity in vitro. *Environ. Pollut.* **2009**,*157*, 1127-1133.

11. Zhang, H.; Ji, H.; Xia, T.; Meng, H.; Low-Kam, C.; Liu, R.; Pokhrel, S.; Lin, S.; Wang, X.; Liao, Y.; Wang, M.; Li, L.; Rallo, R.; Damoiseaux, R.; Telesca, D.; Mädler, L.; Cohen, Y.; Zink, J. I.; Nel, A. E. Use of metal oxide nanoparticle band gap to develop a predictive paradigm for oxidative stress and acute pulmonary inflammation. *ACS Nano.* **2012**, *6*, 4349-4368.

12. Wang, Q.; Ma, X.; Zhang, W.; Pei, H.; Chen, Y. The impact of cerium oxide nanoparticles on tomato (*Solanum lycopersicum* L.) and its implications for food safety. *Metallomics*. **2012**, *4*, 1105-1112.

13. Rico, C. M.; Hong, J.; Morales, M. I.; Zhao, L.; Barrios, A. C.; Zhang, J. Y.; Peralta-Videa, J. R.; Gardea-Torresdey, J. L. Effect of cerium oxide nanoparticles on rice: a study involving the antioxidant defense system and in vivo fluorescence imaging. *Environ. Sci. Technol.* **2013**, *47*, 5635-5642.

14. López-Moreno, M. L.; de la Rosa, G.; Hernandez-Viezcas, J. A.; Peralta-Videa, J. R.; Gardea-Torresdey, J. X-ray absorption spectroscopy (XAS) corroboration of the uptake and storage of CeO_2 nanoparticles and assessment of their differential toxicity in four edible plant species. *J. Agric. Food Chem.* **2010**, *58*, 3689-3693.

15. Priester, J. H.; Ge, Y.; Mielke, R. E.; Horst, A.M.; Moritz, S. C.; Espinosa, K.; Gelb, J.; Walker, S. L.; Nisbet, R. M.; An, Y. J.; Schimel, J. P.; Palmer, R. G.; Hernandez-Viezcas, J. A.; Zhao, L.; Gardea-Torresdey, J. L.; Holden, P. A. Soybean susceptibility to manufactured nanomaterials with evidence for food quality and soil fertility interruption. *Proc. Natl. Acad. Sci.***2012**, *109*, 2451-2456.

16. Zhao, L.; Sun, Y.; Hernandez-Viezcas, J. A.; Servin, A. D.; Hong, J.; Niu, G.; Peralta-Videa, J. R.; Duarte-Gardea, M.; Gardea-Torresdey, J. L. Influence of CeO_2 and ZnO

nanoparticles on cucumber physiological markers and bioaccumulation of Ce and Zn: A Life Cycle Study. *J. Agric. Food Chem.* **2013**, *61*, 11945-11951.

17. Ma, Y.; Kuang, L.; He, X.; Bai, W.; Ding, Y.; Zhang, Z.; Zhao, Y.; Chai, Z. Effects of rare earth oxide nanoparticles on root elongation of plants. *Chemosphere*. **2010**, *78*, 273-279.

18. López-Moreno, M. L.; de la Rosa, G.; Hernandez-Viezcas, J. A.; Castillo-Michel, H.; Botez, C. E.; Peralta-Videa, J. R.; Gardea-Torresdey, J. L. Evidence of the differential biotransformation and genotoxicity of ZnO and CeO_2 nanoparticles on soybean (*Glycine max*) plants. *Environ. Sci. Technol*. **2010**, *44*, 7315-7320.

19. McClean, P.; Cannon, S.; Gepts, P.; Hudson, M.; Jackson, S.; Rokhsar, D.; Schmutz, J,; Vance, C. Towards a whole genome sequence of common bean, (*Phaseolus vulgaris*) Background, Approaches, Applications. USDA, http://www.csrees.usda.gov/business/ reporting/stakeholder/pdfs/pl_common_bean.pdf.

20. Meliorum Technologies Inc. website; http://www.meliorum.com/ceriumoxide.htm.

21. Keller, A. A.; Wang, H.; Zhou, D.; Lenihan, H. S.; Cherr, G.; Cardinale, B. J.; Miller, R.; Ji, Z. Stability and aggregation of metal oxide nanoparticles in natural aqueous matrices. *Environ. Sci. Technol*. **2010**, *44*, 1962-1967.

22. Hernandez-Viezcas, J. A.; Castillo-Michel, H.; Servin, A. D.; Peralta-Videa, J. R.; Gardea-Torresdey, J. L. Spectroscopic verification of zinc absorption and distribution in the desert plant *Prosopis juliflora-velutina* (velvet mesquite) grown with ZnO nanoparticles. *Chem. Eng. J.* **2011**, *170*, 346-352.

23. Packer, A. P.; Lariviere, C.; Li, M.; Chen, M.; Fawcett, A.; Nielsen, K.; Mattson, K.; Chatt, A.; Scriver, C.; Erhardt, L. S. Validation of an inductively coupled plasma mass spectrometry (ICP-MS) method for the determination of cerium, strontium, and titanium in ceramic materials used in radiological dispersal devices (RDDs). *Anal. Chim. Acta* **2007**, *588*, 166-172.

24. Susini, J.; Salomé, M.; Neuhaeusler, U.; Dhez, O.; Eichert, D.; Fayard, B.; Somogyi, A.; Bohic, S.; Bleuet, P.; Martinez-Criado, G.; Tucoulou, R.; Simionovici, A.; Barrett, M.; Drakopoulos, R. The X-ray microscopy and micro-spectroscopy facility at the ESRF, Synchrotron Radiat. *News* **2003**, *16*, 35-43.

25. Zhao, L.; Peralta-Videa, J. R.; Varela-Ramirez, A.; Castillo-Michel, H.; Li, C.; Zhang, J.; Aguilera, R. J.; Keller, A. A.; Gardea-Torresdey, J. L. Effect of surface coating and organic matter on the uptake of CeO_2 NPs by corn plants grown in soil: Insight into the uptake mechanism. *J. Hazard. Mater.* **2012**, *225-226*, 131-138.

26. Ravel, B.; Newville, M. ATHENA and ARTEMIS: interactive graphical data analysis using IFEFFIT. *Phys. Scr.* **2005**, *T115*, 1007-1010.

27. Lichtenthaler, H. K.; Buschmann, C. Chlorophylls and carotenoids: measurement and characterization by UV-VIS spectroscopy. *Curr. Protoc. Food Anal. Chem.* **2001**, F4.3.1-F4.3.8.

28. Bradford, M. M. A rapid and sensitive method for the quantitation of microgram quantities of protein utilizing the principle of protein-dye binding. *Anal. Biochem.* **1976**, *72*, 248-254.

29. Heath, R. L.; Packer, L. Photoperoxidation in isolated chloroplasts: I. Kinetics and stoichiometry of fatty acid peroxidation. *Arch. Biochem. Biophys.* **1968**, *125*, 189-198.

30. Gallego, S.; Benavídes, M. P.; Tomaro, M. L. Effect of heavy metal ion excess on sunflower leaves: evidence for involvement of oxidative stress. *Plant Sci.* **1996**, *121*, 151-150.

31. Aebi, H. Catalase. In *Methods of enzymatic analysis*; Bergmeyer, H. U., Eds.; Academic Press Inc: New York 1974; pp 680.

32. Nakano, Y.; Asada, K. Hydrogen peroxide is scavenged by ascorbate-specific peroxidases in spinach chloroplasts. *Plant Cell Physiol.* **1981**, *22*, 867-880.

33. Urbanek, H.; Kuzniak-Gebarowska, E.; Herka, K. Elicitation of defense responses in bean leaves by *Botrytis cinerea* polygalacturonase. *Acta Physiol. Plant.* **1991**, *13*, 43-50.

34. Sajith, V.; Sobhan, C. B.; Peterson, G. P. Experimental investigations on the effects of cerium oxide nanoparticle fuel additives on biodiesel. *Adv. Mech. Eng.* **2010**, Article ID 581407, 6 pages. doi:10.1155/2010/581407.

35. Park, B.; Donaldson, K.; Duffin, R.; Tran, L.; Kelly, F.; Mudway, I.; Morin, J. P.; Guest, R.; Jenkinson, P.; Samaras, Z.; Giannouli, M.; Kouridis, H.; Martin, P. Hazard and risk assessment of a nanoparticulate cerium oxide-based diesel fuel additive - a case study. *Inhalation Toxicol.* **2008**, *20*, 547-566.

36. Scattergood, Oxonica Ltd., cerium oxide nanoparticles as fuel additives. 2004, Patent no. WO2004065529.

37. Demeester, J.; Smedt, S.; Sanders, N.; Haustraete, J. Light scattering. In *Methods for structural analysis of protein pharmaceuticals*; Jiskoot, W., Crommelin, D. J., Eds.; Arlington, AAPS, 2005; pp 255-259.

38. Zhang, Z.; He, X.; Zhang, H.; Ma, Y.; Zhang, P.; Ding, Y.; Zhao, Y. Uptake and distribution of ceria nanoparticles in cucumber plants. *Metallomics* **2011**, *3*, 816-822.

39. Bali, R.; Siegele, R.; Harris, A. T. Biogenic Pt uptake and nanoparticle formation in *Medicago sativa* and *Brassica juncea*. *J. Nanopart. Res.* **2010**, *12*, 3087-3095.

40. Taiz, L.; Zeiger, E. *Plant Physiology*, 2nd, ed., Sinauer, Sunderland, Massachusetts, 1998.

41. Patil, S.; Sandberg, A.; Heckert, E.; Self, W.; Seal, S. Protein adsorption and cellular uptake of cerium oxide nanoparticles as a function of zeta potential. *Biomaterials* **2008**, *28*, 4600-4607.

42. Majumdar, S.; Peralta-Videa, J. R.; Castillo-Michel, H.; Hong, J.; Rico, C. M.; Gardea-Torresdey, J. L. Applications of synchrotron μ-XRF to study the distribution of biologically important elements in different environmental matrices: A review. *Anal. Chim. Acta* **2012**, *755*, 1-16.

43. Zhang, P.; Yuhui, M.; Zhang, Z.; He, X.; Zhang, J.; Guo, Z.; Tai, R.; Zhao, Y.; Chai, Z. Biotransformation of ceria nanoparticles in cucumber plants. *ACS Nano* **2012,** *6*, 9943-9950.

44. Esau, K. *Anatomy of Seed Plants*, 2nd, ed., Wiley, New York, 1977.

45. Sugiyama, A.; Yazaki, K. Root exudates of legume plants and their involvement in interactions with soil microbes. In *Secretions and Exudates in Biological Systems, Signaling and Communication in Plants*; Vivanco, J., Baluška, F., Eds.; Springer-Verlag, Berlin Heidelberg 2012; pp 27-48.

46. Shyam, R.; Aery, N. C. Effect of cerium on growth, dry matter production, biochemical constituents and enzymatic activities of cowpea plants [*Vigna unguiculata* (L.) Walp.]. *J. Soil Sci. Plant Nutr.* **2012**, *12*, 1-14.

47. Neto, A. D. A.; Prisco, J. T.; Gomes-Filho, E. Changes in soluble amino-N, soluble proteins and free amino acids in leaves and roots of salt-stressed maize genotypes. *J. Plant Interact.* **2009**, *4*, 137-144.

48. Nayer, M.; Reza, H. Effects of drought stress on soluble proteins in two maize varieties. *Turk. J. Biol.* **2008**, *32*, 23-30.

49. Sharma, P.; Jha, A. B.; Dubey, R. S.; Pessarakli, M. Reactive oxygen species, oxidative damage, and antioxidative defense mechanism in plants under stressful conditions. *J. Bot.* **2012**, Article ID 217037, doi:10.1155/2012/217037.

50. Zhao, L.; Peng, B.; Hernandez-Viezcas, J.; Rico, C.; Sun, Y.; Peralta-Videa, J.; Tang, X.; Niu, G.; Jin, L.; Varela, A.; Zhang, J.; Gardea-Torresdey, J. Stress response and tolerance of *Zea mays* to CeO_2 nanoparticles: cross talk among H_2O_2, heat shock protein and lipid peroxidation. *ACS Nano* **2012**, *6*, 9615-9622.

51. Heckert, E. G.; Karakoti, A. S.; Seal, S.; Self, W. T. The role of cerium redox state in the SOD mimetic activity of nanoceria. *Biomaterials* **2008**, *29*, 2705-2709.

52. Keating, P. R. L.; Scanlon, D. O.; Morgan, B. J.; Galea, N. M.; Watson, G. W. Analysis of intrinsic defects in CeO_2 using a koopmans-like GGA+U approach. *J. Phys. Chem.* **2012**, *116*, 2443-2452.

53. Ojalvo, I.; Rokem, J. S.; Navon, G.; Goldberg, I. 31P NMR study of elicitor treated *Phaseolus vulgaris* cell suspension cultures. *Plant Physiol.* **1987**, *85*, 716-719.

54. Ashraf, M.; Mehmood, S. Response of four *Brassica* species to drought stress, *Environ. Expt. Bot.* **1990**, *30*, 93-100.

55. Majumdar, S.; Peralta-Videa, J. R.; Bandyopadhyay, S.; Castillo-Michel, H.; Hernandez-Viezcas, J. A.; Sahi, S.; Gardea-Torresdey, J. L. Exposure of cerium oxide nanoparticles to kidney bean shows disturbance in the plant defense mechanisms. *J. Hazard. Mater.* **2014**, 278, 279-287.

CHAPTER 3

1. Keller, A. A.; McFerran, S.; Lazareva, A.; Suh, S. Global life cycle releases of engineered nanomaterials. *J. Nanopart. Res.* **2013**, *15,* 1692.

2. Collin, B.; Auffan, M.; Johnson, A. C.; Kaur, I.; Keller, A. A.; Lazareva, A.; Lead, J. R.; Ma, X.; Merrifield, R.; Svendsen, C.; White, J.; Unrine, J. Environmental release, fate and ecotoxicological effects of manufactured ceria nanomaterials. *Environ. Sci. Nano.* **2014**, DOI 10.1039/C4EN00149D.

3. Judy, J. D.; Unrine, J. M.; Bertsch, P. M. Evidence for Biomagnification of Gold Nanoparticles within a Terrestrial Food Chain. *Environ. Sci. Technol*. **2011**, *45*, 776-781.

4. Gardea-Torresdey, J.; Rico, C.; White, J. Trophic transfer, transformation and impact of engineered nanomaterials in terrestrial environments. *Environ. Sci. Technol*. **2014**, *48*, 2526-2540.

5. Lin, D.; Tian, X.; Wu, F.; Xing, B. Fate and transport of engineered nanomaterials in the environment. *J Environ Qual.* **2010**, *39*, 1896-908.

6. Schwabe, F.; Schulin, R.; Limbach, L. K.; Stark, W.; Bürge, D.; Nowack, B. Influence of two types of organic matter on interaction of CeO_2 nanoparticles with plants in hydroponic culture. *Chemosphere*. **2013**, *91*, 512-520.

7. Yang, K.; Lin, D.; Xing, B. Interactions of Humic Acid with Nanosized Inorganic Oxides. *Langmuir* **2009**, *25*, 3571-3576.

8. Collin, B.; Oostveen, E.; Tsyusko, O. V.; Unrine, J. M. Influence of Natural Organic Matter and Surface Charge on the Toxicity and Bioaccumulation of Functionalized Ceria Nanoparticles in *Caenorhabditis elegans*. *Environ. Sci. Technol*. **2014**, *48*, 1280-1289.

9. Hernandez-Viezcas, J. A.; Castillo-Michel, H.; Andrews, J. C.; Cotte, M.; Rico, C.; Peralta-Videa, J. R.; Ge, Y.; Priester, J. H.; Holden, P. A.; Gardea-Torresdey, J. L. *In situ* synchrotron X-ray fluorescence mapping and speciation of CeO_2 and ZnO nanoparticles in soil cultivated soybean (*Glycine max*). *ACS Nano*, **2013**, *7*, 1415-1423.

10. Majumdar, S.; Peralta-Videa, J. R.; Bandyopadhyay, S.; Castillo-Michel, H.; Hernandez-Viezcas, J. A.; Sahi, S.; Gardea-Torresdey, J. L. Exposure of cerium oxide nanoparticles to kidney bean shows disturbance in the plant defense mechanisms. *J. Hazard. Mater.* **2014**, *278*, 279-287.

11. Zhang, P.; Yuhui, M.; Zhang, Z.; He, X.; Zhang, J.; Guo, Z.; Tai, R.; Zhao, Y.; Chai, Z. Biotransformation of ceria nanoparticles in cucumber plants, *ACS Nano*, **2012**, *6*, 9943-9950.

12. Zhao, L.; Sun, Y.; Hernandez-Viezcas, J. A.; Servin, A. D.; Hong, J.; Niu, G.; Peralta-Videa, J. R.; Duarte-Gardea, M.; Gardea-Torresdey, J. L. Influence of CeO_2 and ZnO nanoparticles on cucumber physiological markers and bioaccumulation of Ce and Zn: A Life Cycle Study. *J. Agric. Food Chem.* **2013**, *61*, 11945-11951.

13. Zhao, L.; Peralta-Videa, J. R.; Varela-Ramirez, A.; Castillo-Michel, H.; Li, C.; Zhang, J.; Aguilera, R. J.; Keller, A. A.; Gardea-Torresdey, J.L. Effect of surface coating and organic matter on the uptake of CeO_2 NPs by corn plants grown in soil: Insight into the uptake mechanism, *J. Hazard. Mater.* **2012**, *225–226*, 131-138.

14. Priester, J. H.; Ge, Y.; Mielke, R. E.; Horst, A. M.; Moritz, S. C.; Espinosa, K.; Gelb, J.; Walker, S. L.; Nisbet, R. M.; An, Y. J.; Schimel, J. P.; Palmer, R. G.; Hernandez-Viezcas, J. A.; Zhao, L.; Gardea-Torresdey, J. L.; Holden, P. A. Soybean susceptibility to

manufactured nanomaterials with evidence for food quality and soil fertility interruption. *Proc. Natl. Acad. Sci.* **2012**, *109,* 2451-2456.

15. Sperazza, M.; Moore, J. N.; Hendrix. M. S. High-resolution particle size analysis of naturally occurring very fi ne-grained sediment through laser diffractometry. *J. Sediment. Res.* **2004**, *74*, 736–743.

16. Keller, A. A.; Wang, H.; Zhou, D.; Lenihan, H. S.; Cherr, G.; Cardinale, B. J.; Miller, R. R.; Ji, Z. Stability and aggregation of metal oxide nanoparticles in natural aqueousmatrices. *Environ. Sci. Technol.* **2010**, *44*, 1962–1967.

17. US Environmental Protection Agency 1986 Test Methods for Evaluating Solid Waste. SW-846 Method 9081 US Environmental Protection Agency Washington D.C. DC

18. AOAC (Association of Official Analytical Chemists). In *Official Methods of Analysis*, 17th ed.; AOAC: Arlington, VA, 2000.

19. Bremner, J. M. Methods of soil analysis part 3 Nitrogen total. In *Chemical methods*, 3rd ed.; Bartels, J. M.; et al. Eds.; ASA, and SSSA. Madison, WI, Book Series, 1996 No. 5. 1085-1121.

20. Packer, A. P.; Lariviere, D.; Li, C.; Chen, M.; Fawcett, A.; Nielsen, K.; Mattson, K.; Chatt, A.; Scriver, C.; Erhardt, L. S. Validation of an inductively coupled plasma mass spectrometry (ICP-MS) method for the determination of cerium, strontium, and titanium in ceramic materials used in radiological dispersal devices (RDDs). *Anal. Chim. Acta*. **2007**, *588*, 166-172.

21. Lichtenthaler, H. K.; Buschmann, C. Chlorophylls and carotenoids: measurement and characterization by UV-VIS spectroscopy, *Curr. Protoc. Food Analyt. Chem.* **2001**, F4.3.1-F4.3.8.

22. Brady, N. C.; Weil, R. R. *The nature and properties of soils*; 13th ed., 2002.

23. Rittner, M. N.; Abraham; T. Nanostructed materials: an overview and commericial analysis. *JOM*, **1998**, *50*, 37-38.

24. Loosli, F.; Coustumer, P. L.; Stoll, S. Effect of natural organic matter on the disagglomeration of manufactured TiO_2 nanoparticles. *Environ. Sci.: Nano*, **2014**, *1*, 154-160.

25. Taiz, L.; Zeiger, E. *Plant Physiology*; 2nd ed., Sinauer, Sunderland, Massachusetts, 1998.

CHAPTER 4

1. Collin, B.; Auffan, M.; Johnson, A. C.; Kaur, I.; Keller, A. A.; Lazareva, A.; Lead, J. R.; Ma, X.; Merrifield, R.; Svendsen, C.; White, J.; Unrine, J. Environmental release, fate and ecotoxicological effects of manufactured ceria nanomaterials. *Environ. Sci. Nano.* **2014**, DOI 10.1039/C4EN00149D.

2. McCormack, R. N.; Mendez, P.; Barkam, S.; Neal, C. J.; Das, S.; Seal, S. Inhibition of Nanoceria's Catalytic Activity due to Ce^{3+} Site-Specific Interaction with Phosphate Ions. *J. Phys. Chem. C.* **2014**, *118*, 18992-19006.

3. Keller, A. A.; McFerran, S.; Lazareva, A.; Suh, S. Global life cycle releases of engineered nanomaterials. *J. Nanopart. Res.* **2013**, *15,* 1692.

4. Rico, C. M.; Morales, M. I.; Barrios, A. C.; McCreary, R.; Hong, J.; Lee, W. Y.; Nunez, J. Peralta-Videa, J. R.; Gardea-Torresdey, J. L. Effect of cerium oxide nanoparticles on the quality of rice (*Oryza sativa* L.) grains. *J. Agric. Food Chem.* **2013**, *61*, 11278-11285.

5. Zhao, L.; Peralta-Videa, J. R.; Varela-Ramirez, A.; Castillo-Michel, H.; Li, C.; Zhang, J.; Aguilera, R. J.; Keller, A. A; Gardea-Torresdey, J. L. Effect of surface coating and organic matter on the uptake of CeO_2 NPs by corn plants grown in soil: Insight into the uptake mechanism. *J. Hazard. Mater.* **2012***, 225–226*, 131-138.

6. Majumdar, S.; Peralta-Videa, J. R.; Bandyopadhyay, S.; Castillo-Michel, H.; Hernandez-Viezcas, J. A.; Sahi, S.; Gardea-Torresdey, J. L. Exposure of cerium oxide nanoparticles to kidney bean shows disturbance in the plant defense mechanisms. *J. Hazard. Mater.* 2014, 278, 279-287.

7. Priester, J. H.; Ge, Y.; Mielke, R. E.; Horst, A. M.; Moritz, S. C.; Espinosa, K.; Gelb, J.; Walker, S. L.; Nisbet, R. M.; An, Y. J.; Schimel, J. P.; Palmer, R. G.; Hernandez-Viezcas, J. A.; Zhao, L.; Gardea-Torresdey, J. L.; Holden, P. A. Soybean susceptibility to manufactured nanomaterials with evidence for food quality and soil fertility interruption. *Proc. Natl. Acad. Sci.* **2012**, *109,* 2451-2456.

8. Wang, Q.; Ma, X.; Zhang, W.; Pei, H.; Chen, Y. The impact of cerium oxide nanoparticles on tomato (*Solanum lycopersicum* L.) and its implications for food safety. *Metallomics*. **2012**, *4*, 1105-1112.

9. Morales, M. I.; Rico, C. M.; Hernandez-Viezcas, J. A.; Nunez, J. E.; Barrios, A. C.; Tafoya, A.; Flores-Marges, J. P.; Peralta-Videa, J. R.; Gardea-Torresdey, J. L.Toxicity assessment of cerium oxide nanoparticles in cilantro (*Coriandrum sativum* L.) plants grown in organic soil. *J. Agric. Food Chem.* **2013**, *61*, 6224-6230.

10. Corral-Diaz, B; Peralta-Videa, J. R.; Alvarez-Parrilla, E.; Rodrigo-García, J.; Morales, M. I.; Osuna-Avila, P.; Niu, G.; Hernandez-Viezcas, J. A.; Gardea-Torresdey, J. L. Cerium oxide nanoparticles alter the antioxidant capacity but do not impact tuber ionome in *Raphanus sativus* (L). *Plant Physiol. Biochem*. **2014**, *84*, 277-285.

11. Hernandez-Viezcas, J. A.; Castillo-Michel, H.; Andrews, J. C.; Cotte, M.; Rico, C.; Peralta-Videa, J. R.; Ge, Y.; Priester, J. H.; Holden, P. A.; Gardea-Torresdey, J. L. *In situ* synchrotron X-ray fluorescence mapping and speciation of CeO_2 and ZnO nanoparticles in soil cultivated soybean (*Glycine max*). *ACS Nano*, **2013**, *7*, 1415-1423.

12. Zhang, Z.; He, X.; Zhang, H.; Ma, Y.; Zhang, P.; Ding, Y.; Zhao, Y. Uptake and distribution of ceria nanoparticles in cucumber plants. *Metallomics,* **2011**, *3*, 816-822.

13. Gardea-Torresdey, J.; Rico, C.; White, J. Trophic transfer, transformation and impact of engineered nanomaterials in terrestrial environments. *Environ. Sci. Technol*. **2014**, *48*, 2526-2540.

14. Zhao, L.; Peralta-Videa, J. R.; Rico, C.; Hernandez-Viezcas, J. A.; Sun, Y.; Niu, G.; Servin, A.; Nunez, J. E.; Duarte-Gardea, M.; Gardea-Torresdey, J. L. CeO_2 and ZnO nanoparticles change the nutritional qualities of cucumber (*Cucumis sativus*). *J. Agric. Food Chem.* **2014**, *62*, 2752-2759.

15. Peralta-Videa, J. R.; Hernandez-Viezcas, J. A.; Zhao, L.; Corral Diaz, B.; Ge, Y.; Priester, J. H.; Holden, P.A.; Gardea-Torresdey, J. L. Cerium dioxide and zinc oxide nanoparticles alter the nutritional value of soil cultivated soybean plants. *Plant Physiol. Biochem*. **2014**, *80*, 128-135.

16. Schwabe, F.; Schulin, R.; Limbach, L. K.; Stark, W.; Bürge, D.; Nowack, B. Influence of two types of organic matter on interaction of CeO_2 nanoparticles with plants in hydroponic culture. *Chemosphere*. **2013**, *91*, 512-520.

17. Ghosh, S.; Mashayekhi, H.; Pan, B.; Bhowmik, P.; Xing, B. Colloidal behavior of aluminum oxide nanoparticles as affected by pH and natural organic matter. *Langmuir*. **2008**, *24*, 12385-12391.

18. Hyung, H.; Fortner, J. D.; Hughes, J. B.; Kim, J. Natural organic matter stabilizes carbon nanotubes in the aqueous phase. *Environ. Sci. Technol*. **2007**, *41*, 179–184.

19. Drewnowski, A. The nutrient rich foods index helps to identify healthy, affordable foods. *Am. J. Clin. Nutr.* **2010**, *91* (suppl), 1095S–1101S.

20. McClean, P.; Cannon, S.; Gepts, P.; Hudson, M.; Jackson, S.; Rokhsar, D.; Schmutz, J.; Vance, C. Towards a whole genome sequence of common bean, (*Phaseolus vulgaris*) Background, Approaches, Applications, USDA. http://www.csrees.usda.gov/business/reporting/stakeholder/pdfs/pl_common_bean.pdf.

21. Keller, A. A.; Wang, H.; Zhou, D.; Lenihan, H. S.; Cherr, G.; Cardinale, B. J.; Miller, R. R.; Ji, Z. Stability and aggregation of metal oxide nanoparticles in natural aqueousmatrices. *Environ. Sci. Technol.* **2010**, *44*, 1962–1967.

22. Packer, A. P.; Lariviere, D.; Li, C.; Chen, M.; Fawcett, A.; Nielsen, K.; Mattson, K.; Chatt, A.; Scriver, C.; Erhardt, L. S. Validation of an inductively coupled plasma mass spectrometry (ICP-MS) method for the determination of cerium, strontium, and titanium in ceramic materials used in radiological dispersal devices (RDDs). *Anal. Chim. Acta*. **2007**, *588*, 166-172.

23. AOAC (Association of Official Analytical Chemists). In *Official Methods of Analysis*, 17th ed.; AOAC: Arlington, VA, 2000.

24. Bremner, J. M. Methods of soil analysis part 3 Nitrogen total. In *Chemical methods*, 3rd ed.; Bartels, J. M.; et al. Eds.; ASA, and SSSA. Madison, WI, Book Series, 1996 No. 5. 1085-1121.

25. Verma, S.; Dubey, R. S. Effect of cadmium on soluble sugars and enzymes of their metabolism in rice. *Biol. Plant.* **2001**, *44*, 117-123.

26. Dubois, M.; Gilles, K. A.; Hamilton, J. K.; Rebers, P. A.; Smith, F. Colorimetric method for determination of sugars and relatedsubstances. *Anal. Chem.***1956**, *26*, 350-356.

27. Zhao, L.; Sun, Y.; Hernandez-Viezcas, J. A.; Servin, A. D.; Hong, J.; Niu, G.; Peralta-Videa, J. R.; Duarte-Gardea, M.; Gardea-Torresdey, J. L. Influence of CeO_2 and ZnO nanoparticles on cucumber physiological markers and bioaccumulation of Ce and Zn: A Life Cycle Study. *J. Agric. Food Chem.* **2013**, *61*, 11945-11951.

28. Buchanan, B. B.; Gruissem, W.; Jones, R. L. *Biochemistry and molecular biology of plants*; 2000.

29. Taiz, L.; Zeiger, E. *Plant Physiology*; 2nd ed., Sinauer, Sunderland, Massachusetts, 1998.

30. Brady, N. C.; Weil, R. R. *The nature and properties of soils*; 13th ed., 2002.

31. Manara, A. Plant responses to heavy metal toxicity. In *Plants and heavy metals*; Furini, A., Eds.; Netherlands 2012; pp 27-53.

32. Synder, C.S. Raise soybean yields and profit potential with phosphorus and potassium fertilization. 2000; http://www.ipni.net/ppiweb/ppinews.nsf/0/1ef10df06662ad9d8525690 3006ac569/$FILE/cssmay00.pdf.

33. Yruela, I. Copper in plants: acquisition, transport and interactions. *Funct. Plant Biol.* **2009**, *36*, 409–430; doi.org/10.1071/FP08288.

34. Kemi, V. E.; Karkkainen, M. U.; Rita, H. J.; Laaksonen, M. M.; Outila, T. A.; Lamberg-Allardt, C. J. Low calcium: phosphorus ratio in habitual diets affects serum parathyroid hormone concentration and calcium metabolism in healthy women with adequate calcium intake. *Br. J. Nutr.* **2010**, *103* (4), 561-568.

35. Hille, R.; Nishino, T.; Bittner, F. Molybdenum enzymes in higher organisms. *Coordin. Chem. Rev*. **2011**, 255, 1179-1205.

36. National Research Council (NRC), Recommended dietary allowances. 10th ed. National Academic Press, Washington DC. 1989.

37. Dokken, K. M.; Davis, L. C. "Infrared monitoring of dinitrotoluenes in sunflower and maize roots". *J. Environ. Qual.* **2011**, 40, 719-730.

38. Taoutaou, A.; Socaciu, C.; Pamfil, D.; Fetea, F.; Balazs, E.; Botez, C. New markers for potato late blight resistance and susceptibility using FTIR spectroscopy. *Notulae Botanicae Horti Agrobotanici Cluj-Napoca*, **2012**, 40.

39. Kole, C.; Kole, P.; Randunu, K. M.; Choudhary, P.; Podila, F.; Ke, P. C.; Rao, A. M.; Marcus, R. K. Nanobiotechnology can boost crop production and quality: first evidence from increased plant biomass, fruit yield and phytomedicine content in bitter melon (*Momordica charantia*). *BMC Biotechnol.* **2013**, *13*, 37.

40. Dokken, K. M.; Davis, L. C.; Marinkovic, N. S. Use of infrared microspectroscopy in plant growth and development. *Appl. Spectrosc. Rev.* **2007**, *40*, 301-326.

CHAPTER 5

1. Karakoti, A. S.; Monteiro-Riviere, N. A.; Aggarwal, R.; Davis, J. P.; Narayan, R. J.; Self, W. T.; McGinnis, J.; Seal, S. Nanoceria as Antioxidant: Synthesis and Biomedical Applications. *JOM (Warrendal 1989)*. **2008**, *60*, 33-37.

2. Lee, S. S.; Song, W.; Cho, M.; Puppala, H. L.; Nguyen, P.; Zhu, H.; Segatori, L.; Colvin, V. L. Antioxidant Properties of Cerium Oxide Nanocrystals as a Function of Nanocrystal Diameter and Surface Coating Lee. *ACS Nano.* **2013**, 7, 9693-9703.

3. Collin, B.; Auffan, M.; Johnson, A. C.; Kaur, I.; Keller, A. A.; Lazareva, A.; Lead, J. R.; Ma, X.; Merrifield, R.; Svendsen, C.; White, J.; Unrine, J. Environmental release, fate and ecotoxicological effects of manufactured ceria nanomaterials. *Environ. Sci. Nano*. **2014**, DOI 10.1039/C4EN00149D.

4. Walkey, C.; Das, S.; Seal, S.; Erlichman O.; Heckman, K.; Ghibelli, L.; Traversa, E.; McGinnisf, J. F.; Self, W. T. Catalytic properties and biomedical applications of cerium oxide nanoparticles. *Environ. Sci.: Nano* **2015**; DOI: 10.1039/c4en00138a.

5. Mittal, S.; Pandey, A. K. "Cerium Oxide Nanoparticles Induced Toxicity in Human Lung Cells: Role of ROS Mediated DNA Damage and Apoptosis". *BioMed Res. Int.* **2014**, *Article ID 891934*, 14 pages; doi10.1155/2014/891934.

6. Arya, A.; Sethy, N. K.; Das, M.; Singh, S. K.; Das, A.; Ujjain, S. K.; Sharma, R. K.; Sharma, M.; Bhargava, K. Cerium oxide nanoparticles prevent apoptosis in primary cortical culture by stabilizing mitochondrial membrane potential. *Free Radical Res.* **2014**, *48*, 784-793.

7. Keller, A. A.; McFerran, S.; Lazareva, A.; Suh, S. Global life cycle releases of engineered nanomaterials. *J. Nanopart. Res.* **2013**, *15*, 1692.

8. Rico, C. M.; Morales, M. I.; Barrios, A. C.; McCreary, R.; Hong, J.; Lee, W. Y.; Nunez, J.; Peralta-Videa, J. R.; Gardea-Torresdey, J. L. Effect of cerium oxide nanoparticles on the quality of rice (*Oryza sativa* L.) grains. *J. Agric. Food Chem.* **2013**, *61*, 11278-11285.

9. Priester, J. H.; Ge, Y.; Mielke, R. E.; Horst, A. M.; Moritz, S. C.; Espinosa, K.; Gelb, J.; Walker, S. L.; Nisbet, R. M.; An, Y. J.; Schimel, J. P.; Palmer, R. G.; Hernandez-Viezcas, J. A.; Zhao, L.; Gardea-Torresdey, J. L.; Holden, P. A. Soybean susceptibility to manufactured nanomaterials with evidence for food quality and soil fertility interruption. *Proc. Natl. Acad. Sci.* **2012**, *109*, 2451-2456.

10. Wang, Q.; Ma, X.; Zhang, W.; Pei, H.; Chen, Y. The impact of cerium oxide nanoparticles on tomato (*Solanum lycopersicum* L.) and its implications for food safety. *Metallomics* **2012**, *4*, 1105-1112.

11. Morales, M. I.; Rico, C. M.; Hernandez-Viezcas, J. A.; Nunez, J. E.; Barrios, A. C.; Tafoya, A.; Flores-Marges, J. P.; Peralta-Videa, J. R.; Gardea-Torresdey, J. L. Toxicity assessment of cerium oxide nanoparticles in cilantro (*Coriandrum sativum* L.) plants grown in organic soil. *J. Agric. Food Chem.* **2013**, *61*, 6224-6230.

12. Corral-Diaz, B; Peralta-Videa, J. R.; Alvarez-Parrilla, E.; Rodrigo-García, J.; Morales, M. I.; Osuna-Avila, P.; Niu, G.; Hernandez-Viezcas, J. A.; Gardea-Torresdey, J. L. Cerium oxide nanoparticles alter the antioxidant capacity but do not impact tuber ionome in *Raphanus sativus* (L). *Plant Physiol. Biochem.* **2014**, *84*, 277-285.

13. Hernandez-Viezcas, J. A.; Castillo-Michel, H.; Andrews, J. C.; Cotte, M.; Rico, C.; Peralta-Videa, J. R.; Ge, Y.; Priester, J. H.; Holden, P. A.; Gardea-Torresdey, J. L. *In situ* synchrotron X-ray fluorescence mapping and speciation of CeO2 and ZnO nanoparticles in soil cultivated soybean (*Glycine max*). *ACS Nano* **2013**, *7*, 1415-1423.

14. Zhao, L.; Peralta-Videa, J. R.; Rico, C.; Hernandez-Viezcas, J. A.; Sun, Y.; Niu, G.; Servin, A.; Nunez, J. E.; Duarte-Gardea, M.; Gardea-Torresdey, J. L. CeO2 and ZnO nanoparticles change the nutritional qualities of cucumber (*Cucumis sativus*). *J. Agric. Food Chem.* **2014**, *62*, 2752-2759.

15. Peralta-Videa, J. R.; Hernandez-Viezcas, J. A.; Zhao, L.; Corral Diaz, B.; Ge, Y.; Priester, J. H.; Holden, P.A.; Gardea-Torresdey, J. L. Cerium dioxide and zinc oxide nanoparticles

alter the nutritional value of soil cultivated soybean plants. *Plant Physiol. Biochem.* **2014**, *80*, 128-135.

16. Horgan, R. P.; Kenny, L.C. 'Omic' technologies: genomics, transcriptomics, proteomics and metabolomics. *Obs. & Gynae.* **2011**, *13*, 189–195.

17. Natarajana, S. S.; Pastor-Corralesa, M. A.; Khana, F. H.; Garrett, W. M. Proteomic Analysis of Common Bean (*Phaseolus vulgaris* L.) by Two-Dimensional Gel Electrophoresis and Mass Spectrometry**. *J. Basic Appl. Sci.* 2013,** *9,* 424-437.

18. Lee, J.; Koh, H. J. A label-free quantitative shotgun proteomics analysis of rice grain development. *Proteome Sci.* **2011**, ***9***, 61.

19. Vannini, C.; Domingo, G.; Onelli, E.; Prinsi, B.; Marsoni, M.; Espen, L.; Bracale, M. Morphological and Proteomic Responses of *Eruca sativa* Exposed to Silver Nanoparticles or Silver Nitrate. *PLoS ONE* **2013**, *8*. doi 10.1371/journal. pone.0068752.

20. Mirzajani, F.; Askari, H.; Hamzelou, S.; Schober, Y.; Römpp, A.; Ghassempour, A.; Spengler, B. Proteomics study of silver nanoparticles toxicity on *Oryza sativa* L. *Ecotox. Environ. Safe.* **2014**, *108*, 335-339.

21. Abdallah, C.; Dumas-Gaudot, E.; Renaut, J.; Sergeant, K. "Gel-Based and Gel-Free Quantitative Proteomics Approaches at a Glance". *Int. J. Plant Genom.* **2012**, *Article ID 494572*, 17 pages; DOI 10.1155/2012/494572.

22. Keller, A. A.; Wang, H.; Zhou, D.; Lenihan, H. S.; Cherr, G.; Cardinale, B. J.; Miller, R. R.; Ji, Z. Stability and aggregation of metal oxide nanoparticles in natural aqueousmatrices. *Environ. Sci. Technol.* **2010**, *44*, 1962–1967.

23. Keller, A.; Nesvizhskii, A. I.; Kolker, E.; Aebersold R. Empirical statistical model to estimate the accuracy of peptide identifications made by MS/MS and database search. *Anal Chem.* **2002**, 74, 5383-92.

24. Nesvizhskii, A. I.; Keller, A.; Kolker, E.; Aebersold R. A statistical model for identifying proteins by tandem mass spectrometry. *Anal Chem.* **2003,** *75*, 4646-58.

25. Nesvizhskii, A. I.; Vitek, O.; Aebersold, R. Analysis and validation of proteomic data generated by tandem mass spectrometry. *Nat Methods*. **2007**, 4, 787-97.

26. Fermin, D.; Basrur, V.; Yocum, A. K.; Nesvizhskii, A. I. Abacus: a computational tool for extracting and pre-processing spectral count data for label-free quantitative proteomic analysis. *Proteomics.* **2011**, *11*, 1340-5.

27. Choi, H., Fermin, D., Nesvizhskii, A. I. Significance analysis of spectral count data in label-free shotgun proteomics. *Mol Cell Proteomics*. **2008**, 7, 2373-85.

28. McClean, P. E.; Lavin, M.; Gepts, P.; Jackson, S.A. *Phaseolus vulgaris*: A Diploid Model for Soybean, in Genetics and Genomics of Soybean Plant Genetics and Genomics: Crops and Models Volume 2, 2008, pp 55-76.

29. López-Moreno, M. L.; de la Rosa, G.; Hernandez-Viezcas, J. A.; Castillo-Michel, H.; Botez, C. E.; Peralta-Videa, J. R.; Gardea-Torresdey, J. L. Evidence of the differential biotransformation and genotoxicity of ZnO and CeO_2 nanoparticles on soybean (*Glycine max*) plants. *Environ. Sci. Technol*. **2010**, *44*, 7315-7320.

30. Hossain, Z.; Komatsu, S. Contribution of proteomic studies towards understanding plant heavy metal stress response. *Front Plant Sci.* **2013**, *25*, 310.

31. Mirouze, M.; Sels, J.; Richard, O.; Czernic, P.; Loubet,S.; Jacquier, A.; François, I. E. J. A.; Cammue, B. P. A.; Lebrun, M.; Berthomieu, P.; Marquès, L. A putative novel role for plant defensins: a defensin from the zinc hyper-accumulating plant, *Arabidopsis halleri*, confers zinc tolerance. *Plant J.* **2006**, *47*, 329–342.

32. Schenk,G.;Mitić,N.;Hanson, G. R.;Comba, P. Purple acid phosphatase: A journey into the function and mechanism of a colorful enzyme, Coordination Chemistry Reviews, **2013**, *257*, 473-482

33. Emani, C.; Hall, T. C.; Phaseolin: Structure and Evolution. *The Open Evolution Journal*, **2008**, *2*, 66-74.

34. Zhang H, Lian C, Shen Z. Proteomic identification of small, copper-responsive proteins in germinating embryos of Oryza sativa. *Ann. Bot.* **2009**, *103*, 923-930.

35. Lalitha R. Gowda, L. R.; Savithri, H. S.; Rao, D. R. The Complete Primary Structure of a Unique Mannose/Glucose-specific Lectin from Field Bean (*Dolichos lab lub*). *J. Biol. Chem.***1994**, *269*, 18789-18793

36. Peumans, W. J.; Van Damme, E. J. Lectins as plant defense proteins. *Plant Physiol.* **1995**,*109*, 347-352.

37. Hamelryck, T. W.; Dao-Thi, M.; Poortman, F.; Chrispeels‖, M. J.; Wyns, L.; Loris, R. The Crystallographic Structure of Phytohemagglutinin-L., *J. Biol. Chem.* **1996**, *271*, 20479-20485.

CHAPTER 6

1. Project on Emerging Nanotechnologies, **2014**. Consumer Products Inventory. Available: http://www.nanotechproject.org/cpi, accessed on November 26, 2014.

2. Rico, C. M.; Majumdar, S.; Duarte-Gardea, M.; Peralta-Videa, J. R.; Gardea-Torresdey, J. L. Interaction of nanoparticles with edible plants and their possible implications in the food chain. *J. Agric. Food Chem.* **2011**, *59*, 3485-3498.

3. Keller, A. A.; McFerran, S.; Lazareva, A.; Suh, S. Global life cycle releases of engineered nanomaterials. *J. Nanopart. Res.* **2013**, *15,* 1692.

4. Collin, B.; Auffan, M.; Johnson, A. C.; Kaur, I.; Keller, A. A.; Lazareva, A.; Lead, J. R.; Ma, X.; Merrifield, R.; Svendsen, C.; White, J.; Unrine, J. Environmental release, fate and ecotoxicological effects of manufactured ceria nanomaterials. *Environ. Sci. Nano.* **2014**, DOI 10.1039/C4EN00149D.

5. Gardea-Torresdey, J.; Rico, C.; White, J. Trophic transfer, transformation and impact of engineered nanomaterials in terrestrial environments. *Environ. Sci. Technol*. **2014**, *48*, 2526-2540.

6. Zhang, H.; Ji, S.; Xia, T.; Meng, H.; Low-Kam, C. *et al.* Use of metal oxide nanoparticle band gap to develop a predictive paradigm for oxidative stress and acute pulmonary inflammation. *ACS Nano* **2012**, 6, 4349-4368.

7. Wang, Q.; Ma, X.; Zhang, W.; Pei, H.; Chen, Y. The impact of cerium oxide nanoparticles on tomato (*Solanum lycopersicum* L.) and its implications for food safety. *Metallomics* **2012**, *4*, 1105-1112.

8. Rico, C. M.; Morales, M. I.; Barrios, A. C.; McCreary, R.; Hong, J.; Lee, W. Y.; Nunez, J. Peralta-Videa, J. R.; Gardea-Torresdey, J. L. Effect of cerium oxide nanoparticles on the quality of rice (*Oryza sativa* L.) grains. *J. Agric. Food Chem.* **2013**, *61*, 11278-11285.

9. Morales, M. I.; Rico, C. M.; Hernandez-Viezcas, J. A.; Nunez, J. E.; Barrios, A. C.; Tafoya, A.; Flores-Marges, J. P.; Peralta-Videa, J. R.; Gardea-Torresdey, J. L.Toxicity assessment of cerium oxide nanoparticles in cilantro (*Coriandrum sativum* L.) plants grown in organic soil. *J. Agric. Food Chem.* **2013**, *61*, 6224-6230.

10. Corral-Diaz, B; Peralta-Videa, J. R.; Alvarez-Parrilla, E.; Rodrigo-García, J.; Morales, M. I.; Osuna-Avila, P.; Niu, G.; Hernandez-Viezcas, J. A.; Gardea-Torresdey, J. L. Cerium oxide nanoparticles alter the antioxidant capacity but do not impact tuber ionome in *Raphanus sativus* (L). *Plant Physiol. Biochem*. **2014**, *84*, 277-285

11. Zhang, Z.; He, X.; Zhang, H.; Ma, Y.; Zhang, P.; Ding, Y.; Zhao, Y. Uptake and distribution of ceria nanoparticles in cucumber plants. *Metallomics,* **2011**, *3*, 816-822.

12. Zhao, L.; Sun, Y.; Hernandez-Viezcas, J. A.; Servin, A. D.; Hong, J.; Niu, G.; Peralta-Videa, J. R.; Duarte-Gardea, M.; Gardea-Torresdey, J. L. Influence of CeO_2 and ZnO nanoparticles on cucumber physiological markers and bioaccumulation of Ce and Zn: a life cycle study. *J. Agric. Food Chem*. **2013**, *61*, 1945-11951.

13. Ferry, J. L.; Craig, P.; Hexel, C.; Sisco, P.; Frey, R.; Pennington, P. L.; Fulton, M. H.; Scott, I. G.; Decho, A. W.; Kashiwada, S.; Murphy, C. J.; Shaw, T. J. Transfer of gold nanoparticles from the water column to the estuarine food web. *Nature Nanotechnol.* **2009**, *4*, 441-444.

14. Zhu, X.; Wang, J.; Zhang, X.; Chang, Y.; Chen, Y. Trophic transfer of TiO2 nanoparticles from daphnia to zebrafish in a simplified freshwater food chain. *Chemosphere* **2010**, *79*, 928-933.

15. Holbrook, R. D.; Murphy, K. E.; Morrow, J. B.; Cole, K. D. Trophic transfer of nanoparticles in a simplified invertebrate food web. *Nature Nanotechnol*. **2008**, *3*, 352-355.

16. Werlin, R.; Priester, J. H.; Mielke, R. E.; Kramer, S.; Jackson, S.; Stoimenov, P. K.; Stucky, G. D.; Cherr, G. N.; Orias, E.; Holden, P. A. Biomagnification of cadmium selenide quantum dots in a simple experimental microbial food chain. *Nature Nanotechnol*. **2011**, *6*, 65-71.

17. Kulacki, K. J.; Cardinale, B. J.; Keller, A. A.; Bier, R.; Dickson, H. How do stream organisms respond to, and influence, the concentration of titanium dioxide nanoparticles? A mesocosm study with algae and herbivores. *Environ.Toxicol. Chem.* **2012**, *31*, 2414-2422.

18. Artells, E.; Issartel, J.; Auffan, M.; Borschneck, D.; Thill, A.; Tella, M.; Brousset, L.; Rose, J.; Bottero, J. Y.; Thiéry, A. Exposure to Cerium Dioxide Nanoparticles Differently Affect Swimming Performance and Survival in Two Daphnid Species. Shah V, ed. *PLoS ONE* **2013**, *8*, e71260. doi:10.1371/journal.pone.0071260.

19. Larguinho, M.; Correia, D.; Diniz, M. S.; Baptista, P. V. Evidence of one-way flow bioaccumulation of gold nanoparticles across two trophic levels. J. Nanopart. Res., **2014**, *16*, 2549.

20. Tella, M.; Auffan, M.; Brousset, L.; Issartel, J.; Kieffer, I.; Pailles, C.; Morel, E.; Santaella, C.; Angeletti, B.; Artells, E.; Rose, J.; Thiéry, A.; Bottero, Transfer, Transformation, and Impacts of Ceria Nanomaterials in Aquatic Mesocosms Simulating a Pond Ecosystem. *J. Environ. Sci. Technol*. **2014**, *48*, 9004-9013.

21. Judy, J. D.; Unrine, J. M.; Bertsch, P. M. Evidence for Biomagnification of Gold Nanoparticles within a Terrestrial Food Chain. *Environ. Sci. Technol*. **2011**, *45*, 776-781.

22. Judy, J. D.; Unrine, J. M.; Rao, W.; Bertsch, P. M. Bioaccumulation of Gold Nanomaterials by *Manduca sexta* through Dietary Uptake of Surface Contaminated Plant Tissue. *Environ. Sci. Technol*. **2012**, *46*, 12672-12678.

23. Hawthorne, J.; De la Torre Roche, R.; Xing, B.; Newman, L. A.; Ma, X.; Majumdar, S.; Gardea-Torresdey, J.; White, J C. Particle-Size Dependent Accumulation and Trophic Transfer of Cerium Oxide through a Terrestrial Food Chain. *Environ. Sci. Technol.***2014**, *48*, 13102-13109.

24. Capinera, J. L. Class Insecta-Insects Order Coleoptera-Beetles, Weevils, White Grubs and Wireworms, In Handbook of Vegetable Pests, Eds. John L. Capinera, Academic Press, San Diego, 2001, pp 49-192, ISBN 9780121588618, http://dx.doi.org/10.1016/B978-012158861-8/50005-3.

25. Keller, A. A.; Wang, H.; Zhou, D.; Lenihan, H. S.; Cherr, G.; Cardinale, B. J.; Miller, R. R.; Ji, Z. Stability and aggregation of metal oxide nanoparticles in natural aqueousmatrices. *Environ. Sci. Technol.* **2010**, *44*, 1962–1967.

26. Majumdar, S.; Peralta-Videa, J. R.; Bandyopadhyay, S.; Castillo-Michel, H.; Hernandez-Viezcas, J. A.; Sahi, S.; Gardea-Torresdey, J. L. Exposure of cerium oxide nanoparticles to kidney bean shows disturbance in the plant defense mechanisms. *J. Hazard. Mater.* **2014**, *278*, 279-287.

27. Robertson, J. L.; Savin, N. E; Preisler, H. K.; Russell, R. M. Bioassays with Arthropods, 2nd Ed., pp16-18

28. Packer, A. P.; Lariviere, D.; Li, C.; Chen, M.; Fawcett, A.; Nielsen, K.; Mattson, K.; Chatt, A.; Scriver, C.; Erhardt, L. S. Validation of an inductively coupled plasma mass spectrometry (ICP-MS) method for the determination of cerium, strontium, and titanium in ceramic materials used in radiological dispersal devices (RDDs). *Anal. Chim. Acta*. **2007**, *588*, 166-172.

29. Priester, J. H.; Ge, Y.; Mielke, R. E.; Horst, A. M.; Moritz, S. C.; Espinosa, K.; Gelb, J.; Walker, S. L.; Nisbet, R. M.; An, Y. J.; Schimel, J. P.; Palmer, R. G.; Hernandez-Viezcas, J. A.; Zhao, L.; Gardea-Torresdey, J. L.; Holden, P. A. Soybean susceptibility to manufactured nanomaterials with evidence for food quality and soil fertility interruption. *Proc. Natl. Acad. Sci.* **2012**, *109,* 2451-2456.

30. López-Moreno, M. L.; de la Rosa, G.; Hernandez-Viezcas, J. A.; Castillo-Michel, H.; Botez, C. E.; Peralta-Videa, J. R.; Gardea-Torresdey, J. L. Evidence of the differential

biotransformation and genotoxicity of ZnO and CeO_2 nanoparticles on soybean (*Glycine max*) plants. *Environ. Sci. Technol.* **2010**, *44*, 7315-7320.

31. Rico, C. M.; Hong, J.; Morales, M. I.; Zhao, L.; Barrios, A. C.; Zhang, J. Y.; Peralta-Videa, J. R.; Gardea-Torresdey, J. L. Effect of cerium oxide nanoparticles on rice: a study involving the antioxidant defense system and in vivo fluorescence imaging. *Environ. Sci. Technol.* **2013**, *47*, 5635-5642.

Appendix I

List of 659 proteins identified combining all the treatments by merging the identified protein lists from all three biological replicates.

Protein ID	DEFLINE	Prot Len
P13917	Basic 7S globulin OS=Glycine max GN=BG PE=1 SV=2	427
C6F117	Putative ribosomal protein S15 OS=Glycine max PE=2 SV=1	130
B0M197	Peroxisomal voltage-dependent anion-selective channel protein OS=Glycine max PE=2 SV=1	276
B0M1A5	Betaine aldehyde dehydrogenase OS=Glycine max GN=BADH2 PE=2 SV=1	503
B2BF98	40S ribosomal protein S6 OS=Glycine max PE=3 SV=1	247
B3TDK6	Lipoxygenase OS=Glycine max GN=Lx3 PE=3 SV=1	857
Q9FQF9	Lipoxygenase OS=Phaseolus vulgaris PE=1 SV=1	874
B3TDK5	Lipoxygenase OS=Glycine max PE=3 SV=1	862
O24320	Lipoxygenase OS=Phaseolus vulgaris PE=1 SV=2	865
K7L7J5	Lipoxygenase OS=Glycine max PE=3 SV=1	861
B3TDK4	Lipoxygenase OS=Glycine max PE=3 SV=1	839
K7L9E5	Uncharacterized protein (Fragment) OS=Glycine max PE=4 SV=1	214
I1KG91	Uncharacterized protein (Fragment) OS=Glycine max PE=4 SV=1	490
B7T1N8	Rack OS=Phaseolus vulgaris GN=RACK PE=2 SV=1	324
C6SV78	Ribosomal protein L15 OS=Glycine max PE=2 SV=1	204
C6SV94	Uncharacterized protein OS=Glycine max PE=2 SV=1	150
C6SVE3	Putative uncharacterized protein OS=Glycine max PE=4 SV=1	91
C6SVF4	Putative uncharacterized protein OS=Glycine max PE=2 SV=1	223
C6SVV7	40S ribosomal protein S12 OS=Glycine max PE=2 SV=1	141
C6SW15	Putative uncharacterized protein OS=Glycine max PE=1 SV=1	236
C6SVZ3	Putative uncharacterized protein OS=Glycine max PE=2 SV=1	193
C6SVZ7	Putative uncharacterized protein OS=Glycine max PE=2 SV=1	215
C6SW04	Uncharacterized protein OS=Glycine max PE=2 SV=1	206
C6SW33	Uncharacterized protein OS=Glycine max PE=2 SV=1	148
C6SWE9	Histone H2B OS=Glycine max PE=2 SV=1	137
C6SWQ4	Proteasome subunit beta type OS=Glycine max PE=2 SV=1	233
C6SWV3	Uncharacterized protein OS=Glycine max PE=2 SV=1	245
C6SWX1	Uncharacterized protein OS=Glycine max PE=4 SV=1	108
C6SXM4	Uncharacterized protein OS=Glycine max PE=2 SV=1	181
T2DN08	ADP-ribosylation factor OS=Phaseolus vulgaris PE=2 SV=1	209
C6SXU0	Putative uncharacterized protein OS=Glycine max PE=2 SV=1	245
C6SWG4	40S ribosomal protein S21 OS=Glycine max PE=3 SV=1	82
C6SYI8	Putative uncharacterized protein OS=Glycine max PE=2 SV=1	164
C6SZN6	Uncharacterized protein OS=Glycine max PE=1 SV=1	164
C6SZ83	Putative uncharacterized protein OS=Glycine max PE=2 SV=1	205
C6T073	Uncharacterized protein OS=Glycine max PE=1 SV=1	197
C6T0H2	Putative uncharacterized protein OS=Glycine max PE=4 SV=1	115
C6T116	Putative uncharacterized protein OS=Glycine max PE=2 SV=1	158
C6T1V2	Uncharacterized protein OS=Glycine max PE=2 SV=1	157
C6SVX0	Putative uncharacterized protein OS=Glycine max PE=2 SV=1	161
C6T2E5	Uncharacterized protein OS=Glycine max PE=2 SV=1	206
C6T4R9	Uncharacterized protein OS=Glycine max PE=2 SV=1	155
C6T514	40S ribosomal protein S8 (Fragment) OS=Glycine max PE=2 SV=1	243
C6T588	Uncharacterized protein OS=Glycine max PE=2 SV=1	158
C6SWV6	40S ribosomal protein S27 OS=Glycine max PE=3 SV=1	90
C6T5N1	Putative uncharacterized protein OS=Glycine max PE=2 SV=1	166
C6T898	Putative uncharacterized protein OS=Glycine max PE=2 SV=1	450
C6T8X3	Putative uncharacterized protein OS=Glycine max PE=2 SV=1	413
C6T977	Uncharacterized protein OS=Glycine max PE=2 SV=1	372
C6TAX1	Putative uncharacterized protein OS=Glycine max PE=2 SV=1	293

C6TB24	Putative uncharacterized protein OS=Glycine max PE=2 SV=1	198
C6TB70	Putative uncharacterized protein OS=Glycine max PE=2 SV=1	218
C6TBY0	Uncharacterized protein OS=Glycine max PE=2 SV=1	260
C6TCC6	Uncharacterized protein OS=Glycine max PE=2 SV=1	316
C6TCX5	Uncharacterized protein OS=Glycine max PE=2 SV=1	394
C6SXC3	Uncharacterized protein OS=Glycine max PE=4 SV=1	112
C6TDL5	Putative uncharacterized protein OS=Glycine max PE=2 SV=1	260
C6TEK4	Putative uncharacterized protein OS=Glycine max PE=2 SV=1	426
C6TG97	Proteasome subunit alpha type OS=Glycine max PE=2 SV=1	249
C6TGA8	Putative uncharacterized protein OS=Glycine max PE=2 SV=1	340
C6TGF3	Putative uncharacterized protein (Fragment) OS=Glycine max PE=2 SV=1	487
C6TH59	Proteasome subunit alpha type OS=Glycine max PE=2 SV=1	235
C6THM7	Serine hydroxymethyltransferase OS=Glycine max PE=1 SV=1	442
C6THN1	Putative uncharacterized protein OS=Glycine max PE=2 SV=1	444
C6TIR2	Putative uncharacterized protein OS=Glycine max PE=2 SV=1	149
Q93VL8	Calmodulin OS=Phaseolus vulgaris GN=CaM PE=2 SV=1	149
C6TIW0	Fructose-bisphosphate aldolase OS=Glycine max PE=1 SV=1	388
C6SZ11	Putative uncharacterized protein OS=Glycine max PE=2 SV=1	234
C6TJT5	Putative uncharacterized protein OS=Glycine max PE=1 SV=1	364
C6TLT3	40S ribosomal protein S3a OS=Glycine max PE=2 SV=1	261
C6TMG1	Fructose-bisphosphate aldolase OS=Glycine max PE=2 SV=1	358
I1JH86	Fructose-bisphosphate aldolase OS=Glycine max PE=3 SV=1	358
I1M6D5	Fructose-bisphosphate aldolase OS=Glycine max PE=3 SV=1	357
C6TNX9	Proteasome subunit alpha type OS=Glycine max PE=2 SV=1	246
C6ZHS4	Eukaryotic translation initiation factor 5A2 OS=Glycine max PE=2 SV=1	160
D2DWA5	Formate dehydrogenase OS=Phaseolus vulgaris PE=3 SV=1	374
C6T9Z5	Uncharacterized protein OS=Glycine max PE=2 SV=1	388
D3W146	Non-specific lipid-transfer protein OS=Phaseolus vulgaris GN=Pha v 3.0101 PE=3 SV=1	115
E7E8T8	60S acidic ribosomal protein P0 OS=Phaseolus vulgaris PE=2 SV=1	320
F8SMB9	Adenosylhomocysteinase OS=Glycine max PE=2 SV=1	485
G3E7M5	Putative rubisco subunit binding-protein alpha subunit OS=Glycine max PE=2 SV=1	584
C6T0H9	Uncharacterized protein OS=Glycine max PE=2 SV=1	140
H2FH46	Glutathione transferase OS=Phaseolus vulgaris GN=GSTF1-1 PE=2 SV=1	215
C6SVD7	Uncharacterized protein OS=Glycine max PE=2 SV=1	215
H6WQB3	Allantoinase 1 OS=Phaseolus vulgaris PE=2 SV=1	512
I1J8H1	Uncharacterized protein OS=Glycine max PE=4 SV=1	901
I1LU53	Uncharacterized protein OS=Glycine max PE=4 SV=1	984
I1LRQ4	Uncharacterized protein OS=Glycine max PE=4 SV=1	984
I1JF86	Uncharacterized protein OS=Glycine max PE=4 SV=2	506
I1JIA0	Clathrin heavy chain OS=Glycine max PE=3 SV=2	1707
I1JR71	Importin subunit alpha OS=Glycine max PE=3 SV=1	532
I1K6C9	Uncharacterized protein OS=Glycine max PE=4 SV=2	853
I1KAB0	Aldehyde dehydrogenase OS=Glycine max PE=3 SV=1	491
I1KAB7	Uncharacterized protein OS=Glycine max PE=3 SV=1	503
K7KUJ1	Uncharacterized protein (Fragment) OS=Glycine max PE=4 SV=1	378
B1Q2X4	Protein disulfide isomerase OS=Glycine max GN=PDIL-1 PE=1 SV=1	525
I1KAY1	Uncharacterized protein OS=Glycine max PE=3 SV=1	98
C6T389	Uncharacterized protein OS=Glycine max PE=2 SV=1	194
I1KD00	Uncharacterized protein OS=Glycine max PE=3 SV=2	753
I1KDM8	Malate dehydrogenase OS=Glycine max PE=3 SV=1	345
C6TGD9	Uncharacterized protein OS=Glycine max PE=2 SV=1	409
I1LH25	Malate dehydrogenase OS=Glycine max PE=3 SV=1	353
I1KFR0	Uncharacterized protein OS=Glycine max PE=4 SV=1	279
I1KJ84	Uncharacterized protein OS=Glycine max PE=4 SV=1	424
I1KP71	Uncharacterized protein OS=Glycine max PE=3 SV=1	350
C6T7T2	Putative uncharacterized protein OS=Glycine max PE=2 SV=1	350
I1KPN3	Uncharacterized protein OS=Glycine max PE=3 SV=1	667
I1MT10	Uncharacterized protein OS=Glycine max PE=3 SV=1	645
Q01899	Heat shock 70 kDa protein, mitochondrial OS=Phaseolus vulgaris PE=1 SV=1	675

I1JGR5	Uncharacterized protein OS=Glycine max PE=3 SV=1	652
K7LZH1	Uncharacterized protein OS=Glycine max PE=3 SV=1	632
K7L2A0	Uncharacterized protein OS=Glycine max PE=3 SV=1	633
K7MVD3	Uncharacterized protein OS=Glycine max PE=3 SV=1	647
I1KQ93	Uncharacterized protein OS=Glycine max PE=3 SV=1	582
K7KCS1	Uncharacterized protein OS=Glycine max PE=4 SV=1	394
I1KTW3	Uncharacterized protein OS=Glycine max PE=3 SV=1	537
I1MJE1	Uncharacterized protein OS=Glycine max PE=3 SV=2	495
I1KU21	Uncharacterized protein OS=Glycine max PE=4 SV=1	843
T2DM33	Elongation factor 2-like protein OS=Phaseolus vulgaris PE=2 SV=1	846
I1KWM7	6-phosphogluconate dehydrogenase, decarboxylating OS=Glycine max PE=3 SV=1	486
C6T498	Putative uncharacterized protein OS=Glycine max PE=2 SV=1	220
I1KXC2	Uncharacterized protein OS=Glycine max PE=4 SV=1	1459
I1KZJ9	Uncharacterized protein OS=Glycine max PE=4 SV=1	725
I1KZT2	Uncharacterized protein OS=Glycine max PE=4 SV=1	287
I1L0N6	Uncharacterized protein OS=Glycine max PE=4 SV=1	313
K7LYD7	Uncharacterized protein OS=Glycine max PE=4 SV=1	307
I1L0Q8	Uncharacterized protein OS=Glycine max PE=4 SV=1	458
I1L8R1	Uncharacterized protein OS=Glycine max PE=4 SV=1	405
I1L934	Histone H4 OS=Glycine max PE=3 SV=1	103
B9MST3	Histone H4 OS=Glycine max PE=3 SV=1	103
I1L957	Uncharacterized protein OS=Glycine max PE=4 SV=1	449
I1LCI1	Uncharacterized protein OS=Glycine max PE=3 SV=1	577
I1LCN7	Uncharacterized protein OS=Glycine max PE=4 SV=1	1218
C6T4A1	Glutathione peroxidase OS=Glycine max PE=2 SV=1	166
I1LEE5	Uncharacterized protein OS=Glycine max PE=4 SV=1	631
I1JAY8	Uncharacterized protein OS=Glycine max PE=4 SV=2	643
I1LQL0	Uncharacterized protein OS=Glycine max PE=4 SV=1	195
I1LT76	Uncharacterized protein OS=Glycine max PE=4 SV=1	242
K7KWZ7	Uncharacterized protein OS=Glycine max PE=4 SV=1	282
I1LWR4	Phosphorylase OS=Glycine max PE=3 SV=1	978
I1LXQ1	Uncharacterized protein OS=Glycine max PE=4 SV=2	725
I1LZ82	Uncharacterized protein OS=Glycine max PE=4 SV=1	811
I1KCD7	Uncharacterized protein OS=Glycine max PE=4 SV=2	814
I1JXA0	Uncharacterized protein OS=Glycine max PE=4 SV=1	814
I1M0U7	Annexin OS=Glycine max PE=3 SV=1	314
C6T7M2	Annexin OS=Glycine max PE=2 SV=1	312
I1MBR7	Uncharacterized protein OS=Glycine max PE=4 SV=1	469
I1LM73	Uncharacterized protein OS=Glycine max PE=4 SV=1	475
I1MC31	Uncharacterized protein OS=Glycine max PE=3 SV=1	847
I1JJL6	Uncharacterized protein OS=Glycine max PE=3 SV=1	702
I1L314	Uncharacterized protein OS=Glycine max PE=3 SV=1	699
D6C500	HSP90-2 OS=Glycine max PE=1 SV=1	699
I1MD61	Uncharacterized protein OS=Glycine max PE=4 SV=1	330
I1M561	Uncharacterized protein OS=Glycine max PE=4 SV=1	331
P49231	Profilin-1 OS=Phaseolus vulgaris PE=1 SV=1	131
C6TCF1	Putative uncharacterized protein OS=Glycine max PE=2 SV=1	241
I1MDT4	Uncharacterized protein OS=Glycine max PE=3 SV=1	377
C6TGZ9	Putative uncharacterized protein OS=Glycine max PE=2 SV=1	377
O65016	Actin 4 OS=Glycine max GN=SAc4 PE=3 SV=1	376
I1MDY5	Uncharacterized protein OS=Glycine max PE=4 SV=1	524
I1MJC7	Phosphoglycerate kinase OS=Glycine max PE=3 SV=1	401
I1MJC6	Phosphoglycerate kinase OS=Glycine max PE=3 SV=1	377
I1MJU7	Uncharacterized protein OS=Glycine max PE=3 SV=1	689
I1MM08	Malic enzyme OS=Glycine max PE=3 SV=2	591
I1K5Y5	Malic enzyme OS=Glycine max PE=3 SV=1	633
I1MQS6	Uncharacterized protein OS=Glycine max PE=4 SV=1	420
I1MTR0	Uncharacterized protein OS=Glycine max PE=3 SV=1	553
I1N2Z5	Uncharacterized protein OS=Glycine max PE=4 SV=1	112

C6T0L2	Uncharacterized protein OS=Glycine max PE=4 SV=1	101
I1N8M5	Uncharacterized protein OS=Glycine max PE=4 SV=1	201
I1NAI7	Uncharacterized protein OS=Glycine max PE=3 SV=1	444
I1JPW5	Uncharacterized protein OS=Glycine max PE=3 SV=1	444
C6TDL9	Putative uncharacterized protein OS=Glycine max PE=2 SV=1	219
I1NEH6	Uncharacterized protein OS=Glycine max PE=4 SV=1	328
I1NFS4	ATP synthase subunit beta OS=Glycine max PE=3 SV=1	559
I1NIE7	Uncharacterized protein OS=Glycine max PE=3 SV=2	557
I1NJ85	Uncharacterized protein OS=Glycine max PE=3 SV=1	636
I1LFG6	Uncharacterized protein OS=Glycine max PE=3 SV=1	636
K7L7D2	Uncharacterized protein OS=Glycine max PE=4 SV=1	330
K7LQ69	Uncharacterized protein OS=Glycine max PE=4 SV=1	812
Q9SWB4	Poly [ADP-ribose] polymerase 3 OS=Glycine max GN=PARP3 PE=2 SV=1	815
K7LWE4	Uncharacterized protein OS=Glycine max PE=4 SV=1	186
K7MIV6	Uncharacterized protein OS=Glycine max PE=4 SV=1	214
K7VK11	UDP-glucuronic acid decarboxylase 1-like isoform 1 OS=Phaseolus vulgaris PE=2 SV=1	342
I1LQS4	Uncharacterized protein OS=Glycine max PE=4 SV=1	343
O23959	Ca+2-binding EF hand protein OS=Glycine max GN=GmPM13 PE=2 SV=1	239
C6TFP4	Uncharacterized protein OS=Glycine max PE=1 SV=1	123
O24319	Purple acid phosphatase OS=Phaseolus vulgaris GN=pap PE=1 SV=1	459
P80366	Fe(3+)-Zn(2+) purple acid phosphatase OS=Phaseolus vulgaris PE=1 SV=2	432
Q39856	Epoxide hydrolase OS=Glycine max PE=2 SV=1	341
C6TK81	Putative uncharacterized protein OS=Glycine max PE=2 SV=1	318
Q41108	Pv42p OS=Phaseolus vulgaris PE=2 SV=1	379
Q41119	Peptidyl-prolyl cis-trans isomerase OS=Phaseolus vulgaris GN=Cyp PE=1 SV=1	172
K7LNW4	Peptidyl-prolyl cis-trans isomerase OS=Glycine max PE=3 SV=1	195
Q5JZZ3	Triosephosphate isomerase OS=Phaseolus vulgaris var. nanus GN=tpi PE=1 SV=1	254
Q71EW8	Methionine synthase OS=Glycine max PE=1 SV=1	763
T2DLV0	5-methyltetrahydropteroyltriglutamate homocysteine methyltransferase like isoform 1 OS=Phaseolus vulgaris PE=2 SV=1	763
I1MW49	Uncharacterized protein OS=Glycine max PE=3 SV=2	765
Q8GTA3	Sucrose synthase OS=Phaseolus vulgaris PE=1 SV=1	805
Q8W1A0	Cysteine synthase OS=Glycine max PE=1 SV=1	325
Q9M7M4	Mannose lectin FRIL (Fragment) OS=Phaseolus vulgaris PE=2 SV=1	279
P05088	Erythroagglutinating phytohemagglutinin OS=Phaseolus vulgaris GN=DLEC1 PE=1 SV=1	275
P05087	Leucoagglutinating phytohemagglutinin OS=Phaseolus vulgaris GN=DLEC2 PE=1 SV=1	272
Q43628	Phytohemagglutinin OS=Phaseolus vulgaris PE=4 SV=1	274
T2DN52	Phytohemagglutinin OS=Phaseolus vulgaris PE=2 SV=1	274
D7F7K7	Lectin OS=Glycine max GN=Le4 PE=4 SV=1	280
P15231	Leucoagglutinating phytohemagglutinin OS=Phaseolus vulgaris GN=PDLEC2 PE=3 SV=1	273
Q9XIS6	Granule-bound starch synthase I OS=Phaseolus vulgaris GN=pvgbss1 PE=2 SV=1	606
C6TGT0	Uncharacterized protein OS=Glycine max PE=2 SV=1	290
T2DLI2	Glyceraldehyde-3-phosphate dehydrogenase OS=Phaseolus vulgaris PE=2 SV=1	338
C6TD56	Uncharacterized protein OS=Glycine max PE=1 SV=1	340
I1K135	Uncharacterized protein OS=Glycine max PE=3 SV=1	337
T2DLJ5	Calnexin-like protein OS=Phaseolus vulgaris PE=2 SV=1	546
T2DLM1	Acetohydroxyacid isomeroreductase OS=Phaseolus vulgaris PE=2 SV=1	581
T2DLN1	Tubulin beta chain OS=Phaseolus vulgaris PE=2 SV=1	449
I1JT28	Uncharacterized protein OS=Glycine max PE=3 SV=1	449
I1KRC0	Uncharacterized protein OS=Glycine max PE=3 SV=1	443
I1KPA1	Uncharacterized protein OS=Glycine max PE=3 SV=1	445
T2DLN4	60S ribosomal protein l9 OS=Phaseolus vulgaris PE=2 SV=1	193
T2DLR9	Alcohol dehydrogenase 1 OS=Phaseolus vulgaris PE=2 SV=1	380
I1KAJ5	Uncharacterized protein OS=Glycine max PE=3 SV=1	337
I1MAE6	Uncharacterized protein OS=Glycine max PE=3 SV=1	380
C6TA60	Putative uncharacterized protein OS=Glycine max PE=2 SV=1	379
I1JY29	Uncharacterized protein OS=Glycine max PE=3 SV=1	381
T2DLS9	Quinone-oxidoreductase-like protein OS=Phaseolus vulgaris PE=2 SV=1	337
T2DLT1	60S ribosomal protein L3-like protein OS=Phaseolus vulgaris PE=2 SV=1	388

T2DM56	GTP-binding nuclear protein Ran-3 OS=Phaseolus vulgaris PE=2 SV=1	221
T2DMQ9	60S ribosomal protein L18-3-like protein OS=Phaseolus vulgaris PE=2 SV=1	222
C6SWN7	Putative uncharacterized protein OS=Glycine max PE=2 SV=1	187
C6THM9	Annexin OS=Glycine max PE=2 SV=1	313
T2DMX0	Alcohol dehydrogenase class III OS=Phaseolus vulgaris PE=2 SV=1	379
T2DNI1	Hydroxyacylglutathione hydrolase OS=Phaseolus vulgaris PE=2 SV=1	258
T2DNM6	Proteasome subunit beta type-6-like protein OS=Phaseolus vulgaris PE=2 SV=1	233
T2DNN1	Steroid binding protein OS=Phaseolus vulgaris PE=2 SV=1	232
K7MIH4	Uncharacterized protein OS=Glycine max PE=4 SV=1	222
T2DNN6	NADPH-specific isocitrate dehydrogenase OS=Phaseolus vulgaris PE=2 SV=1	412
T2DNR4	Alpha-1,4-glucan-protein synthase [UDP-forming]-like protein OS=Phaseolus vulgaris PE=2 SV=1	363
C6TD94	Putative uncharacterized protein (Fragment) OS=Glycine max PE=1 SV=1	315
K7MUF4	Uncharacterized protein OS=Glycine max PE=4 SV=1	347
C6TAB7	Uncharacterized protein OS=Glycine max PE=2 SV=1	357
T2DNT1	40S ribosomal protein S5-like protein OS=Phaseolus vulgaris PE=2 SV=1	207
T2DNW6	CHP-rich zinc finger protein OS=Phaseolus vulgaris PE=2 SV=1	244
T2DNZ6	In2-1 protein OS=Phaseolus vulgaris PE=2 SV=1	237
T2DP01	14-3-3 protein OS=Phaseolus vulgaris PE=2 SV=1	259
T2DMA9	14-3-3 family protein OS=Phaseolus vulgaris PE=2 SV=1	256
T2DNK7	14-3-3 protein OS=Phaseolus vulgaris PE=2 SV=1	258
I1M3M0	Uncharacterized protein OS=Glycine max PE=3 SV=1	260
C6TGW2	Uncharacterized protein OS=Glycine max PE=2 SV=1	262
C6TJB9	Putative uncharacterized protein OS=Glycine max PE=2 SV=1	243
T2DP18	Cbs domain protein OS=Phaseolus vulgaris PE=2 SV=1	206
T2DP50	Elongation factor 1-beta OS=Phaseolus vulgaris PE=2 SV=1	223
T2DN56	Elongation factor 1 beta OS=Phaseolus vulgaris PE=2 SV=1	231
T2DPD6	Profilin OS=Phaseolus vulgaris PE=2 SV=1	131
T2DPE5	Nucleoside diphosphate kinase 1 OS=Phaseolus vulgaris PE=2 SV=1	149
T2DPK7	Malate dehydrogenase OS=Phaseolus vulgaris PE=2 SV=1	332
rev_tr|C4B4V1|C4B4V1_BYMV	DECOY PROTEIN	3056
C6TEC2	Putative uncharacterized protein OS=Glycine max PE=2 SV=1	499
C6SV88	Peptidyl-prolyl cis-trans isomerase OS=Glycine max PE=2 SV=1	147
C6SX09	Putative uncharacterized protein (Fragment) OS=Glycine max PE=2 SV=1	252
C6SZ88	Uncharacterized protein OS=Glycine max PE=2 SV=1	194
C6TKH0	Uncharacterized protein OS=Glycine max PE=2 SV=1	294
T2DMN2	Aquaporin PIP-type 7a-like protein OS=Phaseolus vulgaris PE=2 SV=1	289
C6SWE3	Putative uncharacterized protein OS=Glycine max PE=2 SV=1	215
I1M0B5	Uncharacterized protein OS=Glycine max PE=4 SV=1	490
T2DMJ8	Intracellular protease OS=Phaseolus vulgaris PE=2 SV=1	388
B2YDQ6	Gly m Bd 28K allergen (Fragment) OS=Glycine max PE=4 SV=1	373
I1JR88	Uncharacterized protein OS=Glycine max PE=4 SV=1	318
K7K5A8	Uncharacterized protein OS=Glycine max PE=4 SV=1	1129
T2DP56	Acid phosphatase OS=Phaseolus vulgaris PE=2 SV=1	256
T2DP66	Cysteine proteinase OS=Phaseolus vulgaris PE=2 SV=1	385
C6T6K1	Putative uncharacterized protein (Fragment) OS=Glycine max PE=2 SV=1	212
C6TKP4	Putative uncharacterized protein OS=Glycine max PE=2 SV=1	255
C6TNT8	Putative uncharacterized protein OS=Glycine max PE=2 SV=1	391
I1J8K1	Uncharacterized protein OS=Glycine max PE=4 SV=2	1004
T2DP23	Basic 7S globulin OS=Phaseolus vulgaris PE=2 SV=1	486
A5JVZ7	Superoxide dismutase OS=Glycine max PE=1 SV=1	241
C6SZF9	Putative uncharacterized protein OS=Glycine max PE=2 SV=1	231
I1LTJ5	Beta-galactosidase OS=Glycine max PE=3 SV=1	840
I1JPI7	Uncharacterized protein OS=Glycine max PE=4 SV=1	397
Q7X9E6	Heat shock cognate protein 70 (Fragment) OS=Phaseolus vulgaris PE=2 SV=1	37
I1KMP3	Uncharacterized protein OS=Glycine max PE=3 SV=1	497
C6TBI1	Putative uncharacterized protein OS=Glycine max PE=2 SV=1	280
C6TKW9	Putative uncharacterized protein OS=Glycine max PE=2 SV=1	458

T2DPW3	Beta-glucosidase 44-like protein OS=Phaseolus vulgaris PE=2 SV=1	518
K7KSG7	Uncharacterized protein OS=Glycine max PE=4 SV=1	170
rev_tr|I1L3Y5|I1L3Y5_SOYBN	DECOY PROTEIN	722
I1JXQ5	Uncharacterized protein OS=Glycine max PE=4 SV=2	1011
C6SZK1	Putative uncharacterized protein OS=Glycine max PE=2 SV=1	152
rev_tr|K7LFI1|K7LFI1_SOYBN	DECOY PROTEIN	1205
C6T0K5	Reticulon-like protein (Fragment) OS=Glycine max PE=2 SV=1	125
I1N7G4	Uncharacterized protein OS=Glycine max PE=3 SV=1	582
I1NF29	Uncharacterized protein OS=Glycine max PE=4 SV=1	766
I1JY87	Uncharacterized protein OS=Glycine max PE=4 SV=2	565
C6TLJ9	Proteasome subunit beta type OS=Glycine max PE=2 SV=1	272
I1K565	Uncharacterized protein OS=Glycine max PE=4 SV=1	991
C6TAZ2	Putative uncharacterized protein OS=Glycine max PE=2 SV=1	211
C6TGR8	Putative uncharacterized protein OS=Glycine max PE=2 SV=1	421
C6TID1	Putative uncharacterized protein OS=Glycine max PE=1 SV=1	315
rev_tr|Q39871|Q39871_SOYBN	DECOY PROTEIN	463
C6SWE8	Superoxide dismutase [Cu-Zn] OS=Glycine max PE=2 SV=1	152
I1LJP3	Uncharacterized protein OS=Glycine max PE=4 SV=1	331
I1M5L7	Uncharacterized protein OS=Glycine max PE=3 SV=1	863
I1MA56	Uncharacterized protein OS=Glycine max PE=3 SV=1	432
C6SW24	Uncharacterized protein OS=Glycine max PE=2 SV=1	204
P84869	Antifungal lectin PVAP (Fragment) OS=Phaseolus vulgaris PE=1 SV=1	10
C6TM35	Putative uncharacterized protein OS=Glycine max PE=2 SV=1	309
C6TIJ2	Putative uncharacterized protein (Fragment) OS=Glycine max PE=2 SV=1	303
I1J6Z7	Uncharacterized protein OS=Glycine max PE=4 SV=1	313
I1LDX0	Uncharacterized protein OS=Glycine max PE=4 SV=1	628
K7M3E3	Uncharacterized protein OS=Glycine max PE=4 SV=1	773
rev_tr|I1L957|I1L957_SOYBN	DECOY PROTEIN	449
Q9S8B3	GNL-1 alpha SUBUNIT=LECTIN (Fragment) OS=Phaseolus vulgaris PE=1 SV=1	24
T2DNM1	Uncharacterized protein OS=Phaseolus vulgaris PE=2 SV=1	366
C6SZQ3	Uncharacterized protein OS=Glycine max PE=2 SV=1	151
I1JD78	Uncharacterized protein OS=Glycine max PE=3 SV=1	501
I1K8E3	Uncharacterized protein OS=Glycine max PE=4 SV=1	873
D7EYG6	V-H(+)-ATPase subunit A OS=Glycine max PE=2 SV=1	623
Q41125	Proline-rich 14 kDa protein OS=Phaseolus vulgaris PE=2 SV=1	127
rev_tr|I1LGJ3|I1LGJ3_SOYBN	DECOY PROTEIN	736
C6T7V6	Triosephosphate isomerase OS=Glycine max PE=1 SV=1	309
T2DNF1	60S ribosomal protein L13a OS=Phaseolus vulgaris PE=2 SV=1	206
C6SWE0	Uncharacterized protein OS=Glycine max PE=2 SV=1	162
C6SX72	Putative uncharacterized protein OS=Glycine max PE=2 SV=1	181
I1JJP2	Glucose-1-phosphate adenylyltransferase OS=Glycine max PE=3 SV=1	515
S5RUY3	Sporulation related domain-containing protein OS=Rhizobium etli bv. mimosae str. Mim1 GN=REMIM1_CH01868 PE=4 SV=1	1063
C6SVF1	Actin depolymerizing factor 1 OS=Glycine max GN=ADF1 PE=2 SV=1	139
K7KD30	Uncharacterized protein (Fragment) OS=Glycine max PE=4 SV=1	199
E9NZS9	Putative uncharacterized protein OS=Phaseolus vulgaris PE=4 SV=1	804
K7N193	Uncharacterized protein OS=Glycine max PE=4 SV=1	111
rev_tr|I1MUI4|I1MUI4_SOYBN	DECOY PROTEIN	1217
K7ME55	Uncharacterized protein OS=Glycine max PE=4 SV=1	747
I1J8V9	Uncharacterized protein OS=Glycine max PE=4 SV=1	630
I1JSP6	Coatomer subunit gamma OS=Glycine max PE=3 SV=1	886
B0M199	Peroxisomal fatty acid beta-oxidation multifunctional protein OS=Glycine max PE=1 SV=1	723
K7LDT9	Uncharacterized protein OS=Glycine max PE=4 SV=1	950
I1KQE8	Uncharacterized protein OS=Glycine max PE=4 SV=1	1006

rev_tr|C6TGT4|C6TGT4_SOYBN	DECOY PROTEIN	419
rev_tr|K7KPD2|K7KPD2_SOYBN	DECOY PROTEIN	621
F8QXP7	Legumin OS=Phaseolus vulgaris PE=2 SV=1	606
Q39890	Calmodulin OS=Glycine max GN=SCaM-4 PE=1 SV=1	150
I1JCI6	Uncharacterized protein OS=Glycine max PE=3 SV=1	250
rev_tr|K7KME7|K7KME7_SOYBN	DECOY PROTEIN	327
I1JVE0	Uncharacterized protein OS=Glycine max PE=3 SV=1	283
I1J7G5	Uncharacterized protein OS=Glycine max PE=4 SV=1	170
I1N3A6	Uncharacterized protein OS=Glycine max PE=4 SV=1	410
I1JQX3	Uncharacterized protein OS=Glycine max PE=3 SV=1	515
O24323	Cysteine proteinase OS=Phaseolus vulgaris PE=1 SV=1	455
C6TJH2	Uncharacterized protein OS=Glycine max PE=2 SV=1	192
rev_tr|C6T2L7|C6T2L7_SOYBN	DECOY PROTEIN	228
F8QXP8	Albumin-2 OS=Phaseolus vulgaris PE=2 SV=1	227
I1KZJ0	Uncharacterized protein OS=Glycine max PE=3 SV=1	439
C6T7Z3	Putative uncharacterized protein OS=Glycine max PE=1 SV=1	210
Q01527	Maturation protein OS=Glycine max GN=gGmpm9 PE=2 SV=1	152
rev_tr|I1M0H3|I1M0H3_SOYBN	DECOY PROTEIN	373
I1JPV5	Pyruvate kinase OS=Glycine max PE=3 SV=1	527
rev_tr|I1KR15|I1KR15_SOYBN	DECOY PROTEIN	699
K7L2I5	Uncharacterized protein OS=Glycine max PE=4 SV=1	376
C6TAN1	Putative uncharacterized protein OS=Glycine max PE=2 SV=1	423
K7K978	Uncharacterized protein OS=Glycine max PE=4 SV=1	582
I1JW22	Uncharacterized protein OS=Glycine max PE=3 SV=1	605
F8QXP9	Defensin D1 OS=Phaseolus vulgaris PE=4 SV=1	75
K7LDQ4	Uncharacterized protein OS=Glycine max PE=3 SV=1	323
rev_tr|I1KJP8|I1KJP8_SOYBN	DECOY PROTEIN	285
I1KNH4	Uncharacterized protein OS=Glycine max PE=4 SV=1	568
C6TLQ4	Putative uncharacterized protein OS=Glycine max PE=2 SV=1	245
K7MMG8	Uncharacterized protein OS=Glycine max PE=4 SV=1	641
C6T1L4	Uncharacterized protein OS=Glycine max PE=2 SV=1	176
A8C8H3	Glutamate decarboxylase OS=Glycine max GN=GAD PE=1 SV=1	503
C6SV85	Uncharacterized protein OS=Glycine max PE=4 SV=1	110
C6SVD3	Peptidyl-prolyl cis-trans isomerase OS=Glycine max PE=4 SV=1	112
C6SVH1	Putative uncharacterized protein OS=Glycine max PE=2 SV=1	143
I1J4X9	Uncharacterized protein OS=Glycine max PE=3 SV=1	787
C6SVL1	Ribosomal protein OS=Glycine max PE=2 SV=1	216
C6SW37	Putative uncharacterized protein OS=Glycine max PE=4 SV=1	64
C6SWE2	Putative uncharacterized protein OS=Glycine max PE=1 SV=1	191
C6T7C4	Putative uncharacterized protein (Fragment) OS=Glycine max PE=2 SV=1	245
C6T827	Uncharacterized protein OS=Glycine max PE=2 SV=1	360
C6TAW4	Proteasome subunit alpha type OS=Glycine max PE=2 SV=1	250
C6TBD8	Putative uncharacterized protein OS=Glycine max PE=1 SV=1	384
C6TBS6	Proteasome subunit beta type OS=Glycine max PE=2 SV=1	271
C6TCC4	Putative uncharacterized protein OS=Glycine max PE=2 SV=1	155
C6TD18	Putative uncharacterized protein (Fragment) OS=Glycine max PE=2 SV=1	241
I1J582	Eukaryotic translation initiation factor 3 subunit I OS=Glycine max PE=3 SV=1	326
C6TG44	Putative uncharacterized protein OS=Glycine max PE=2 SV=1	340
C6THE3	Aspartate aminotransferase OS=Glycine max PE=2 SV=1	344
C6THG4	Putative uncharacterized protein OS=Glycine max PE=2 SV=1	271
C6THU7	Putative uncharacterized protein OS=Glycine max PE=2 SV=1	269
C6TI56	Putative uncharacterized protein OS=Glycine max PE=1 SV=1	341
C6TL09	Putative uncharacterized protein OS=Glycine max PE=2 SV=1	282

C6TLF4	Uncharacterized protein OS=Glycine max PE=2 SV=1	310
F8QXQ1	Albumin-1A OS=Phaseolus vulgaris PE=2 SV=1	127
I1JKR6	Pectinesterase OS=Glycine max PE=3 SV=2	490
I1JSF3	Uncharacterized protein OS=Glycine max PE=4 SV=1	194
I1J6K4	Uncharacterized protein OS=Glycine max PE=4 SV=2	928
I1K5E5	Uncharacterized protein OS=Glycine max PE=4 SV=1	610
I1LJ01	Uncharacterized protein OS=Glycine max PE=4 SV=2	124
I1LMP2	Uncharacterized protein OS=Glycine max PE=4 SV=1	309
I1MC13	Uncharacterized protein OS=Glycine max PE=4 SV=1	490
K0GYZ0	DRE-binding protein 2D1 OS=Glycine max GN=DREB2D;1 PE=2 SV=1	524
K7KAJ1	Uncharacterized protein OS=Glycine max PE=3 SV=1	243
K7MPQ1	Uncharacterized protein OS=Glycine max PE=4 SV=1	302
Q43453	G.max mRNA from stress-induced gene (H4) OS=Glycine max PE=1 SV=1	158
T2DLE1	Uncharacterized protein OS=Phaseolus vulgaris PE=2 SV=1	321
T2DNW9	Fasciclin-like arabinogalactan protein 1-like protein OS=Phaseolus vulgaris PE=2 SV=1	420
I1J7C7	Uncharacterized protein OS=Glycine max PE=4 SV=1	229
I1K4F3	Uncharacterized protein OS=Glycine max PE=4 SV=2	640
I1NBD9	Uncharacterized protein OS=Glycine max PE=4 SV=1	860
C6SXE1	Cyanate hydratase OS=Glycine max GN=CYN PE=2 SV=1	165
C6SWE6	Uncharacterized protein OS=Glycine max PE=2 SV=1	168
C6SXB4	Uncharacterized protein OS=Glycine max PE=2 SV=1	133
C6T9C2	Putative uncharacterized protein OS=Glycine max PE=2 SV=1	309
C6TL04	Putative uncharacterized protein OS=Glycine max PE=2 SV=1	298
C6TMQ9	Putative uncharacterized protein OS=Glycine max PE=2 SV=1	372
I1JNC7	Uncharacterized protein OS=Glycine max PE=4 SV=1	984
C6K8D1	Seed biotinylated protein 68 kDa isoform OS=Glycine max PE=2 SV=1	643
I1J8M6	Uncharacterized protein OS=Glycine max PE=4 SV=1	365
I1K7F4	Uncharacterized protein OS=Glycine max PE=4 SV=1	547
I1KIP9	Uncharacterized protein OS=Glycine max PE=3 SV=1	724
I1LNE6	Uncharacterized protein OS=Glycine max PE=3 SV=1	535
I1N696	Uncharacterized protein OS=Glycine max PE=4 SV=1	495
K7KYL8	Uncharacterized protein OS=Glycine max PE=4 SV=1	407
C6T4R2	Putative uncharacterized protein OS=Glycine max PE=2 SV=1	213
rev_tr|I1M7A0|I1M7A0_SOYBN	DECOY PROTEIN	926
C6SWG9	Uncharacterized protein OS=Glycine max PE=2 SV=1	181
I1JYK1	Uncharacterized protein OS=Glycine max PE=3 SV=1	231
I1J8A4	Thioredoxin reductase OS=Glycine max PE=3 SV=2	370
I1JDH6	Uncharacterized protein OS=Glycine max PE=3 SV=1	275
K7LKJ0	Uncharacterized protein OS=Glycine max PE=4 SV=1	81
B8R511	NBS-LRR type putative disease resistance protein CNL-J1 OS=Phaseolus vulgaris PE=4 SV=1	1186
C6SY23	Putative uncharacterized protein OS=Glycine max PE=1 SV=1	180
C6TNC2	Putative uncharacterized protein OS=Glycine max PE=2 SV=1	371
I1JQD9	Eukaryotic translation initiation factor 3 subunit C OS=Glycine max PE=3 SV=1	926
I1KTQ4	Citrate synthase OS=Glycine max PE=3 SV=1	472
K7KWB0	Uncharacterized protein OS=Glycine max PE=3 SV=1	488
T2DP13	Endo-1314-beta-D-glucanase-like protein OS=Phaseolus vulgaris PE=2 SV=1	255
I1JGP8	Uncharacterized protein OS=Glycine max PE=3 SV=1	570
I1KM24	Uncharacterized protein OS=Glycine max PE=4 SV=1	515
I1L5K0	Uncharacterized protein OS=Glycine max PE=4 SV=1	1148
K7LY40	Uncharacterized protein OS=Glycine max PE=4 SV=1	2020
rev_tr|K7K8N7|K7K8N7_SOYBN	DECOY PROTEIN	944
I1JMB4	Uncharacterized protein OS=Glycine max PE=3 SV=1	418
I1K1C9	Uncharacterized protein OS=Glycine max PE=4 SV=1	352
I1MUR2	Uncharacterized protein OS=Glycine max PE=3 SV=1	338
rev_tr|N6V087|N6V087_9RHIZ	DECOY PROTEIN	518

I1L4U3	Uncharacterized protein OS=Glycine max PE=3 SV=2	787
C6SXD0	Uncharacterized protein OS=Glycine max PE=2 SV=1	153
I1JJB5	Uncharacterized protein OS=Glycine max PE=3 SV=1	464
C6SX86	Uncharacterized protein OS=Glycine max PE=2 SV=1	146
L0LIZ4	Uncharacterized protein OS=Rhizobium tropici CIAT 899 GN=RTCIAT899_CH10025 PE=4 SV=1	2231
K7MKC3	Uncharacterized protein OS=Glycine max PE=4 SV=1	213
rev_tr|C6TH30|C6TH30_SOYBN	DECOY PROTEIN	383
E9NZT0	Ribosomal protein L19 OS=Phaseolus vulgaris PE=3 SV=1	209
T2DN63	Oleosin 16 kDa-like protein OS=Phaseolus vulgaris PE=2 SV=1	160
Q41111	Dehydrin OS=Phaseolus vulgaris PE=1 SV=1	202
I1LK14	Uncharacterized protein OS=Glycine max PE=4 SV=2	678
S5RYF5	TonB-dependent hemoglobin/transferrin/lactoferrin family receptor protein OS=Rhizobium etli bv. mimosae str. Mim1 GN=REMIM1_CH03122 PE=4 SV=1	752
T2DNK2	Plasminogen activator inhibitor 1 RNA-binding protein OS=Phaseolus vulgaris PE=2 SV=1	411
I1JLC8	Uncharacterized protein OS=Glycine max PE=4 SV=1	105
K7LJS8	Uncharacterized protein OS=Glycine max PE=4 SV=1	633
L0LF18	Multidrug and toxin extrusion (MATE) family efflux pump OS=Rhizobium tropici CIAT 899 GN=RTCIAT899_CH02970 PE=4 SV=1	449
C6SZN4	Ribosomal protein L37 OS=Glycine max PE=3 SV=1	95
Q9FT25	Pyridoxal biosynthesis protein PDX1 OS=Phaseolus vulgaris GN=PDX1 PE=2 SV=1	312
rev_tr|K7KXF5|K7KXF5_SOYBN	DECOY PROTEIN	507
I1LFG4	Uncharacterized protein OS=Glycine max PE=4 SV=1	742
rev_tr|L0LRE1|L0LRE1_RHITR	DECOY PROTEIN	331
rev_tr|K7LKK0|K7LKK0_SOYBN	DECOY PROTEIN	273
I1LGX3	Uncharacterized protein OS=Glycine max PE=4 SV=1	132
I1JTY8	Uncharacterized protein OS=Glycine max PE=4 SV=1	805
I1MQT7	Uncharacterized protein OS=Glycine max PE=4 SV=2	1218
rev_tr|K7MM29|K7MM29_SOYBN	DECOY PROTEIN	1030
I1K5F0	Uncharacterized protein OS=Glycine max PE=4 SV=1	479
rev_tr|I1K773|I1K773_SOYBN	DECOY PROTEIN	898
I1LAA7	Uncharacterized protein OS=Glycine max PE=4 SV=1	969
rev_tr|K7LCF8|K7LCF8_SOYBN	DECOY PROTEIN	902
I1L2M6	Uncharacterized protein OS=Glycine max PE=4 SV=1	222
I1JXH8	Uncharacterized protein OS=Glycine max PE=3 SV=1	487
rev_tr|K7M2P0|K7M2P0_SOYBN	DECOY PROTEIN	135
T2DMX7	Heat-shock protein OS=Phaseolus vulgaris PE=2 SV=1	703
rev_tr|K0VUA4|K0VUA4_9RHIZ	DECOY PROTEIN	236
C6TMA8	Uncharacterized protein OS=Glycine max PE=1 SV=1	119
C6TNT7	Putative uncharacterized protein (Fragment) OS=Glycine max PE=2 SV=1	213
C6TK38	Putative uncharacterized protein OS=Glycine max PE=2 SV=1	484
rev_tr|C6T865|C6T865_SOYBN	DECOY PROTEIN	312
Q9AU12	Phosphoenolpyruvate carboxylase OS=Phaseolus vulgaris PE=1 SV=1	968
C6TCQ8	Carbonic anhydrase OS=Glycine max PE=2 SV=1	259
I1K5S7	Uncharacterized protein OS=Glycine max PE=4 SV=2	576
C6TFA0	Putative uncharacterized protein OS=Glycine max PE=1 SV=1	214
C6T7U0	Putative uncharacterized protein OS=Glycine max PE=2 SV=1	221
I1JXS8	Uncharacterized protein OS=Glycine max PE=4 SV=1	990
L0LT14	Chaperone protein HtpG OS=Rhizobium tropici CIAT 899 GN=htpG PE=3 SV=1	629

rev_tr|K0VZH8|K0VZH8_9RHIZ	DECOY PROTEIN	320
rev_tr|K7MXZ9|K7MXZ9_SOYBN	DECOY PROTEIN	527
K0VRX2	Capsular polysaccharide biosynthesis protein (Fragment) OS=Rhizobium sp. Pop5 GN=RCCGEPOP_15776 PE=4 SV=1	459
I1K764	Glucose-1-phosphate adenylyltransferase OS=Glycine max PE=3 SV=1	519
rev_tr|I1KRY3|I1KRY3_SOYBN	DECOY PROTEIN	593
I1K547	Uncharacterized protein OS=Glycine max PE=4 SV=1	372
I1MB04	Uncharacterized protein OS=Glycine max PE=3 SV=1	1292
T2DPD1	60S acidic ribosomal protein P1-3-like protein OS=Phaseolus vulgaris PE=4 SV=1	112
K7M2P3	Uncharacterized protein OS=Glycine max PE=4 SV=1	537
K7LJB3	Uncharacterized protein OS=Glycine max PE=4 SV=1	611
I1KGY6	Uncharacterized protein OS=Glycine max PE=3 SV=1	768
C6SXV0	Putative uncharacterized protein OS=Glycine max PE=2 SV=1	132
rev_tr|K7KZI3|K7KZI3_SOYBN	DECOY PROTEIN	1090
C6SVV1	Uncharacterized protein OS=Glycine max PE=2 SV=1	164
I1K8F4	Uncharacterized protein OS=Glycine max PE=4 SV=1	352
S5SWM9	Sugar ABC transporter substrate-binding protein OS=Rhizobium etli bv. mimosae str. Mim1 GN=REMIM1_PF00622 PE=4 SV=1	428
K7LID1	Uncharacterized protein OS=Glycine max PE=4 SV=1	235
Q9M507	Beta-ketoacyl-ACP synthetase I-2 OS=Glycine max PE=2 SV=1	469
C6TGG3	Putative uncharacterized protein OS=Glycine max PE=2 SV=1	363
rev_tr|I1JXW9|I1JXW9_SOYBN	DECOY PROTEIN	715
I1N5N0	Pyruvate kinase OS=Glycine max PE=3 SV=1	510
I1KH65	Uncharacterized protein OS=Glycine max PE=4 SV=1	912
C6SZ18	Uncharacterized protein OS=Glycine max PE=4 SV=1	65
C6T8Y7	Putative uncharacterized protein OS=Glycine max PE=2 SV=1	488
I1J5A5	Uncharacterized protein OS=Glycine max PE=3 SV=1	538
I1KY39	Citrate synthase OS=Glycine max PE=3 SV=1	513
I1N484	Uncharacterized protein OS=Glycine max PE=4 SV=1	110
C6SVK9	Putative uncharacterized protein OS=Glycine max PE=4 SV=1	117
I1KU96	Uncharacterized protein OS=Glycine max PE=3 SV=1	536
C6TA32	Putative uncharacterized protein OS=Glycine max PE=2 SV=1	460
rev_tr|I1KRB5|I1KRB5_SOYBN	DECOY PROTEIN	527
I1L1Q8	Uncharacterized protein OS=Glycine max PE=3 SV=1	509
I1JTT1	Uncharacterized protein OS=Glycine max PE=4 SV=2	384
I1LH56	Uncharacterized protein OS=Glycine max PE=4 SV=1	298
I1L362	Uncharacterized protein OS=Glycine max PE=4 SV=2	1336
I1MKY2	Uncharacterized protein OS=Glycine max PE=4 SV=1	672
C6TMV0	Putative uncharacterized protein OS=Glycine max PE=2 SV=1	162
C6T0M2	Uncharacterized protein OS=Glycine max PE=4 SV=1	75
I1J8K6	Uncharacterized protein OS=Glycine max PE=4 SV=1	318
rev_tr|K0VUV5|K0VUV5_9RHIZ	DECOY PROTEIN	116
I1L3S2	Proteasome subunit alpha type OS=Glycine max PE=3 SV=1	285
K0VSU2	Secretion protein HlyD family protein OS=Rhizobium sp. Pop5 GN=RCCGEPOP_14127 PE=4 SV=1	402
K7MZR8	Uncharacterized protein OS=Glycine max PE=4 SV=1	209
I1LF29	Uncharacterized protein OS=Glycine max PE=3 SV=1	505
I1KG78	Uncharacterized protein OS=Glycine max PE=3 SV=1	857
C6T2W8	Uncharacterized protein OS=Glycine max PE=4 SV=1	103
I1KJN4	Uncharacterized protein OS=Glycine max PE=3 SV=1	420
I1L655	Uncharacterized protein OS=Glycine max PE=3 SV=1	489
I1KMQ9	Uncharacterized protein OS=Glycine max PE=4 SV=1	770
I1L849	Uncharacterized protein OS=Glycine max PE=4 SV=1	262

I1MRX8	Uncharacterized protein OS=Glycine max PE=4 SV=1	503
I1KWC6	Uncharacterized protein OS=Glycine max PE=4 SV=1	538
rev_tr|I1KU45|I1KU45_SOYBN	DECOY PROTEIN	422
rev_tr|K7LI39|K7LI39_SOYBN	DECOY PROTEIN	592
N6V5Q7	Putative fructose transport system kinase OS=Rhizobium freirei PRF 81 GN=RHSP_19647 PE=4 SV=1	210
I1LBD0	Uncharacterized protein OS=Glycine max PE=4 SV=1	447
I1JGR4	Uncharacterized protein OS=Glycine max PE=4 SV=1	784
I1JRF2	Uncharacterized protein OS=Glycine max PE=3 SV=1	557
L0LEG7	Major facilitator superfamily (MFS) transporter OS=Rhizobium tropici CIAT 899 GN=RTCIAT899_CH01800 PE=4 SV=1	405
K7LM33	Uncharacterized protein OS=Glycine max PE=4 SV=1	1384
K7MZ08	Uncharacterized protein OS=Glycine max PE=4 SV=1	450
I1LH18	Uncharacterized protein OS=Glycine max PE=4 SV=1	438
C6T172	Uncharacterized protein OS=Glycine max PE=1 SV=1	236
I1MMH5	Uncharacterized protein OS=Glycine max PE=4 SV=1	414
rev_tr|I1MYD0|I1MYD0_SOYBN	DECOY PROTEIN	613
rev_tr|I1JJ51|I1JJ51_SOYBN	DECOY PROTEIN	283
I1LVC1	Uncharacterized protein OS=Glycine max PE=4 SV=1	135
K0VF89	Excinuclease ABC subunit B (Fragment) OS=Rhizobium sp. Pop5 GN=RCCGEPOP_30134 PE=4 SV=1	365
rev_tr|I1L748|I1L748_SOYBN	DECOY PROTEIN	1772
I1ME45	Proline iminopeptidase OS=Glycine max PE=3 SV=1	391
I1LIN0	Uncharacterized protein OS=Glycine max PE=3 SV=1	513
Q9XES8	Seed maturation protein PM28 OS=Glycine max GN=PM28 PE=4 SV=1	89
C6SVG3	Putative uncharacterized protein OS=Glycine max PE=2 SV=1	155
C6T8Y2	Uncharacterized protein OS=Glycine max PE=2 SV=1	478
C6TCN9	Putative uncharacterized protein OS=Glycine max PE=2 SV=1	407
A4PIT0	Isoamylase-type starch-debranching enzyme 3 OS=Phaseolus vulgaris GN=PvISA3 PE=2 SV=1	783
I1MN39	Proteasome subunit alpha type OS=Glycine max PE=3 SV=1	249
K7KM59	Uncharacterized protein OS=Glycine max PE=4 SV=1	785
A4GG90	ATP synthase subunit beta, chloroplastic OS=Phaseolus vulgaris GN=atpB PE=3 SV=1	498
C6TEA4	Putative uncharacterized protein OS=Glycine max PE=2 SV=1	236
C6T250	Uncharacterized protein OS=Glycine max PE=4 SV=1	75
I1LVQ5	Uncharacterized protein OS=Glycine max PE=4 SV=1	184
S3HK98	Crp/Fnr family transcriptional regulator OS=Rhizobium grahamii CCGE 502 GN=RGCCGE502_06569 PE=4 SV=1	250
I1MSU1	Xylose isomerase OS=Glycine max PE=3 SV=1	480
rev_tr|I1N5T6|I1N5T6_SOYBN	DECOY PROTEIN	2175
I1KDV2	Uncharacterized protein OS=Glycine max PE=4 SV=1	422
I1M4W1	Uncharacterized protein OS=Glycine max PE=4 SV=1	180
L0LRX3	XylR-type repressor OS=Rhizobium tropici CIAT 899 GN=RTCIAT899_PB00875 PE=4 SV=1	433
rev_tr|C0JJG7|C0JJG7_SOYBN	DECOY PROTEIN	496
rev_tr|K7KYD8|K7KYD8_SOYBN	DECOY PROTEIN	958
I1LVR2	Uncharacterized protein OS=Glycine max PE=4 SV=1	241
rev_tr|K7LYS3|K7LYS3_SOYBN	DECOY PROTEIN	252
C6TKL2	Reticulon-like protein OS=Glycine max PE=2 SV=1	253
I1MV76	Glutamate dehydrogenase OS=Glycine max PE=3 SV=2	412

rev_tr|L0LFL9|L0LFL9_RHITR	DECOY PROTEIN	260
rev_tr|I1J9K8|I1J9K8_SOYBN	DECOY PROTEIN	596
rev_tr|Q69F89|Q69F89_PHAVU	DECOY PROTEIN	529
N6V3T9	ABC transporter integral membrane protein OS=Rhizobium freirei PRF 81 GN=RHSP_79899 PE=4 SV=1	884
K7L730	Uncharacterized protein OS=Glycine max PE=4 SV=1	122
L0LS48	Chemotaxis protein CheW OS=Rhizobium tropici CIAT 899 GN=RTCIAT899_PC01215 PE=4 SV=1	154
K7MRI3	Uncharacterized protein OS=Glycine max PE=4 SV=1	516
C6SYC1	Uncharacterized protein OS=Glycine max PE=2 SV=1	168
rev_tr|K0VQA3|K0VQA3_9RHIZ	DECOY PROTEIN	323
K7LX62	Uncharacterized protein (Fragment) OS=Glycine max PE=3 SV=1	206
rev_tr|S3HGD3|S3HGD3_9RHIZ	DECOY PROTEIN	200
rev_tr|S3IJG3|S3IJG3_9RHIZ	DECOY PROTEIN	468
C6SZW2	Uncharacterized protein OS=Glycine max PE=2 SV=1	153
S3I214	Transcriptional regulator OS=Rhizobium grahamii CCGE 502 GN=RGCCGE502_07104 PE=4 SV=1	214
rev_tr|I1N0C7|I1N0C7_SOYBN	DECOY PROTEIN	496
K7MND3	Uncharacterized protein (Fragment) OS=Glycine max PE=4 SV=1	103
I1JCE8	Uncharacterized protein OS=Glycine max PE=4 SV=2	418
I1KN71	Uncharacterized protein OS=Glycine max PE=4 SV=2	787
S5SL82	Tetratricopeptide repeat-containing TonB-dependent receptor protein OS=Rhizobium etli bv. mimosae str. Mim1 GN=REMIM1_CH02733 PE=4 SV=1	1239
K9UTZ9	Epidermis-specific secreted glycoprotein EP1-like protein OS=Phaseolus vulgaris PE=2 SV=1	431
O24439	PvLEA-18 OS=Phaseolus vulgaris GN=Pvlea-18 PE=4 SV=1	86
O24442	Group 4-late embryogenesis abundant protein PvLEA4-25 (Fragment) OS=Phaseolus vulgaris GN=Pvlea4-25 PE=2 SV=1	91
Q2N1E0	Group 3 late embryogenesis abundant protein OS=Phaseolus vulgaris GN=LEA3 PE=4 SV=1	468
A7L5M4	Voltage-dependent anion channel (Fragment) OS=Phaseolus vulgaris PE=2 SV=1	60
Q39801	51 kDa seed maturation protein OS=Glycine max PE=2 SV=1	473
Q84UT1	Glucose-1-phosphate adenylyltransferase OS=Phaseolus vulgaris GN=pvagpS1 PE=2 SV=1	515
Q8VX07	Starch branching enzyme (Fragment) OS=Phaseolus vulgaris GN=pvsbe2 PE=4 SV=1	184
Q9FE12	Peroxiredoxin OS=Phaseolus vulgaris GN=2-Cys PRx PE=1 SV=1	260
Q9FPW5	IAA-protein conjugate OS=Phaseolus vulgaris GN=iap1 PE=2 SV=1	318
Q9XER5	Seed maturation protein PM22 OS=Glycine max GN=PM22 PE=2 SV=1	152
Q9XET0	Seed maturation protein PM30 OS=Glycine max GN=PM30 PE=2 SV=1	140
T2DM51	Zinc finger CCCH domain-containing protein OS=Phaseolus vulgaris PE=2 SV=1	186
T2DMU1	Vacuolar-sorting receptor OS=Phaseolus vulgaris PE=2 SV=1	625
T2DN44	60S ribosomal protein L13-2-like protein OS=Phaseolus vulgaris PE=2 SV=1	207
A7XTY1	Cytosolic glutathione reductase OS=Phaseolus vulgaris GN=cGR PE=1 SV=1	506
T2DNF5	S-formylglutathione hydrolase OS=Phaseolus vulgaris PE=2 SV=1	285
T2DNY2	Mitochondrial aldehyde dehydrogenase OS=Phaseolus vulgaris PE=2 SV=1	535
T2DP67	Xylose isomerase OS=Phaseolus vulgaris PE=2 SV=1	480
T2DPA0	Nucleoredoxin 1-like protein OS=Phaseolus vulgaris PE=2 SV=1	571
O22518	40S ribosomal protein SA OS=Glycine max PE=1 SV=1	310
C6TEJ6	40S ribosomal protein SA OS=Glycine max PE=2 SV=1	313
P01060	Bowman-Birk type proteinase inhibitor 2 OS=Phaseolus vulgaris GN=BBI PE=1 SV=3	107
A0T2V2	Alpha amylase inhibitor-1 OS=Phaseolus vulgaris PE=4 SV=1	244
Q6J2U4	Alpha amylase inhibitor-1 OS=Phaseolus vulgaris PE=4 SV=1	244
Q9S9E1	Alpha-amylase inhibitor beta subunit, PHA-I beta subunit OS=Phaseolus vulgaris PE=4 SV=1	137

P04771	Glutamine synthetase PR-2 OS=Phaseolus vulgaris PE=2 SV=1	356
C6TJN5	Glutamine synthetase OS=Glycine max PE=2 SV=1	356
O82560	Glutamine synthetase cytosolic isozyme 2 OS=Glycine max PE=1 SV=1	356
P07219	Phaseolin, alpha-type OS=Phaseolus vulgaris PE=1 SV=1	436
P02853	Phaseolin, beta-type OS=Phaseolus vulgaris PE=1 SV=2	421
Q43632	Phaseolin OS=Phaseolus vulgaris GN=Phs PE=2 SV=1	421
Q43633	Phaseolin OS=Phaseolus vulgaris GN=Phs PE=2 SV=1	430
Q41115	Alpha-phaseolin OS=Phaseolus vulgaris PE=4 SV=1	430
P80463	Phaseolin OS=Phaseolus lunatus GN=PHA PE=1 SV=2	428
P24459	ATP synthase subunit alpha, mitochondrial OS=Phaseolus vulgaris GN=ATPA PE=1 SV=1	508
M1FPH1	ATP synthase subunit alpha OS=Glycine max GN=atp1-3 PE=3 SV=1	508
A9CPA7	Protein disulfide isomerase family OS=Glycine max GN=GmPDIM PE=2 SV=1	438
P25699	Ferritin, chloroplastic OS=Phaseolus vulgaris GN=PFE PE=1 SV=1	254
T2DPX5	Ferritin 3 chloroplastic-like protein OS=Phaseolus vulgaris PE=2 SV=1	260
P25985	Pathogenesis-related protein 1 OS=Phaseolus vulgaris PE=1 SV=2	156
Q43634	Intracellular pathogenesis related protein OS=Phaseolus vulgaris GN=Ypr10 PE=3 SV=1	155
I1LCI3	Superoxide dismutase OS=Glycine max PE=3 SV=1	244
I1KDL4	Uncharacterized protein OS=Glycine max PE=3 SV=1	967
C6TNF0	Ferritin OS=Glycine max PE=2 SV=1	247
I1JBH2	Proteasome subunit alpha type OS=Glycine max PE=3 SV=1	237
C6SVR5	Putative uncharacterized protein OS=Glycine max PE=2 SV=1	211
A0A762	Calreticulin-1 OS=Glycine max GN=Gm crt-1 PE=1 SV=1	420
I1NF03	Uncharacterized protein OS=Glycine max PE=3 SV=1	451
A2VBN4	Trypsin/chymotrypsin inhibitor OS=Phaseolus vulgaris GN=BBI PE=3 SV=1	120
Q8L6E6	Double-headed trypsin inhibitor (Fragment) OS=Phaseolus vulgaris GN=bbi20 PE=3 SV=1	104
Q84RP7	Double-headed trypsin inhibitor (Fragment) OS=Phaseolus vulgaris GN=bbi PE=3 SV=1	104
A7L3U9	Elongation factor 1-alpha (Fragment) OS=Phaseolus vulgaris GN=EF1-a PE=2 SV=1	201
T2DPT7	Elongation factor 1-alpha OS=Phaseolus vulgaris PE=2 SV=1	447
O04299	Elongation factor-1 alpha (Fragment) OS=Glycine max GN=TefS1 PE=4 SV=1	127
C6EVF9	Elongation factor 1-alpha OS=Glycine max GN=EF-1A PE=2 SV=1	447

Appendix II

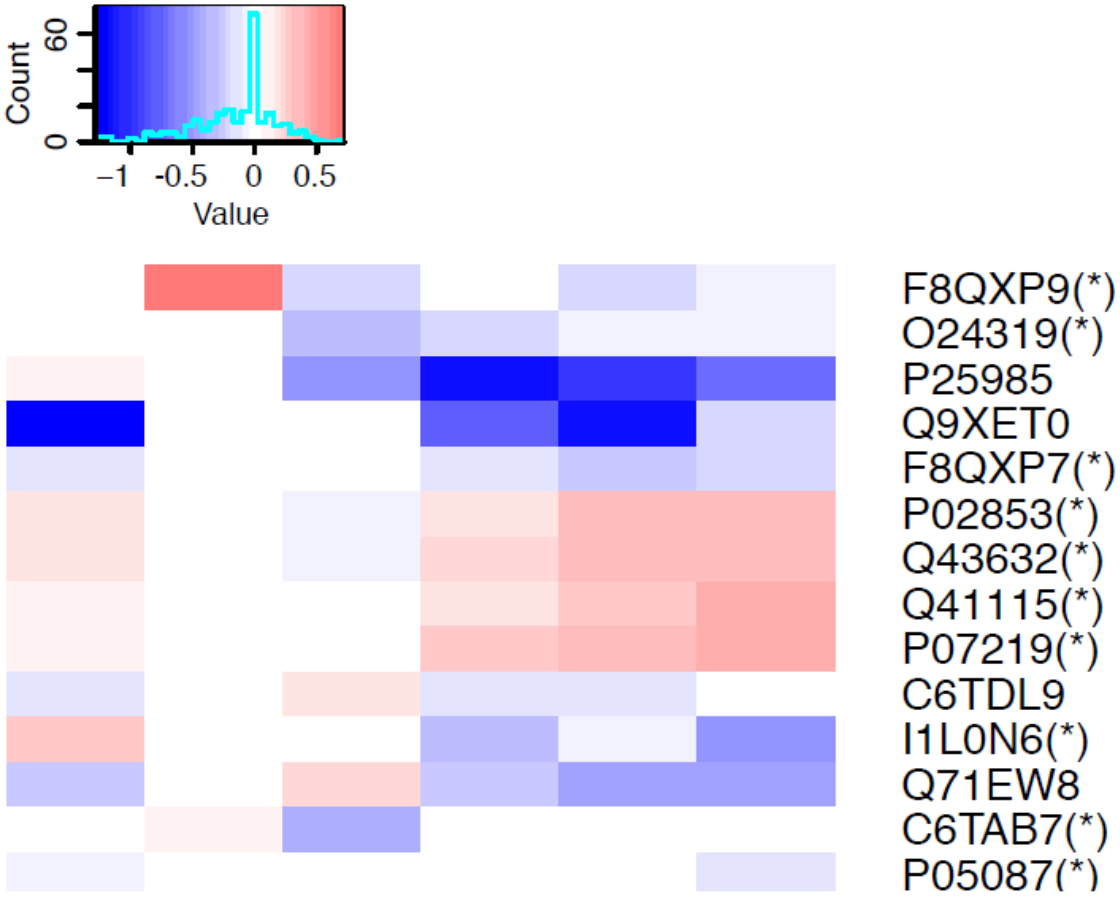
Count
60
0
−1
-0.5
0
0.5
Value
F8QXP9(*)
O24319(*)
P25985
Q9XET0
F8QXP7(*)
P02853(*)
Q43632(*)
Q41115(*)
P07219(*)
C6TDL9
I1L0N6(*)
Q71EW8
C6TAB7(*)
P05087(*)

Vita

Sanghamitra Majumdar earned her Bachelor of Science (Honors) degree in Botany from University of Delhi, INDIA in 2005. She pursued her Masters of Science in Environmental Science in 2007 from Visva Bharati University, INDIA, and was awarded the Central University merit scholarship for being the top-most student in 2006-2007. Then, she worked as a Research assistant at The National Environmental Engineering Research Institute, The Council of Scientific & Industrial Research (CSIR), Government of India, on environmental remediation, regulations, risk management and sustainability. In 2010, she joined the Chemistry PhD program at The University of Texas at El Paso under the supervision of Dr. Jorge Gardea-Torresdey.

Ms. Majumdar has been a recipient of numerous honors and award including George A. Krutilek Memorial Scholarship and Dodson Research grant from Graduate School. During the period of her PhD, she worked as a research associate and teaching assistant at the Department of Chemistry. She has been a member and research assistant at the University of California's Center for Environmental Implications of Nanotechnology, while pursuing her doctoral degree. She was also involved with various leadership and professional development on-campus activities like World Leaders Council, Student Government Association and chaired as the President of the Indian Student Association from 2013-2014. She was also selected to represent research from chemistry department in undergraduate orientation programs.

In January 2015, she will be joining as a Post-doctoral Research Scientist at the Connecticut Agricultural Experiment Station, funded through the U.S FDA towards food safety. Dr. Majumdar has presented her research in numerous national and international conferences. She won the best poster award at the Sustainable Nanotechnology organization Conference 2014 at Boston, and the best oral presenter at the Graduate Research Expo organized by Graduate School, UTEP. She has authored and coauthored six publications during her PhD tenure in high impact factor journals. She has two other research papers under review process and three more under preparation.

Dr. Majumdar's dissertation, *Nanoceria exposure to kidney beans (Phaseolus vulgaris): implications on plant physiology, nutrition and their transfer to next trophic level,* was supervised by Dr. Jorge L. Gardea-Torresdey.

Honors and awards:

- Best Oral Presentation Award, Graduate Research Expo 2014, Graduate School, The University of Texas at El Paso, 14 November, 2014. El Paso, TX
- First place in Poster Session at Sustainable Nanotechnology Organization (SNO) Conference, November, 2014. Boston, Massachusetts, USA.
- Sustainable Nanotechnology Organization (SNO) Student Award 2014
- Graduate School Dodson Research Grant, Graduate School, UTEP, January 2014
- Phytoscholar Award, 2013, awarded by the International Phytotechnology Society (IPS) and the National Institute of Environmental Health Sciences (NIEHS) at 10th International Phytotechnologies Conference, 1-5 October, 2013, Syracuse, New York, USA
- George A. Krutilek Memorial Graduate Scholarship, Office of Scholarship, UTEP, July 2013 (One student selected among 250 applicants)
- Dodson Travel Grant, College of Science, The University of Texas at El Paso, 2013
- Student Government Association Travel Award, The University of Texas at El Paso, 2013
- President, The Indian Student Association, The University of Texas at El Paso, 2013-14
- Judge, COURI Symposium 2012, Campus Office of Undergraduate Research Initiatives
- Dodson Travel Grant, College of Science, The University of Texas at El Paso, 2012
- Central University Merit Scholarship: First class first award in Masters of Science (Environmental Sciences), 2007
- Indira Gandhi Post Graduate National Scholarship by University Grants Commission, INDIA, 2005-06
- Second prize, Environmental Poster competition, National Science Day *2006*, Centre for Biotechnology and Department of Zoology, Visva Bharati, Santiniketan, West Bengal, India, sponsored by Department of Biotechnology, Govt. of India.

Professional memberships and positions:

1. *Invited Board Member,* World Leaders' Council, UTEP, Since January 2014

2. *Invited Member,* International Phytotechnology Society, Since 2013

3. *Member, Sustainable Nanotechnology Organization,* Since 2013

4. *Reviewer,* Environmental Science and Technology, Since 2012

5. *Member,* American Chemical Society, Since 2012

6. *President,* Indian Student Association, UTEP (Non-profit organization, Community services), January 2013- Present

7. *Member,* UC Centre for Environmental Implications of Nanotechnology, NSF-EPA, Since May 2010

8. *Secretary of Botanical Society*, Daulat Ram College, University of Delhi, 2003-04

9. *Joint-Secretary of Botanical Society*, Daulat Ram College, University of Delhi, 2002-03

Publications (reverse chronological order)

1. Hawthorne, J.; De la Torre Roche, R.; Xing, B.; Newman, L. A.; Ma, X.; Majumdar, S.; Gardea-Torresdey, J.; White, J C. Particle-size dependent accumulation and trophic transfer of cerium oxide through a terrestrial food chain. *Environ. Sci. Technol.* **2014**, *48*, 13102-13109.

2. ***Majumdar, S***.; Peralta-Videa, J. R.; Bandyopadhyay, S.; Castillo-Michel, H.; Hernandez J. A.; Bartonjo, J.; Sahi, S.; Gardea-Torresdey, J. L., Exposure of cerium oxide nanoparticles to kidney bean shows disturbance in the plant defense mechanisms. *J. Hazard. Mater.* **2014**, *278*, 279-287.

3. Trujillo-Reyes, J.; ***Majumdar, S***.; Botez, C. E.; Peralta-Videa, J. R.; Gardea-Torresdey, J. L., Exposure studies of core-shell Fe/Fe_3O_4 and Cu/CuO NPs to lettuce (*Lactuca sativa*) plants: Are they a potential physiological and nutritional hazard? *J. Hazard. Mater.* **2014**, *267*, 255-263.

4. Trujillo-Reyes, J.; Vilchis-Nestor, A. R.; ***Majumdar, S***.; Peralta-Videa, J. R.; Gardea-Torresdey, J. L., Citric acid modifies surface properties of commercial CeO_2 nanoparticles reducing their toxicity and cerium uptake in radish (*Raphanus sativus*) seedlings, *J. Hazard. Mater*. **2013**, *263*, 677-684.

5. ***Majumdar, S.;*** Peralta-Videa, J. R.; Castillo-Michel, H.; Hong, J.; Rico, C. M.; Gardea-Torresdey, J. L., Applications of synchrotron μ-XRF to study the distribution of

biologically important elements in different environmental matrices: A review. *Anal. Chim. Acta.* **2012**, *755*, 1-16. **"*Cover article for the journal, November 2012 Issue*"**

6. Rico, C. M.; ***Majumdar, S***.; Duarte-Gardea, M.; Peralta-Videa, J. R.; Gardea-Torresdey, J. L., Interaction of nanoparticles with edible plants and their possible implications in the food chain, *J. Agric. Food Chem.* **2011**, *59*, 3485-3498. **"*American Chemical Society Press release*"**

Noteworthy presentations:

1. ***Majumdar, S.,*** Peralta-Videa, J.R., Gardea-Torresdey, J.L. **2014**. Trophic transfer of cerium oxide nanoparticles along a terrestrial food chain: an ecological risk. Graduate Research Expo 2014, Graduate School, The University of Texas at El Paso, 14 November, 2014. El Pasi, TX (Oral). "*Won best oral presenter award"*

2. ***Majumdar, S.,*** Peralta-Videa, J.R., Gardea-Torresdey, J.L. **2014**. Trophic transfer of metal oxide nanoparticles along a terrestrial food chain: an ecological risk. Third Sustainable Nanotechnology Organization Conference, 2-4 November, 2014. Boston, Massachusetts, USA (Poster). *"Won the best poster award"*

3. ***Majumdar, S.,*** Peralta-Videa, J.R., Trujillo-Reyes, J., Gardea-Torresdey, J.L. **2013**. Fate of nanoceria in Red kidney beans and its filial generation: Differential response to soil quality. 2013 Conference of the Sustainable Nanotechnology Organization, 3-5 November, 2013. Santa Barbara, California, USA (Oral).

4. ***Majumdar, S.,*** Peralta-Videa, J.R., Gardea-Torresdey, J.L. **2013**. Nanoceria biotransform in root epidermis of Kidney bean (*Phaseolus vulgaris*) and demonstrate antioxidant properties in the tissues. SETAC North America 34th Annual Meeting, 17-21 November 2013, Nashville, TN, USA (Oral).

5. ***Majumdar, S.,*** Trujillo-Reyes, J., Peralta-Videa, J.R., Gardea-Torresdey, J.L. **2013.** Translocation of cerium oxide nanoparticles in kidney bean plants and their effects on plant metabolism and seed nutrition quality. 10th International Phytotechnologies Conference, 1-5 October 2013, Syracuse, New York, USA (Poster).

6. White, J.C., De la Torre-Roche, R., Musante, C., ***Majumdar, S.***, Gardea-Torresdey, J, Xing, B., Newman, L.A., Ma, X., Trophic transfer potential of cerium oxide nanoparticles through a terrestrial food chain. 10th International Phytotechnologies Conference, 1-5 October 2013, Syracuse, New York, USA (Poster).

7. Trujillo-Reyes, J., ***Majumdar, S.***, Peralta-Videa, J.R., Gardea-Torresdey J.L. Physiological effects of iron and copper nanostructured oxides on lettuce (*Lactuca sativa*) and onion (*Allium cepa*). XII International Congress and XVIII National Congress of Environmental Sciences, June 5-7, 2013. Ciudad Juárez, Chihuahua, México (Oral).

8. ***Majumdar, S.***, Peralta-Videa, J.R., Gardea-Torresdey, J.L., Impact of cerium oxide nanoparticles on Kidney beans. 244th ACS National Meeting, August 19-23, 2012, Philadelphia, Pennsylvania (Oral).

Permanent address: Flat no.2, ANANDAM, 96/2 K. N. Sen Road

Kolkata, West Bengal, INDIA- 700042

This thesis/dissertation was typed by Sanghamitra Majumdar